

THE ACOUSTICS OF THE VIOLIN.

BY

ERIC JOHNSON

This Thesis is presented in part  
fulfilment of the degree of  
Doctor of Philosophy at the  
University of Salford.

Department of Applied Acoustics  
University of Salford  
Salford, Lancashire.  
30 September, 1981.

TABLE OF CONTENTS

Chapter 1: The Violin.	page 1
Introduction	1
A Brief History of the Violin	2
Building the Violin	5
The Best Violins and What Makes Them Different	11
References	15
Chapter 2: Experimental and Theoretical Methods.	16
Measuring the Frequency Response	16
Holography	24
The Green's Function Technique	34
References	40
Chapter 3: Dynamics of the Bowed String.	41
The Bowed String	41
The Wolf- Note	53
References	58
Chapter 4: An Overview of Violin Design.	59
The Violin's Design	59
The Bridge as a Transmission Element	69
The Function of the Soundpost and Bassbar	73
Modelling the Helmholtz and Front Plate Modes	76
Other Air Modes in the Violin Cavity	79
References	84
Chapter 5: Modelling the Response of the Violin.	85
The Model	85
Evaluating the Model	93
Investigating Violin Design	99
References	106
Chapter 6: Mass- Production Applications	107
Manufacturing Techniques	107
References	116

ACKNOWLEDGEMENTS

In a work such as this it is difficult to thank all those who played a part in its evolution. Ideas and help came from so many directions that some, whose aid was appreciated, have no doubt been left out in my acknowledgements. Those who played the most conspicuous role in the writing of this thesis are listed below but the list is by no means complete. The University itself made possible this work by means of a research grant and this financial help was augmented by the Department of Applied Acoustics. Mr. D. O'Connor, who supervised the work, should receive special thanks for the considerable amount of time he was willing to give and for his valuable suggestions. Dr. R. Ford and Dr. D. Saunders also deserve to be thanked for the many times they have listened to my questions and ideas. The subject of violins has always been of interest to D. Vallance, Prof. Lord, and the violin maker, D. Vernon, and discussions with these three have been fruitful and interesting. Finally, A. Jackson helped in uncounted ways and P. Yeoman always advised me on any question concerning photography.

To these and the many others who helped me in this work I give my thanks.

To those who helped me in a more personal way during four years away from the United States, who made England a friendly and hospitable place, there is no way for me to repay your kindness.

ABSTRACT

The violin is a highly complex vibrating system which, quite without the aid of science, evolved to a high level of sophistication. Wood, which varies considerably from one sample to another, requires individual attention to be fashioned into the plates of a good violin. It is not therefore surprising that mass-produced instruments are of very poor quality. It is the improvement of these instruments which is the objective of this thesis.

After identifying those features of the response upon which the violin's quality most depend a model is developed and used to answer several questions about violin design. As it is extremely difficult to include the sound post in the model it is suggested that an additional structural element, designed to match the back's impedance, is used to support the post. The amount of acoustic radiation from the back is shown to be small so that this change does not greatly affect the output level.

Finally it is shown that, using such a construction, the low frequency response of the violin may be predicted before assembly. A description of an automated production process in which the violin plates are cut and tested by micro-processor controlled machinery concludes the work.

Introduction.

Scientific investigations of the violin family are by no means uncommon today. It seems that nearly every aspect of this subject has been looked at, and yet every advance shows that it is the subtlest details of its action which are the mark of a good violin. Thus, like climbing over a series of ridges, the solution of one problem inevitably brings to view another, more distant one.

In this thesis it is not the smallest details which are investigated. Some interesting problems are elucidated, such as the principles which govern the violin's design, the consequences of the highly non-linear bowing process, and the parameters which determine the origin of the wolf-note, but such problems are only incidental to the purpose of this work. The real goal is to find a way in which to improve the vast majority of new violins, those mass-produced for students, in a way which does not add to their market price.

As a first step towards this goal the most obvious characteristics of good violins are studied. These are evident in the frequency response curves measured by many other researchers. Then, after modelling the action of the violin, a method for predicting the response of a complete violin over part of the frequency range is developed, based on the properties of the component parts. This makes it possible to adjust the violin's frequency response before assembly, while it is still easy to alter the plates. Finally, the possibility of applying this prediction technique in a mass-production situation is briefly explored.

In adopting this approach the importance of the steady-state vibrations is perhaps stressed too much. No doubt the transient response of a violin is also very important, yet the quality of most

mass-produced instruments is so low that, even ignoring a large proportion of the overall problems, the situation can only be improved. Perhaps some day a more detailed analysis of the importance of transients will be carried out, but at this time only the most general questions should be addressed.

#### A Brief History of the Violin.

The origins of the violin have long been the subject of debate among scholars. It has been variously assumed to have evolved from the rebec, lute, viol, or crewth, but it seems most likely that viols and violins developed as two distinct families from these earlier examples of string instruments [1,2].

While nearly everyone is familiar with the violin, a viol is rarely seen today. It had a flat back, five, six, but occasionally more strings, and a very slightly arched belly of very thin wood, in other respects resembling a violin. The advantages which the violins enjoyed over the viols proved to be significant enough to lead to the complete disappearance of all but the bass viol until a recent revival in medieval and renaissance music.

Many luthiers (this term was formerly applied to lute makers but now is more universally applied to the makers of any stringed instruments) have been given the credit for developing the violin. Duiffopruggar (1514-1570), a Bavarian who became a nationalized Frenchman, has often been named as the originator of the violin. This is probably due to the violins made by Vuillaume which were thought by many to be copies of instruments by Duiffopruggar. They were in fact modelled on his viols, some of which exist today [2]. Gaspar da Salo (1540-1609), Andrea Amati (c1535-c1611), and Maggini of Brescia have

all been given credit, but while violins attributed to the first two named still exist, it is impossible to decide this question conclusively. What can be said, however, is that once created the violin evolved rapidly, with the names of the Amatis, the Guarnaeris, and Stradiverius, along with the school of their followers in Cremona, standing above all of the others. Aesthetics and tone were both valued by these luthiers, who with their undoubted genius in craftsmanship and musicianship made violins which are seldom equaled today. Perhaps their dominance in their field is unfortunate for us today, for many

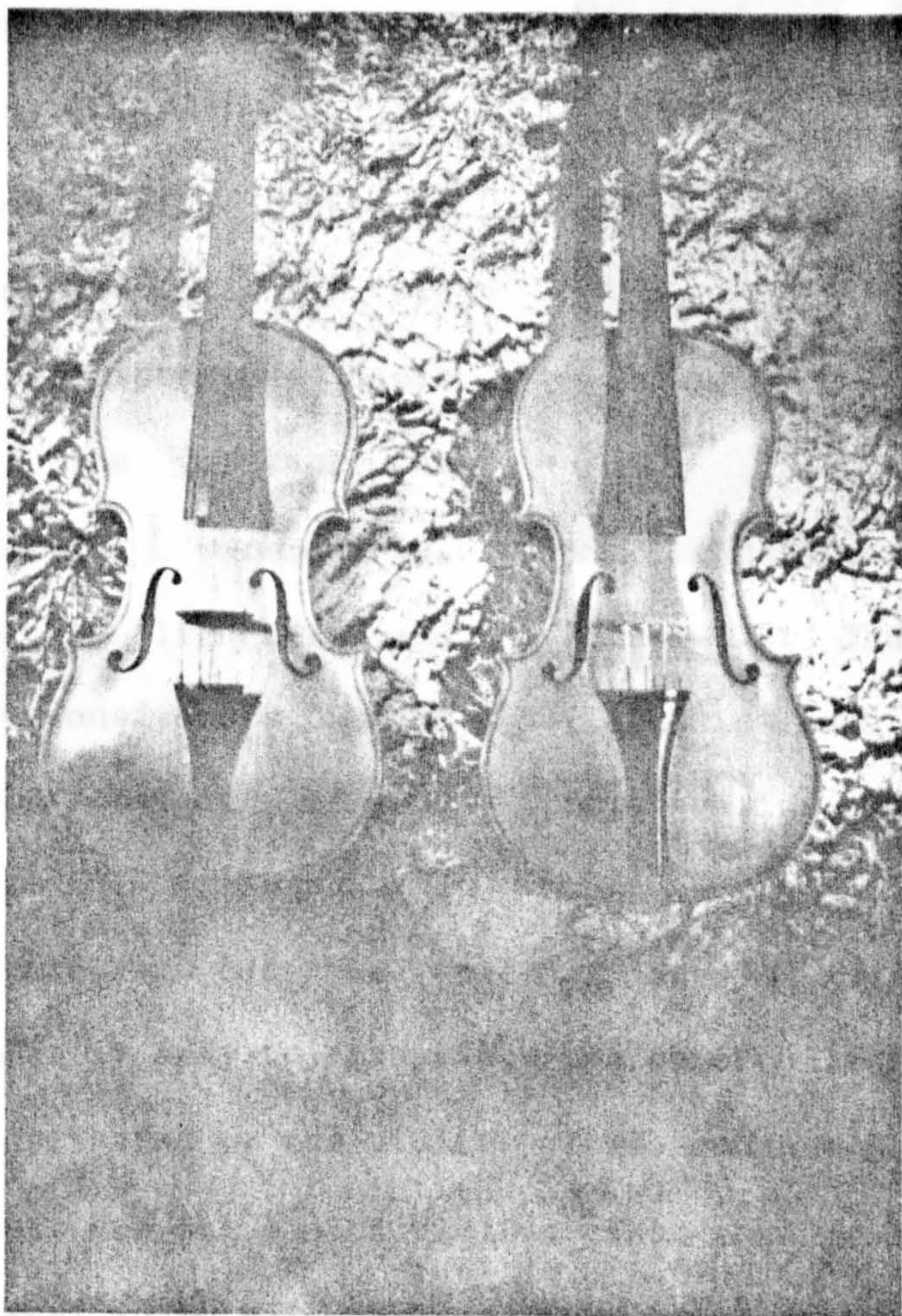


Figure 1.1: Modern copies of violins by Stradavarius (right) and Stainer (left). Note the differently shaped f-holes.

luthiers began to copy these great master's violins and originality and experimentation, which had so quickly developed the violin, were discarded. There were of course exceptions- the German school of violin-making, led by Jacob Stainer (1621-1683), produced instruments of exceptional beauty in both form and tone- but these and the old Italian violins were almost universally copied for many years.

Before beginning the investigation of the acoustics of the violin one should spare a few moments to look at the two violins which appear in figures 1.1 and 1.2, a few moments in which to appreciate the beauty of a well made violin. It is impossible to appreciate the depth of the varnish, the careful workmanship, or the lightness and responsiveness which characterize a good violin, in a

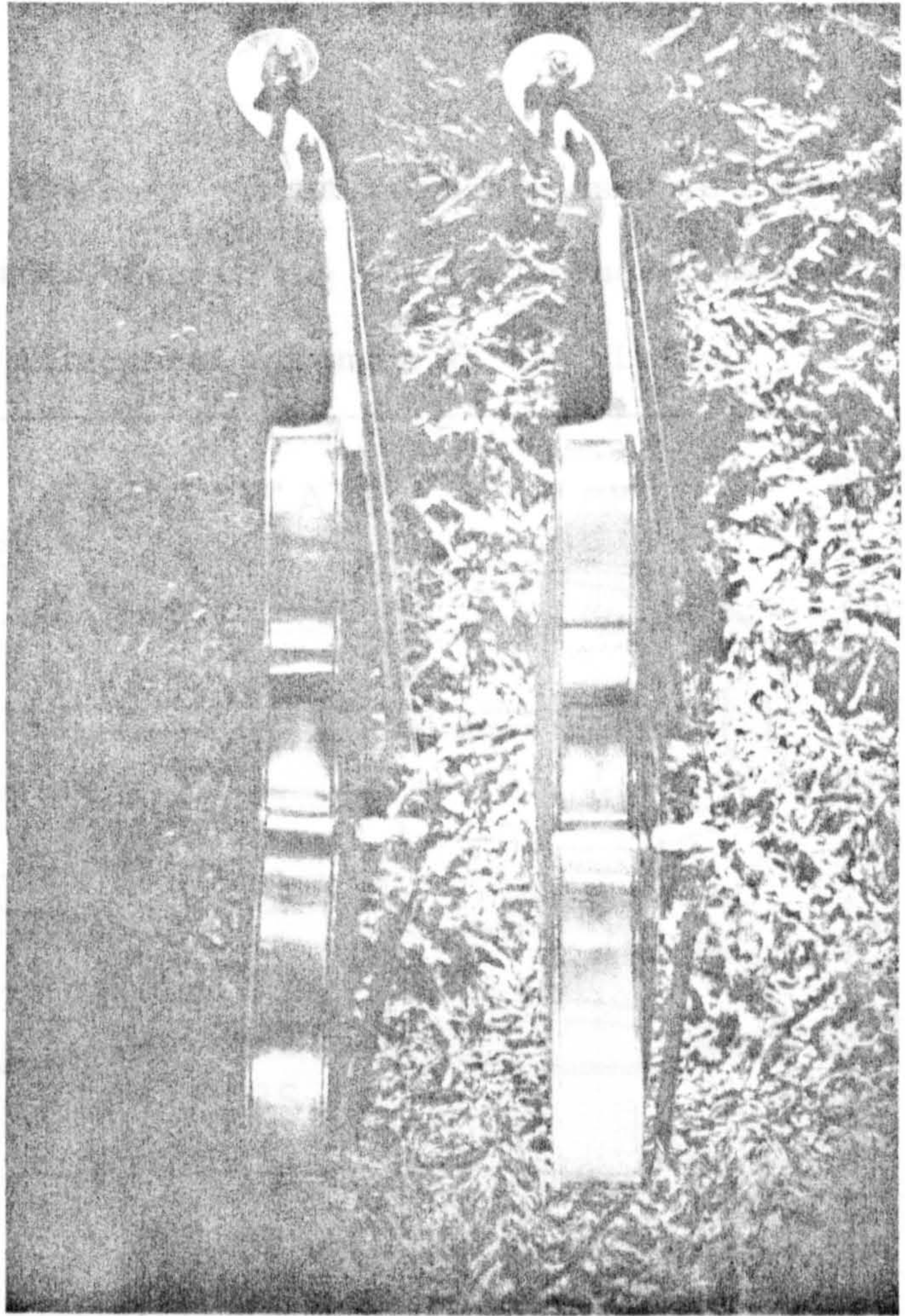


Figure 1.2: The arching of the Stainer copy (left) is much more abrupt than that of the Stradavarius copy (right).

photograph but the graceful arching and the beautifully marked wood make it easy to appreciate how some collectors who cannot even play are fascinated by the violin. This, and not its acoustic properties, often sets the price of a violin. That the genuine old Cremonese violins excel in both is the real reason for their demand.

Building the Violin.

Figure 1.3 illustrates the many pieces which are used to construct a violin. Most of the internal pieces, the blocks, corners, and rib-liners, are present to give structural strength to the violin

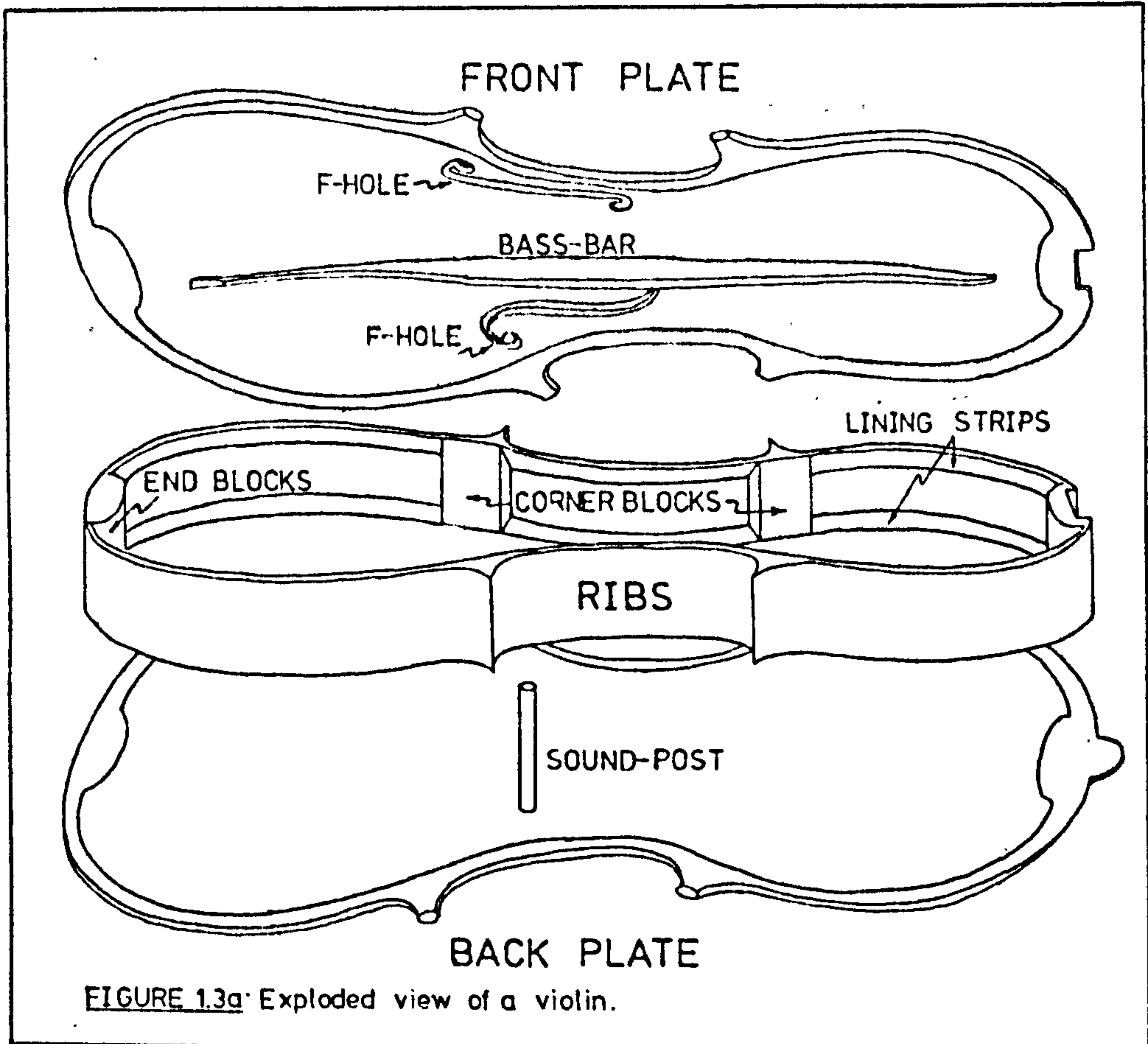


FIGURE 1.3a Exploded view of a violin.

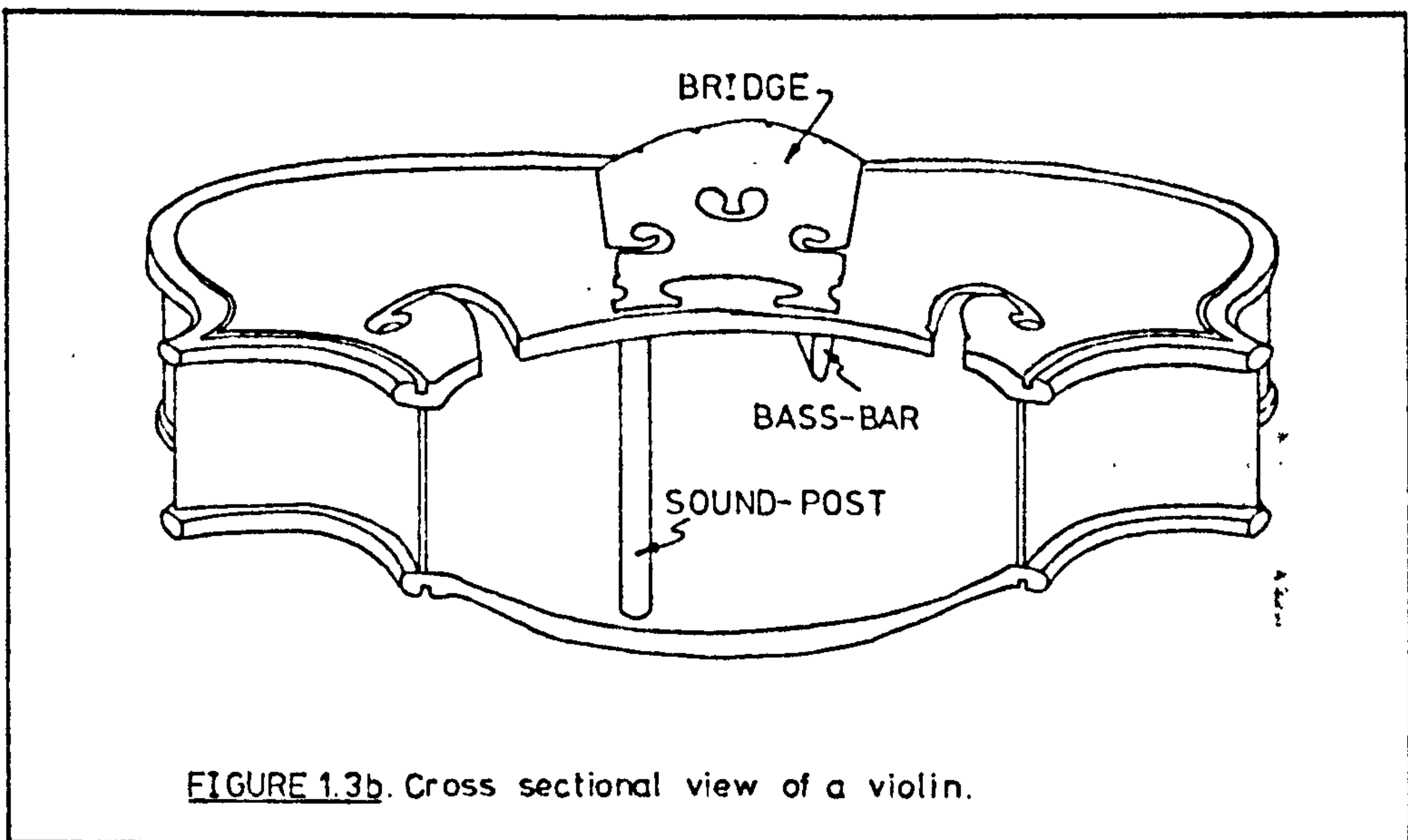


FIGURE 1.3b. Cross sectional view of a violin.

sound-box. The method of construction of the box is itself a fascinating story.

The luthier begins by constructing a set of ribs from strips of sycamore or maple, which he thins to about 1 mm. so that they may be easily bent. The ribs are built with the aid of a mould to which all of the pieces may be clamped and glued. When using an inside mould, such as that shown in figure 1.4, blocks of spruce are lightly glued to it and cut to shape. These pieces form the corners and end blocks of the violin and remain firmly glued to the ribs when they are removed from the mould.

Once the strips have been thinned they are cut into pieces to form the six sections, known as bouts, of the ribs. Starting with one of the C-shaped bouts, the luthier dips the strip of wood in water and then very slowly bends it over a hot, rounded



bending-iron until the piece fits snugly against the mould. The remaining pieces are then bent in the same way. Next the luthier rubs the mould with soap, being very careful not to coat the blocks, so that the glue will not stick to it.

Figure 1.4: A nearly complete set of ribs are held on an inside mould while the luthier traces their outline onto a maple slab.

A hot, organic glue is used to join the bouts together, with the blocks giving strength to the glue joints and clamps holding all of the pieces firmly in place. Some two to ten hours later the glue has hardened, but changes in its strength may occur over a much longer period.

The mould and ribs are constructed so that the latter project about 1 cm. above the surface of the mould. This is necessary so that a lining strip of spruce, about 2 mm. thick, and 7 mm. high, may be glued to the inside of the ribs. First, however, the ribs are cut so that from a height of 32 mm. at the lower block, they taper to 30 mm. at the top. This imperceptible slope is present in the great Italian violins and luthiers, ever mindful to copy these instruments exactly, perform this task without exception.

After the lining strips, which are used only to provide a wider glueing surface for the plates, have been bent and glued into place, they are reduced to a triangular section. This must be done after they have been installed for trying to bend a triangular sectioned strip of wood is an impossible task! Little notches in the blocks and corners secure the linings at their ends.

Carving the two plates is the most important step in making a violin. Much of the final sound and beauty depends on the luthier's skill in executing this task. The plates are often carved with the same arching so that the only major differences in their appearance are the wood used, the f-holes in the front, and the small projection at the top of the back, known as the tongue, which meets the neck. Maple or sycamore is used for the back and spruce for the front. Each plate may be made from a single piece of wood, or from two matching pieces. If two pieces are used for a plate then two adjacent, wedge-shaped slabs are cut, their thickest edges planed and are then glued together. In this way the marking in the wood appears nearly symmetric when the



Figure 1.5: Templates are used by the luthier to check the arching of the plates.

plate is finished. This also ensures that the narrowest part of the grain is at the center.

A tracing of the desired plate outline is next made on the slab, which is then shaped by saw, knife, and scraper. Then with the slab clamped to the working surface, the arching is begun using a curved gouge. Real skill is needed here for carrying away a single large splinter could spoil the work. Once the lengthwise arch has been

cut to match a template, the arch between the central bouts is cut and again matched to a template. After doing the same at the widest portion of the lower and upper bouts, a small plane is used to remove the gouge marks and to sink a shallow groove about 3 mm. from the edges in which the purfling will eventually be cut and set. These two operations bring important aesthetic and practical benefits. The wide groove allows the luthier to use a thick, strong edge without flawing the graceful arching of the thin plate. The purfling, usually consisting of three strips of wood, is set into a narrow groove and emphasizes the violin's shape. More importantly it stops any crack

from propagating from the plate's edge into the vibrating region. Scrapers and glass-paper are used to complete the outside surface of the plate.

Using a caliper to check the thickness, the plate is next hollowed out to its final thickness, which for the belly is about 3.5 mm. at the centre and 1.5 mm. at the edges. The back also varies in its thickness, from about 4mm. to 2 mm.

The front plate must finally have the f-holes cut and its bass bar fitted. Two drill holes and a sharp knife enable the luthier to cut the holes, while the bass-bar must be shaped so that it must be slightly bent in order to be glued in place inside the plate. This done, the belly is placed on the unlined edge of the ribs and a couple of small holes drilled through it into the blocks. These are located where the purfling groove will later be cut, and serve as locating points into which small pegs are stuck. The ribs are removed from the mould, the other set of rib liners glued in place, and then the belly glued on with the pegs in place to keep the ribs from warping. After this the back is attached, the purfling cut, the edges rounded, and the violin body is complete except for varnish. The fashioning of the neck is of little concern here, for although it provides the craftsman with an opportunity to demonstrate his skill in carving the beautiful scroll, it is of no consequence to the violin's acoustics.

Varnishing provides the luthier with another chance to show his expertise, for a well applied oil-varnish enhances and colours the wood, besides providing it with a protective coating which will withstand centuries of use. Spirit varnishes are also used because of the ease with which they may be applied, but these lack the beautiful qualities of the oil varnishes. Despite the claims of countless people the varnish used by the Italian masters was not the secret of their

success, for although the varnish does affect the violin, particularly its damping, the effects are of minor importance when compared with the frequency response and the normal modes of the plates [3].

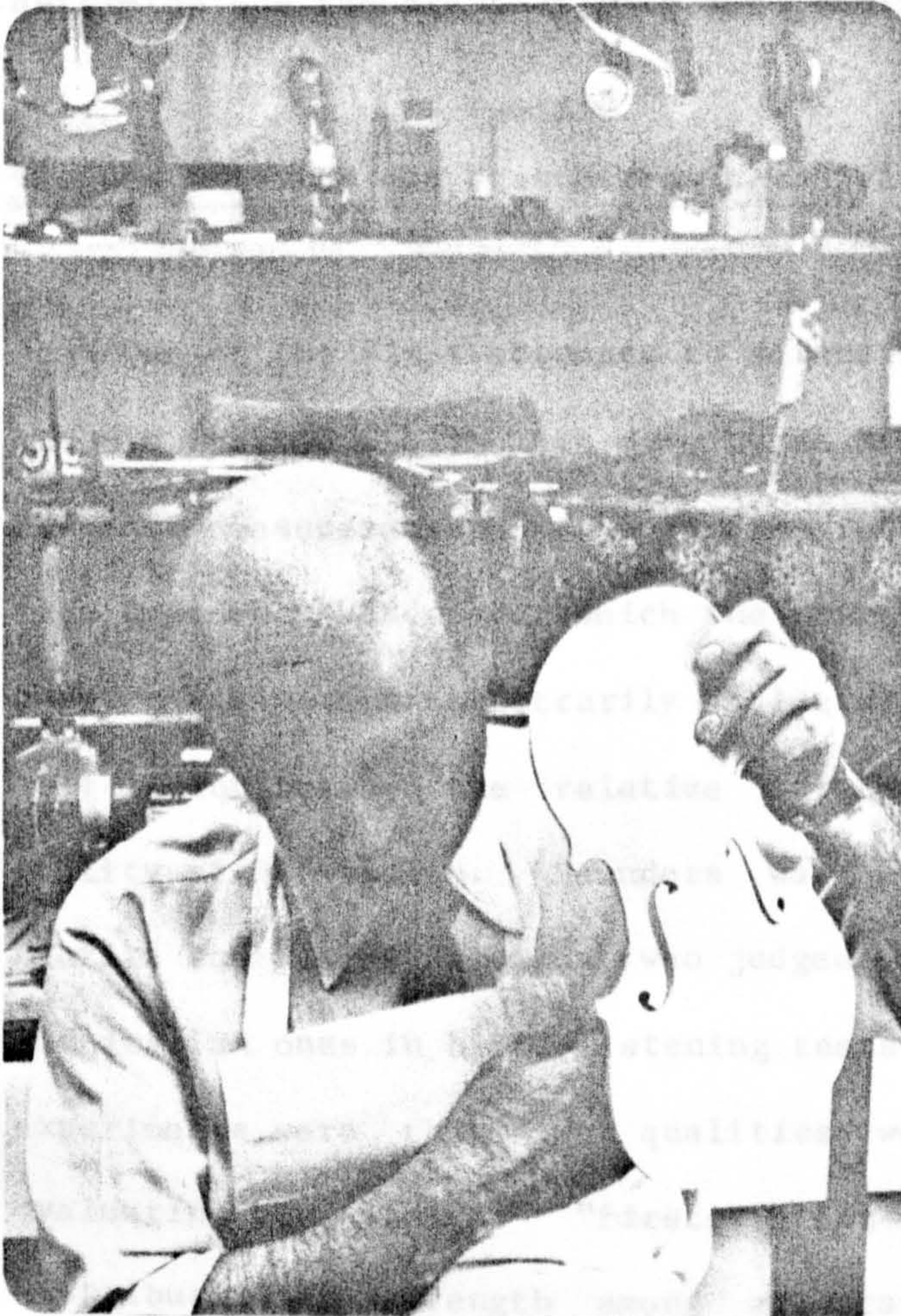


Figure 1.6: Tap tones make it possible to compensate for the individuality of wooden plates by tuning the lowest resonance to a specific pitch.

Today many violin-makers employ tap-tones to help obtain the best possible sound from their instruments. When making the final adjustments of the plate thickness they hold a plate loosely between thumb and finger, about  $4/5$  of the way along the plate length, and rap it sharply with a knuckle as demonstrated in figure 1.6. This excites many modes of vibration and by carving as little as 0.1 mm. of wood from a few square centimetres of the plate, they may be altered perceptibly [4]. Many luthiers adjust their plates until the predominant mode has a pitch of D# for the back, and D for the front plate. This seems to give good results in most cases.

The use of tap tones is perhaps the most important aspect of violin making to which scientific method has been applied. It is by no

means the only one. Most of the important work in this field is utilized in subsequent chapters, but before it is possible to build on this work to improve mass-produced instruments it is necessary to determine the factors that make some violins universally admired.

### The Best Violins and What Makes Them Different.

One of the first attempts to scientifically explain the esteem of the old Italian violins was made by F. Saunders [5]. He made frequency response measurements of many fine instruments, both old and new, in five frequency bands over which the response was averaged. Although these ranges were arbitrarily selected as in table 1.1, he found a correlation between the relative strength of these bands and the quality of a violin. Saunders was assisted in this work by Jascha Hiefitz and Sascha Jacobson, who judged many modern instruments against old Italian ones in blind listening tests. His conclusions from these experiments were that two qualities were of prime importance when evaluating the violin: "first, great power, second, an even distribution of strength among all ranges of frequency, the lowest octave being of special importance" [5]. Another point which he makes is of historic interest:

"Many violins, including two or three of the seven Strads for which we have curves... show a weakness in the range 1300 to 1800 or 2000 cps., amounting to a drop of 4 to 8 dB. This appears... to have no important effect on the reputation of the violins concerned."

Subsequent research has revealed the irony of this statement.

Other attempts at evaluating the violin by a small number of frequency bands have been made, notably by Lottermoser and Meyer [6], who used seven bands, and by Meinel [7], who averaged the frequency response over spectral fifths. These experiments shared the same

disadvantage as did Saunders' tests: the bands were too coarse, and important features were lost among other information in a band. This explains how the weakness which Saunders noted in many good violin's response curves failed to correlate with the quality of the violin. More recent work has shown that this feature is of the highest importance in determining the sound quality of a violin! [8,9].

These early researchers did not ignore the question of transient response. Meinel postulated that as the transient response of the highest resonances is fast, these should have as low an output as possible so that the bowed string articulates well [10]. Saunders made measurements of the logarithmic decrement for various violin modes but concluded that there is no general correlation between this and sound quality [5]. Recent work has concentrated on the importance of the frequency response.

Yankovskii used third octave bands to record the response of many violins and tried to correlate some of the subjective terms which violinists use to describe their instruments with the average response in certain bands [8]. In order to make these tests as meaningful as possible six judges were required to describe many violins with nine subjective terms. All of the instruments were played twice, in a different order, and only those which received the same subjective term from every judge were used in the experiment. The response of a violin to which a subjective description had been unanimously applied was then compared to that of the average for the entire group and the differences related to subjective terms. A list of these appears below in table 1.2.

The most important conclusions about violin frequency response are those arising from a study by Garielsson and Jansson in which "Long time averaged spectra" (LTAS) were used to rate the qualities of

Experimenter	Bands	Frequency range	Remarks
Saunders	5	196-	Arbitrarily selected.
Lottemoser et al	7		Chosen to correspond to vowel formants of U, O, A, E, I, the sibilant S, and the second nasal formant.
Meinel	10	194-12K	Spectral fifths.
Yankowski	17	180- 9K	1/3 Octave bands.
Jansson	24	<180->10K	The Bark frequency scale.

Table 1.1: The frequency bands used by early researchers to describe the quality of violins.

violins [9].

In this process whole tone scales were played over three octaves on each violin as loudly as possible. The results were averaged in twenty-two bands from about 100 Hz. to 9.5 kHz. over a long period of time. By comparing the LTAS of twenty-two good violins which had been judged in a violin-making competition they found a very good correlation between the response in seven of these bands and the rated quality of the violin. The frequency bands of greatest importance proved to be similar to those found by their predecessors, but with a greater accuracy and in a definite order of importance.

The most important characteristics which appeared in their tests were: a high response up to 500 Hz., low response around 1.3 kHz., rising quickly to 2 kHz., and then a rapid drop above 4kHz. The authors point out that the judging of the violins was done by only two men and may not have been of a representative group of violins, but their findings are still of great significance.

The goals are now clear and the work may progress. It will shortly be demonstrated that the bridge is primarily responsible for

Subjective term	Characteristic frequency response
Soprano	Bands at 250, 500, 800, and 1250 show strong response with the 1250 Hz. band dominant. The best violins fall in this category.
Bright	High output between 2500 and 4000 Hz.
Noble, soft	Body resonance in 500 Hz. band strongest.
Nasal	Frequencies from 1.2 to 2KHz. cause this irritating tone quality.
Tight, thin	Relatively uniform response between 500 and 6300 Hz. when averaged over 1/3 octave bands.
Piercing	Any radiation above 4KHz. may cause this.
Treble, shrill	Little radiation below 500 Hz.
Contralto	The lowest band has a relatively high level.

Table 1.2: The subjective terms studied by Yankowskii and the physical interpretation of these terms.

the production of sound at frequencies above about 1.5 kHz., so it is the lowest of the frequency ranges just described which will yield the greatest results. As more information about the violin and its unique design come to light, understanding will not dull the awe, nor remove the mystery, which envelope this amazing creation of man's genius some 400 years ago.

- [1] Sheila Nelson, The Violin and Viola, Ernest Bean Ltd., London, (1972).
- [2] Alberto Bachman, An Encyclopedia of the Violin, reprinted in English, Da Capo Press, New York, (1965).
- [3] John Schelleng, "The acoustical effects of violin varnish", JASA, vol. 44, pp. 1175-1183, (1968).
- [4] M. McIntyre and J. Woodhouse, "The acoustics of stringed musical instruments", Interdisciplinary Science Reviews, vol. 3, no. 2, (1978).
- [5] F. Saunders, "The mechanical action of instruments of the violin family", JASA, vol. 17, p. 169, (1946).
- [6] W. Lottemoser and E. Meyer, "Resonanzen von Gergendecker und Boden", Z. Instrumentebau, vol. 13, no. 7, pp. 185-189, (1959).
- [7] H. Meinel, "Scientific principles of violin construction", reported in Soviet Physics: Acoustics, vol. 6, pp. 149-161, (1960).
- [8] B. Yankovskii, "Objective appraisal of violin tone quality", Soviet Physics: Acoustics, vol. 11, pp. 231-245, (1966).
- [9] A. Gabrielsson and E. Jansson, "Long-time average-spectra and rated qualities of twenty-two violins", Acustica, vol. 42, pp. 47-55, (1979).
- [10] H. Meinel, "Regarding the sound quality of violins and a scientific basis for violin construction", JASA, vol. 29, pp. 817-822, (1957).

Measuring the Frequency Response.

Measuring the frequency response of a violin can be surprisingly difficult. Ideally the method employed would be quick, reproducible, and reflect the way in which the violin is held. The problems of excitation, instrumentation, and mounting a violin for study in an anechoic chamber will be discussed briefly below.

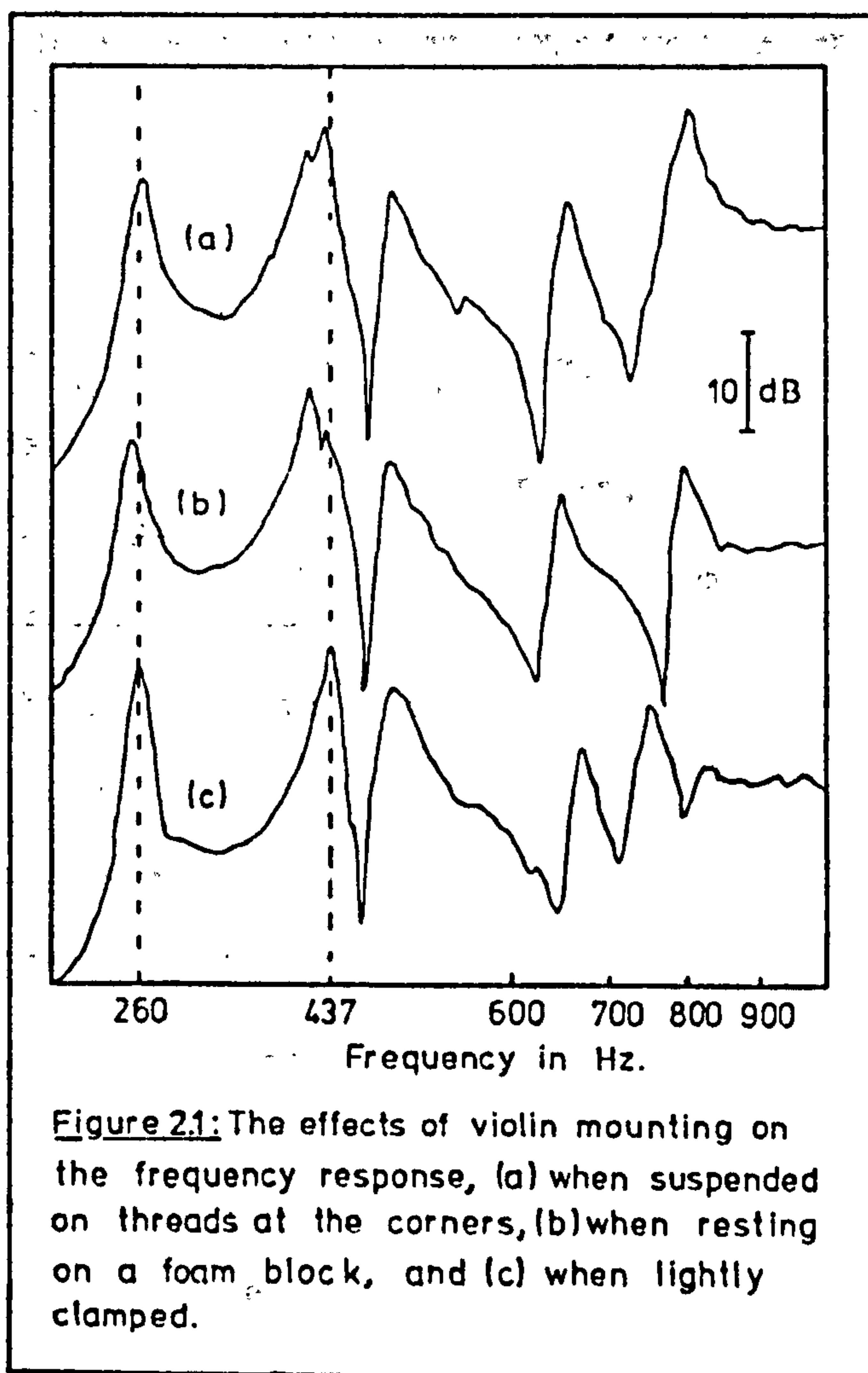
Most experimenters have used some form of bowed excitation, either mechanical or by hand. Mechanical bowing, by a swinging pendulum or a rotating wheel, is inherently reproducible but the construction of such a device is difficult. By contrast, hand bowing requires only a practiced hand and a good ear to produce surprisingly consistent results. It is the behavior of the bowed string and the nearly constant limit in bowing force, as first shown by C. V. Raman, which makes this possible [1]. He showed that, if the bow's speed and its position on the string are held constant, exceeding a certain force between the bow and string destroys the oscillating regime. A raucous, unpleasant sound is produced which the musician instinctively avoids. This limit is very important for, although the frequency content and amplitude of the string depend on all of these factors, the bowing force is the most difficult for the musician to control. Saunders, who was one of the first to employ this method to study the violin's response, demonstrated the remarkable degree to which such results may be reproduced [2]. Since that time the "equal loudness curves", as response measurements made in this way have become known, have been used in most experiments.

Loudness against pitch, rather than the frequency response, is measured when some form of bowed excitation is used to drive the violin. This is essentially what one hears when a violin is played for

each pitch is a combination of partials, each of which contributes to the loudness, rather than a pure tone. While such measurements are useful in many circumstances, they obscure much of the frequency information making it difficult to isolate the resonant frequency of individual modes. Also, by its nature, the "equal loudness curve" must be plotted at discreet frequency intervals, usually a semitone apart. This spacing is wide enough so that, even with the provision of a tracking filter to obtain a true frequency response, details such as the split which sometimes occurs in the Helmholtz resonance may be missed. Although these details are probably of no real significance in the tone quality of a violin they may help one to gain valuable insights into the violin's action.

Mechanical excitation of the violin bridge avoids these problems. In most cases the strings have been left in place when measuring the frequency response in this way, but throughout this thesis the strings have been removed during testing. This eliminates spurious resonances which occur when the driving frequency is that of a string mode, for even when the strings are heavily damped they still affect the frequency response curve. The presence of strings and bridge, and an assembly for driving them, also obscures a large portion of the belly, a problem when making holograms.

In order to measure the violin's response, force was applied to the violin body by an electro-magnetic transducer, B&K type MM0002, which drove a small metallic disk with a high magnetic permeability. As its mass was only 0.3 gm. the disc had a very minor effect on the violin's mode shapes and resonance frequencies. The transducer mount, and that of the violin itself, had a marked effect on the frequency response curve. Other workers have been beset by similar problems which have prompted an effort to standardize mounting techniques [3]. Figure 2.1



shows the degree to which the results may be affected. In obtaining these response curves the same violin was mounted in three different manners: suspended on threads at the corners; resting freely on a foam block; and loosely clamped in a frame which also supported the transducer mounting. With the first two methods the transducer was fixed to an adjustable cantilever.

The measurements took place one after the other with no detectable change in either the temperature, pressure, or humidity, so that it is only the form of mounting which is responsible for the large discrepancies which the curves display.

In two of these response curves the second resonance appears to form a double peak which is caused by the interaction of the violin-plate and the transducer mounting. As a lengthy cantilever was required to support the transducer in the anechoic test chamber it proved to be impossible to eliminate this doublet. Even with the transducer mounted upon a framework in which the violin was clamped, great care was needed to prevent its influencing the violin's frequency response, as figures 2.2 and 2.3 demonstrate.

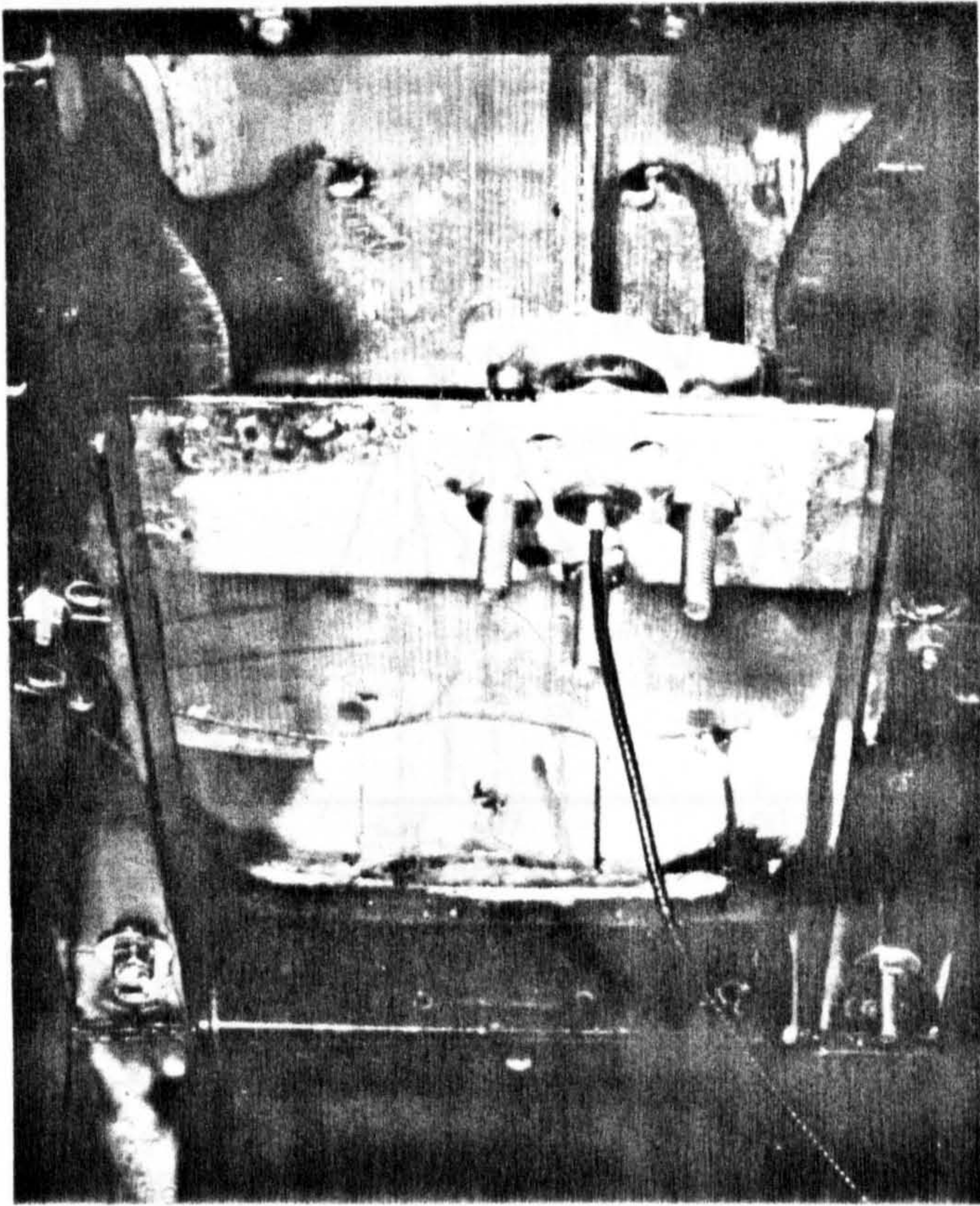
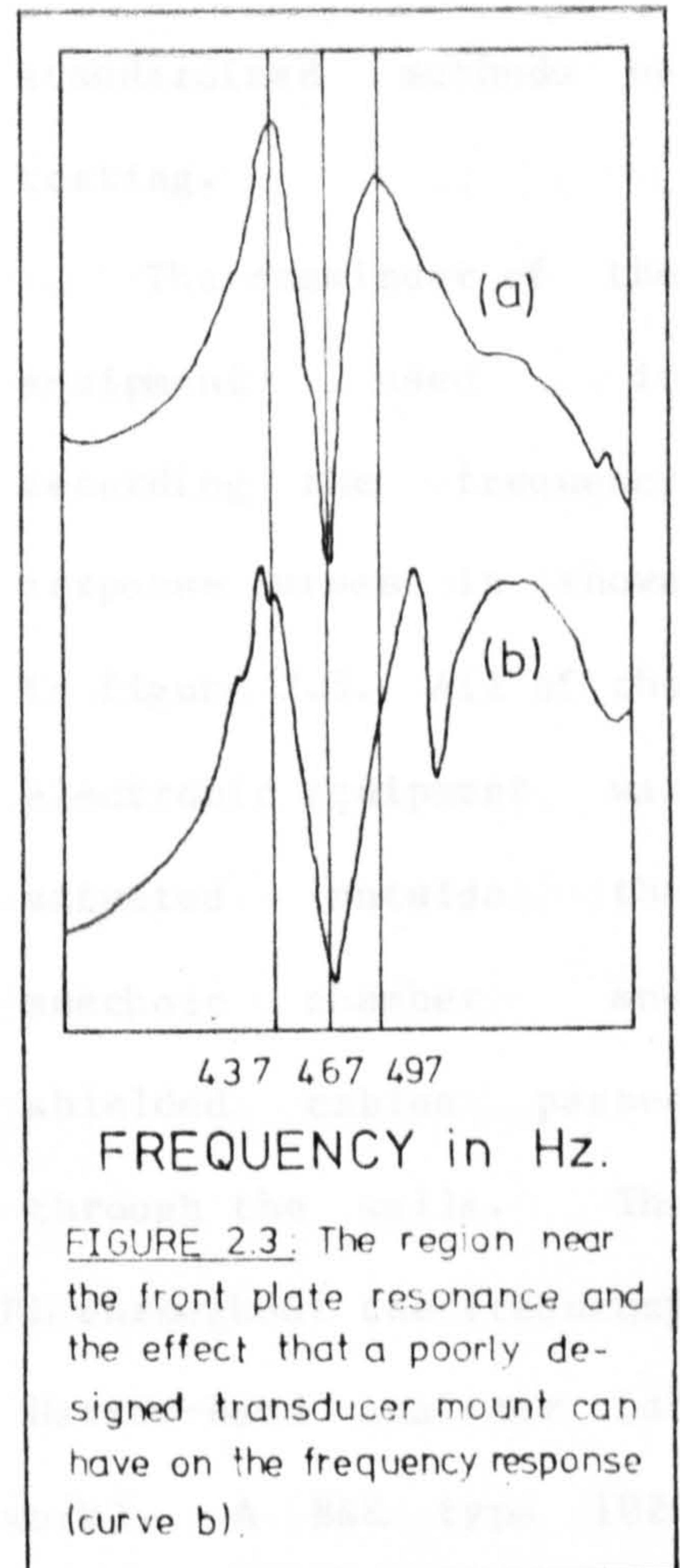
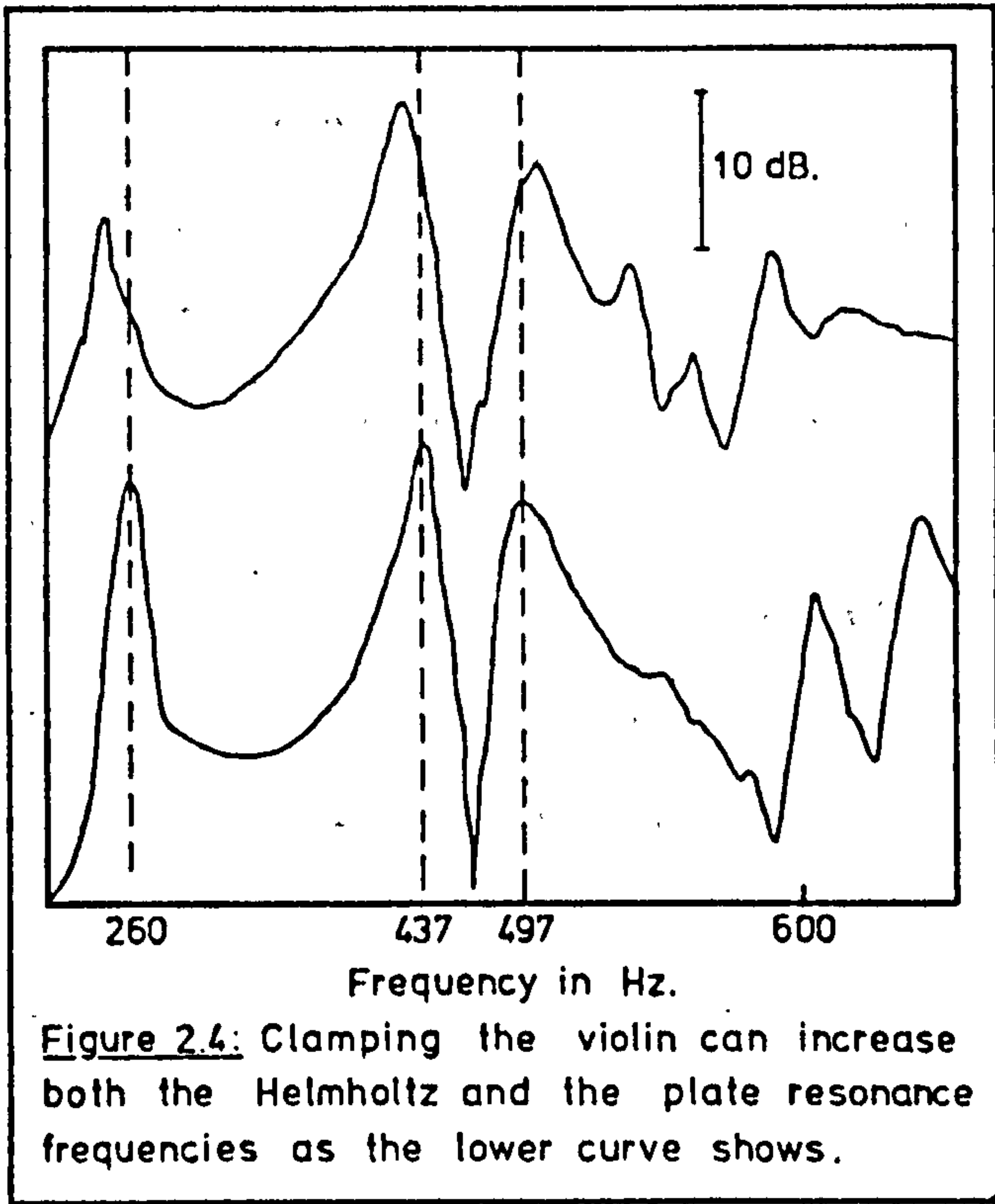


Figure 2.2: The violin front plate and the mounted transducer for driving it.



The clamping of the violin within the framework could also affect its response. Clamping all four corners often introduced a distortion of the violin body which drastically altered its resonance frequencies, as shown in figure 2.4. Light clamping of only three corners eliminated this problem.

The frame for mounting the violin and transducer was used throughout this work as it proved to be the simplest method of eliminating the interaction between the transducer mounting and the violin. It had an additional advantage in that the entire assembly could be quickly and easily transferred to the holography laboratory and used to secure both the violin and transducer to the anti-vibration table in this facility. Overall this system demonstrated its



superiority over the standardized methods of testing.

The remainder of the equipment used in recording the frequency response curves is shown in figure 2.5. All of the electronic equipment was situated outside the anechoic chamber and shielded cables passed through the walls. The

noise floor was typically -5 to -10 dB SPL throughout the frequency range of interest when measured on the Narrow-Band analyzer (dB re.  $2 \times 10^{-5}$  Pa. are used throughout this work). A B&K type 1024 sine-random generator was used to drive the transducer, whose impedance was constant throughout the frequency range. Either a white noise or single frequency sinusoid could be used as an input with this instrument.

A single high-sensitivity microphone, B&K type 4165, was used to pick up the

acoustic output.

The signal was

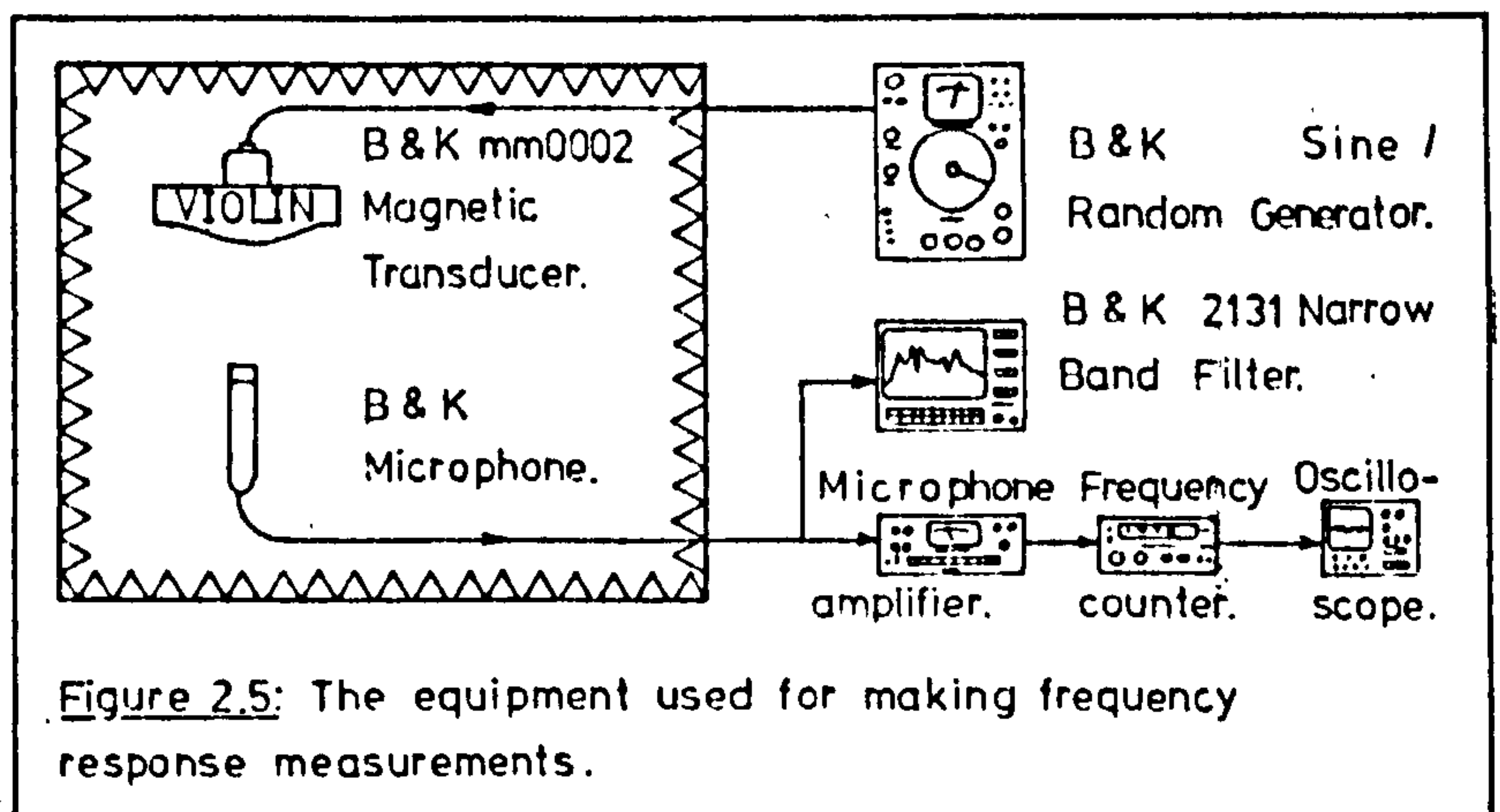
processed in

either a B&K

type 2610

measuring amp-

lifier or a B&K



2131 narrow-band analyzer.

A white noise input was generally used to record a frequency response and the narrow-band analyzer was used for averaging and displaying the signal. As the response was usually required from 190 to 600 Hz. the analyzer was used in the 0 to 1 kHz. mode. Linear averaging was used exclusively. The 400 line linear frequency display then gave excellent definition with only a 2.5 Hz. band-width. On those occasions when a wider response was measured, the 0 to 5 kHz. range was selected. As this instrument is sensitive to frequencies virtually down to D.C., low frequency noise often appears in the response curves, although it was possible to measure the noise first, store it in memory, and then subtract it from any subsequent measurement within the machine.

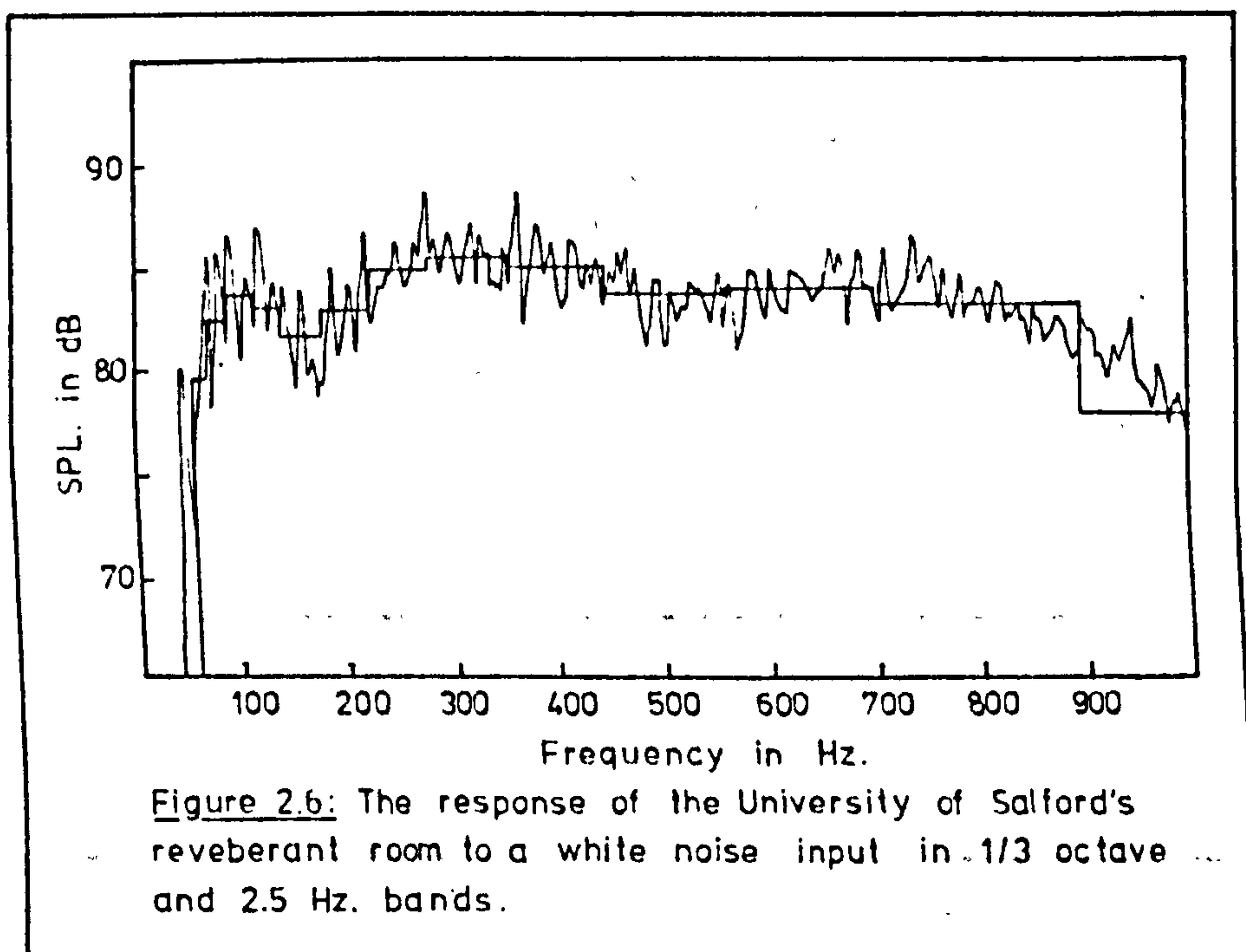
The acoustic output of the violin was often measured at less than 10 dB SPL at certain frequencies and so outside sources of noise could noticeably affect the response even when the triple set of doors which led to the anechoic room were sealed. A long averaging time was therefore used to minimize any such effects, 2048 samples over about five minutes being common.

The Hanning window was used exclusively during experiments as it minimized the problems associated with digital sampling (the linear window should only be used when recording transients). If a small number of wavelengths are recorded in the sample then any frequency component that does not have a whole number of wavelengths in the signal can greatly change the Fourier transform. A Hanning window uses a weighting function to minimize the importance of the beginning and ending of a sample thereby eliminating this problem.

Once a response curve had been recorded it was possible to output it to a level recorder or an x-y plotter.

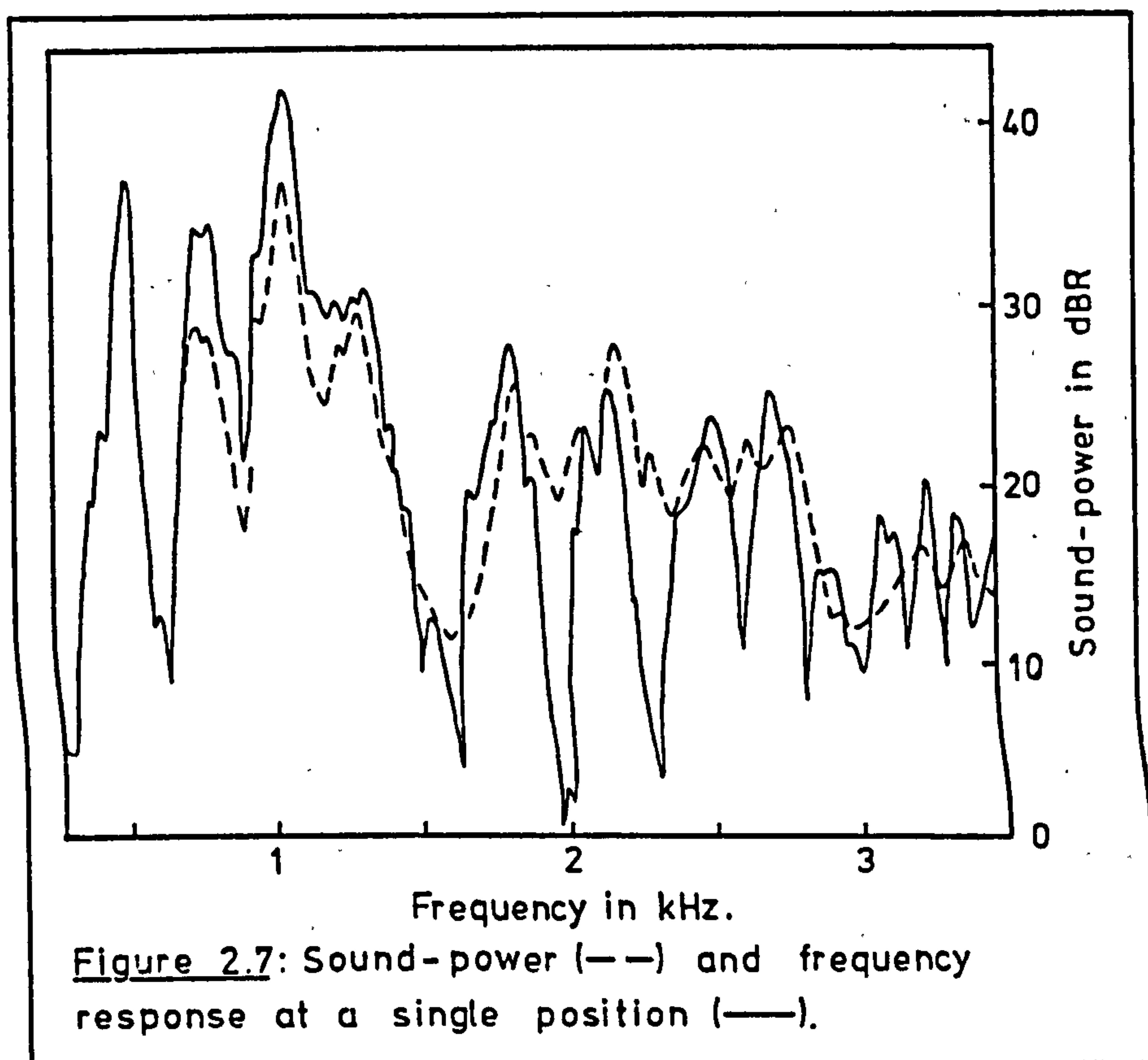
Another useful feature of the narrow-band analyzer was its ability to stop after a number of samples, and continue averaging again after an indefinite interruption. This made it much easier to perform sound-power measurements.

Early in the experimental work the method of measuring the response, whether it should be made in an anechoic or reverberant chamber, and whether sound-power or a single position frequency response should be used, were the subjects of much debate. Figure 2.6 shows the multitude of resonances which occur in the reverberant room at the University of Salford's Department of Applied Acoustics. Although these resonances are so narrow that they do not affect third octave bands in the frequency range covered by a violin they make it impossible to obtain meaningful response curves.



A series of sound-power tests were made to see if the violin's directionality was important at frequencies as low as 600 Hz. Seventeen microphone positions were used at a distance of one meter from the center of the belly, in the hemisphere into which it would

radiate if mounted in a baffle. A frequency response curve was then made using a single microphone position, one meter on the axis normal to the center of the belly. Comparison of the two curves in figure 2.7 shows that, although directionality greatly influences the readings taken at high frequencies, in the range of interest it was not necessary to make sound-power measurements. Of course, the shape of a radiator whose dimensions are less than a quarter wavelength of sound in air does not greatly affect the radiation pattern, but experimental confirmation of this was deemed necessary. Single position frequency response measurements are used throughout this thesis.



Once a frequency response curve had been recorded, the resonant frequencies and half-power points were determined using the sinusoidal output of the generator and the measuring amplifier, frequency counter, and oscilloscope. The amplifier had a 22.5 Hz. high-pass filter which made it possible to obtain a steady position on the meter. Noise was much greater in these instruments than in the analyzer, typically 10 dB

SPL, but as this equipment was only used to measure resonances it caused no difficulties.

Measurements of the resonance frequencies were accurate to within about 0.5 Hz, the error involved mostly due to the difficulty in locating the maximum which has a slope approaching zero at the peak. It was much more difficult to obtain the Q-factor accurately for the output of the sine-random generator varied as much as one dB while trying to locate the 3-dB-down points. Averaging a large number of tests produced figures for Q accurate to about 5%.

Results obtained from the techniques described above were generally reproducible, although with no control over atmospheric conditions some variations occasionally occurred. The method of mounting the violin made it possible to make an accurate and rapid measurement of the frequency response and then to move it to the holography laboratory to study the behavior of individual modes of vibration.

### Holography

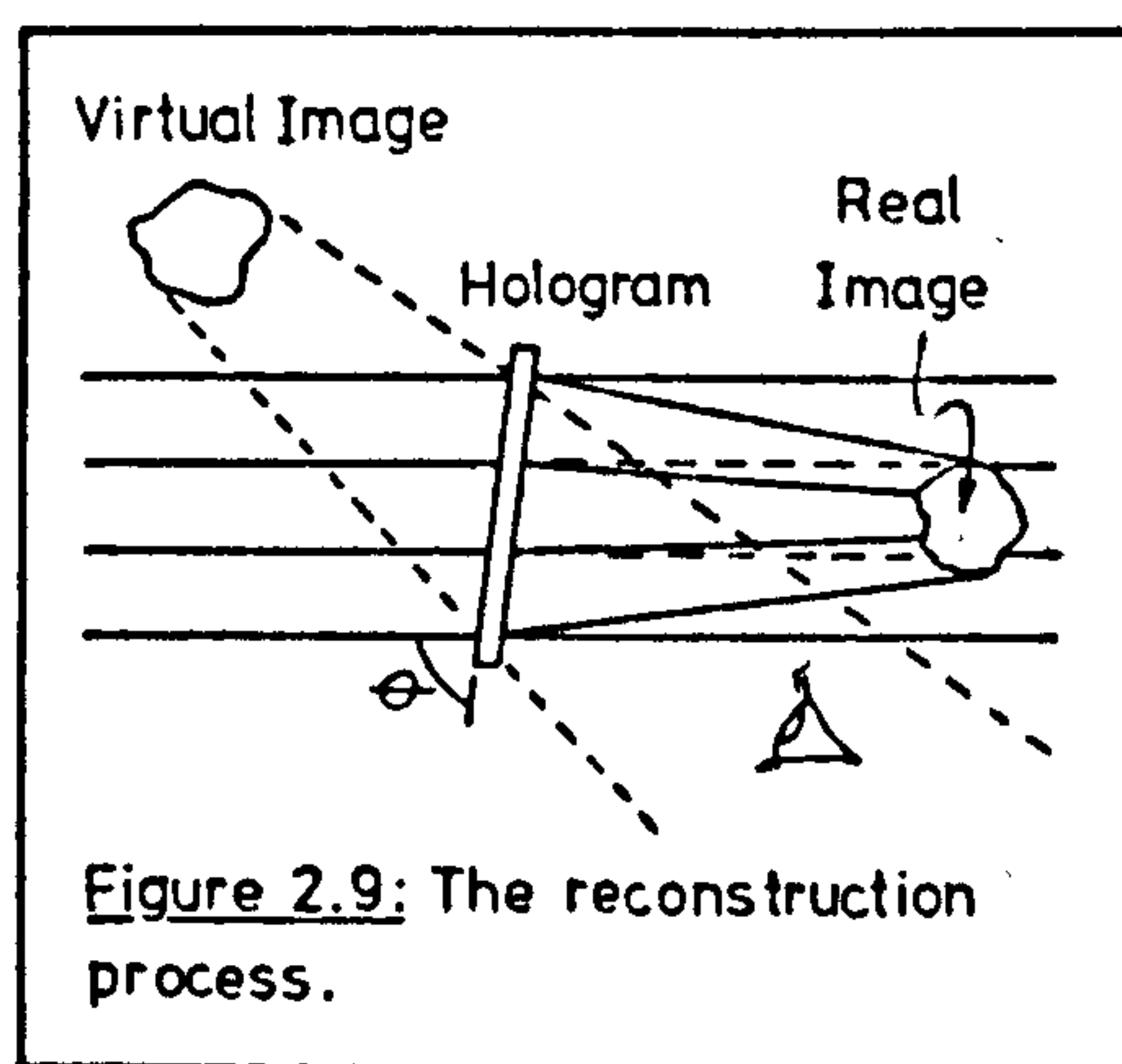
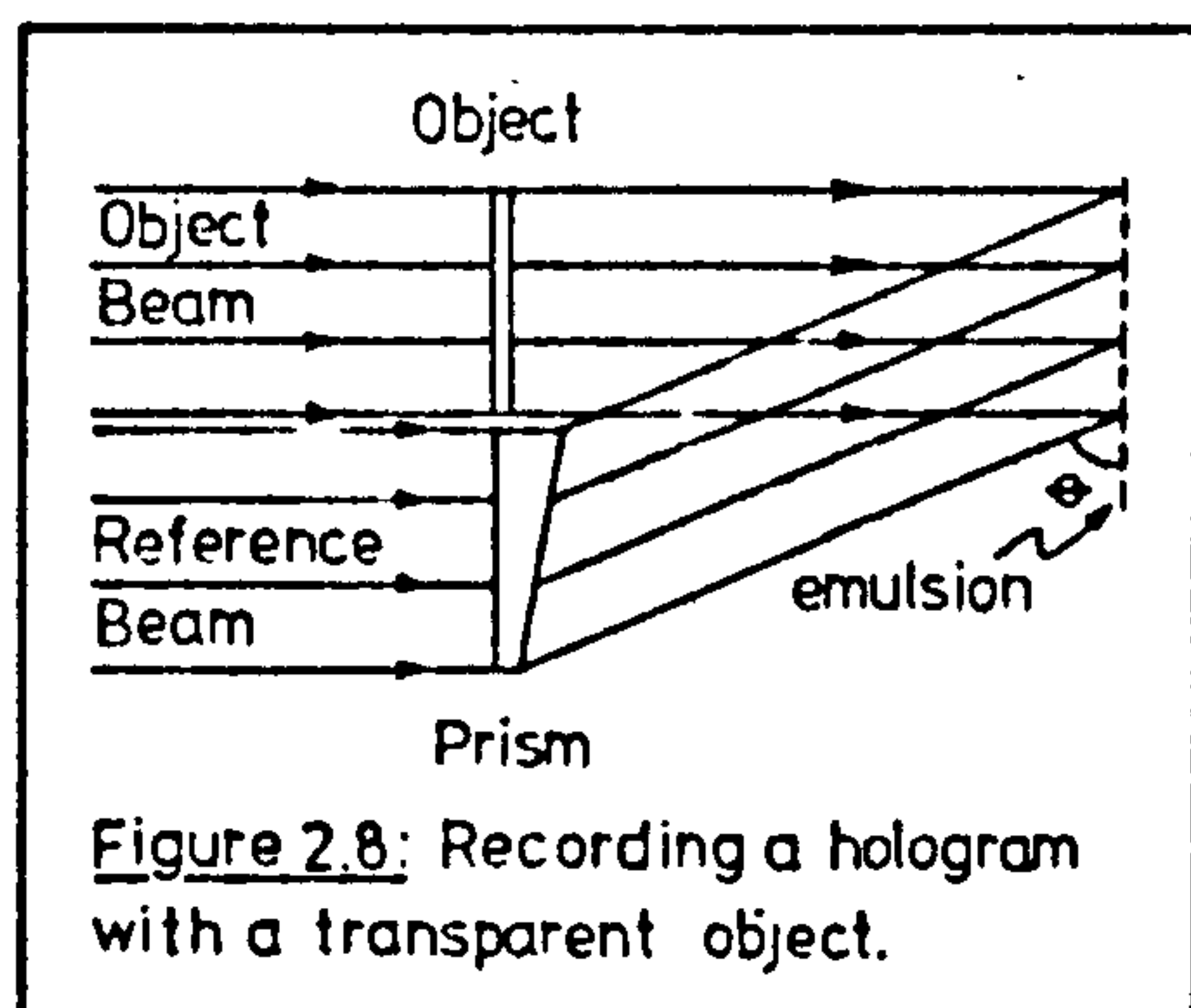
Holography has proven to be a useful tool for investigating the vibrations of stringed musical instruments. In modelling the violin it was found necessary to know precisely the mode shapes and the plate velocity distribution, and although the former could be deduced from Chladni patterns it was vibration holography that made the latter possible. The first investigation using this method was conducted by Reinicke and Cremer who studied the modes of vibration of violins [4]. A similar study by Gabrielson and Jansson established this technique as a valuable tool for the acoustician [5]. It is described in some detail below.

Although the holographic process was envisaged by Gabor as early as 1947, it was not successfully employed until after the laser had been developed [6]. It was the special properties of a laser beam, a coherent, single frequency beam of light, which proved to be the breakthrough that made holography possible.

There are many types of laser in use, but the most common is the helium-neon gas type, which produces a continuous beam with a wavelength of 633 nm. An electric discharge starts the beam by exciting the electrons of the neon atoms to a higher energy level. When these electrons fall to their normal level they release a photon with one of the three wavelengths characteristic of neon. Only the 633 nm. wavelength is in the visible range. The population of excited neon atoms is initially very high and many photons are released. When one of these photons collides with an excited atom, it too releases a photon. Only a small current is necessary to sustain the process once lasing has begun, just enough to maintain a large proportion of excited electrons in the discharge tube.

The discharge tube in which this occurs has mirrors at each end which are arranged so that light travelling along the axis with a wavelength of 633 nm. will form a standing wave. A small portion of this beam, which must necessarily be of uniform phase and non-diverging to form the standing wave, is allowed to escape through a partially silvered mirror. If, however, the number of photons in the tube is allowed to decline below a certain level the process cannot sustain itself and the lasing action ceases. This limits the light intensity of the laser beam to a small fraction of that in the tube, typically 1 to 2%. It is the stimulated emission of a photon which occurs when an atom with a high-level electron is hit by another photon that gives the laser its name- Light Amplification by Stimulated Emission Radiation.

A hologram is a type of photographic emulsion in which both the amplitude and phase information of light from an object are recorded. In ordinary photographs the phase information is lost, but by allowing a second beam of light to interfere with the light from the object, a series of fringes occur which, when recorded in some form, retain all of the information about the object. If these fringes have been recorded on a photographic plate one needs only to develop and fix it,



and then to insert it once more into the reference beam to reconstruct the original object. It will appear behind the plate and retains perspective so that the image may be viewed in three dimensions from different angles.

The theory which describes both the formation and reconstruction of holograms may be simply explained with reference to figures 2.8 and 2.9.

The light distribution upon the photographic emulsion from the object (this will be referred to as the object beam) may be expressed as

$$(2.1) \quad S(\hat{r}) = S_0(\hat{r}) \exp[j\omega t + j\phi(\hat{r})]$$

where  $\hat{r}$  is the position vector  $x\hat{i} + y\hat{j}$  and lies in the plane of the plate, and where  $S_0(\hat{r})$  and  $\exp[j\omega t + j\phi(\hat{r})]$  represent the amplitude and phase along the surface of an infinitesimally thin emulsion.

The reference beam, which is simply a diverged and collimated

laser beam which retains its coherence, may also be represented in the general form of equation (2.1). This gives

$$(2.2) \quad R(\hat{r}) = R_0 \exp[j\omega t + j(2\pi/\lambda) \cos \theta],$$

where the term  $\exp[j(2\pi/\lambda) \cos \theta]$  accounts for the longer path length produced by the angle  $\theta$ .

The photographic emulsion will respond to the intensity of light which irradiates it and so the term  $[S(\hat{r}) + R(\hat{r})]^2$  must be integrated over a large number of periods. As the number of periods approaches infinity, this gives

$$(2.3) \quad I(\hat{r}) = S_0^2(\hat{r}) + R_0^2 + RS^*(\hat{r}) + R^*S(\hat{r}),$$

where  $*$  denotes a complex conjugate.

Once the emulsion has been developed fringes will appear, whose optical density, and therefore transmission of light, will depend upon the intensity  $I(\hat{r})$  with which it was exposed. A properly developed film will then transmit a beam which is directly proportional to the intensity distribution produced by the interference of the two beams and  $T(\hat{r})$ , the transmitted beam, is

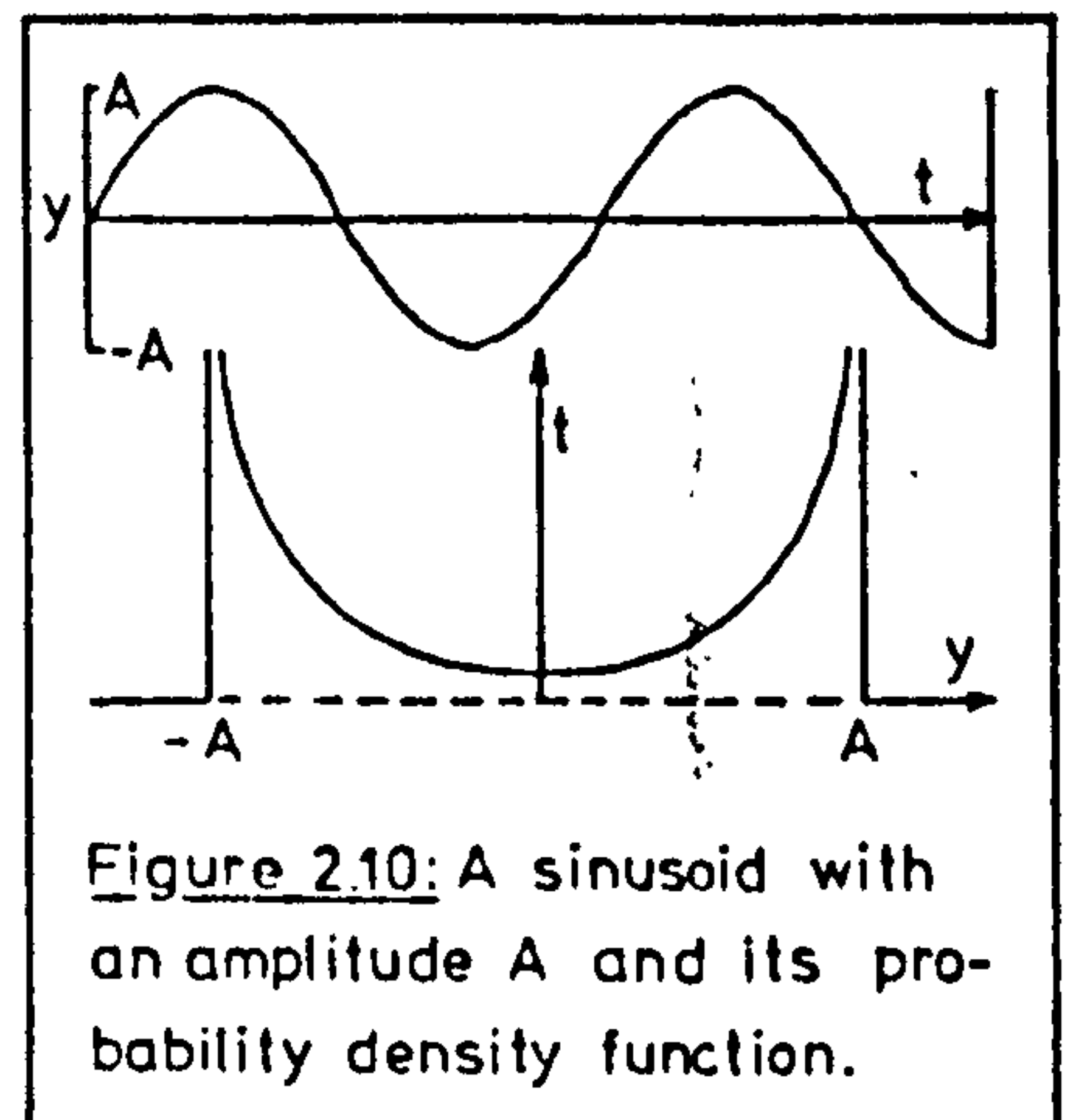
$$(2.4) \quad T(\hat{r}) = AR[S_0^2(\hat{r}) + R_0^2(\hat{r}) + RS^*(\hat{r}) + R^*S(\hat{r})]$$

with  $A$  constant, when the processed holographic plate is reinserted into the reference beam with the object beam removed. Without the interference between the object and reference beam neither of the two terms which contain phase information,  $RS^*(\hat{r})$  nor  $R^*S(\hat{r})$ , would occur and no three-dimensional image would be formed. The term

$AR^2S^*(\hat{r}) = AR_0^2S_0(\hat{r})\exp[j2\alpha - \phi(\hat{r})]$  is the original object beam multiplied by the constant factor  $AR_0^2e^{12\alpha}$ , but with a negative phase  $-\phi(\hat{r})$ , which indicates that the image is converging. This forms the real image and may be viewed by inserting a card or screen at the focal point. The term  $ARR^*S_0(\hat{r})\exp j[2\alpha + \phi(\hat{r})]$  again includes the original object beam, but this time with the phase  $+\phi(\hat{r})$ , indicating that the light is diverging. The virtual image which this produces may be viewed with the eye by looking through the plate, or it may be focussed and photographed with a camera.

As the fringes which are produced on the plate are very close together a movement of even a quarter wavelength in any component of the laboratory setup may degrade or even destroy the hologram. If, however, the object vibrates sinusoidally about a stationary mean, a series of dark and bright fringes appear over the image of the object during reconstruction, each of which is a line of equal amplitude. A vibrating object spends the greatest amount of time at either of its two extremities of displacement, as figure 2.10, the probability density function for a sinusoid, illustrates. The hologram will contain information about all of the infinite positions of the moving object, but as the object spends a greater part of its cycle at the extreme positions than at any other point, these will form fringes with greater contrast on the plate, and consequently the two predominant images on reconstruction.

For the moment only these two main images, and their interaction upon reconstruction, will be considered. If the reconstructed images at a point  $\hat{r}$  ( $x\hat{i} + y\hat{j}$  on a planer object) have



different displacements  $-A$  and  $+A$  which are  $\lambda/2\cos\phi$  apart, destructive interference will occur and a dark spot will appear on the image. Similarly, a dark band will link points on the reconstructed image with a peak to peak displacement of  $3\lambda/2\cos\phi$  or  $5\lambda/2\cos\phi$ , and so-on. In between these dark fringes will be areas where constructive interference takes place. These produce bright fringes connecting points with peak to peak displacements of  $0, \lambda\cos\phi$ , etc.

This is exactly the case in double-exposure holograms, or with a square wave displacement- two distinct images are formed which interfere to produce a

n	$k_n$ , roots of $J_0(k)$	$k_n - k_{n-1}$
1	2.4048	2.4048
2	5.5201	3.1153
3	8.6537	3.1336
4	11.7915	3.1378
5	14.9309	3.1394
6	18.0711	3.1402
7	21.2116	3.1405

Table 1: Roots of  $J_0(k)$  and the difference between subsequent roots.

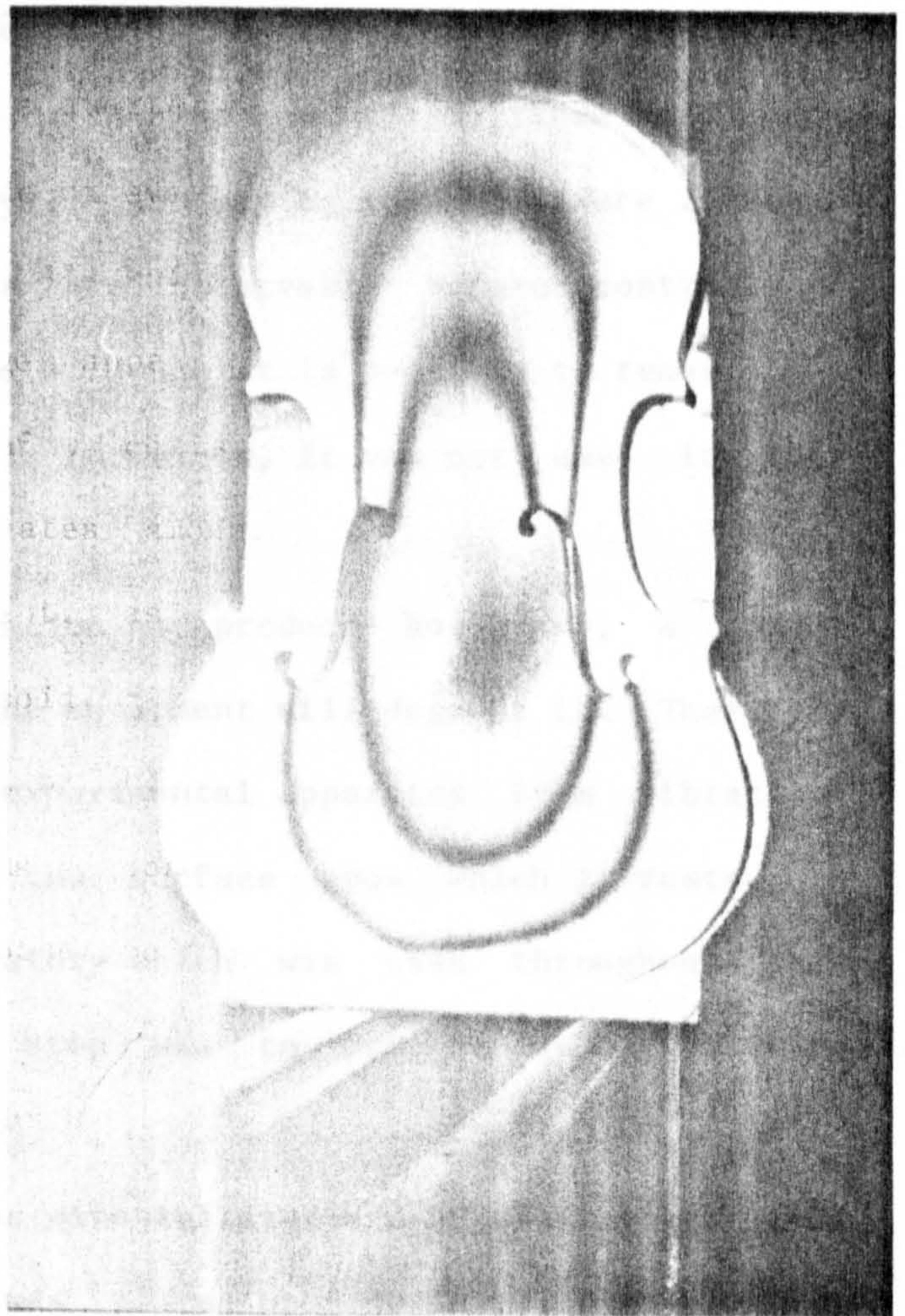


Figure 2.11: A vibration hologram of the front plate's lowest mode.

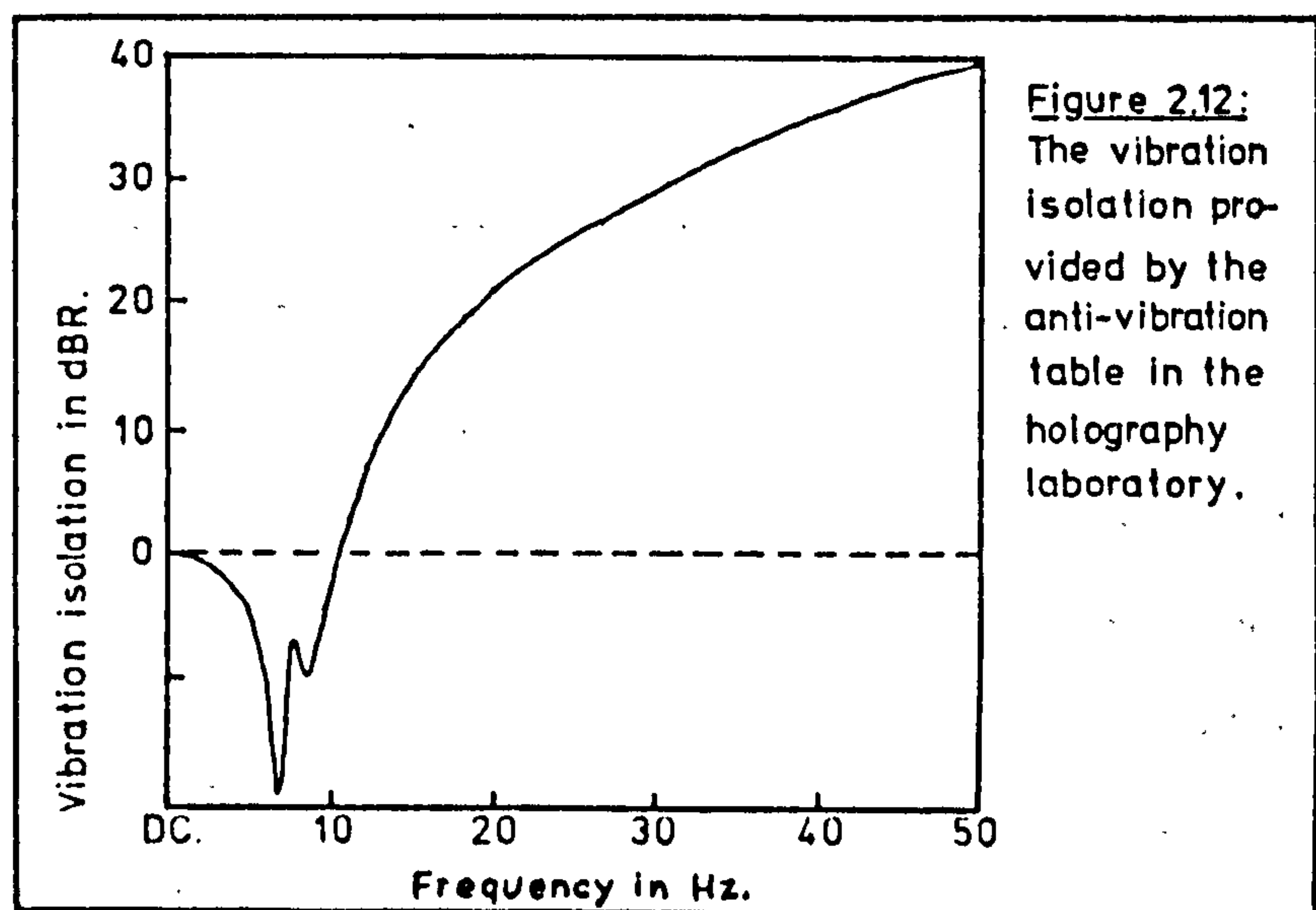
hologram with each successive fringe of equal contrast and representing a change in peak displacement of  $\lambda/2\cos\phi$ .

The presence of the continuous series of images in the vibration hologram slightly alters the way in which the fringes appear, and as the analysis is lengthy, it will not be included herein. Let it suffice to state that in vibration holography the fringes represent peak displacements of  $k_n\lambda/\pi\cos\phi$ , with  $k_n$  the successive roots of the zero-order Bessel function,  $J_0(k)$ , which appear in table 2.1. The spacing between fringes is very nearly the same as that of a double exposure hologram with the exception of the first as the table clearly shows. Contrast also changes with increasing amplitude and each successive fringe appears greyer, as may be seen in figure 2.11. A limit of about fifteen fringes are observable before contrast is reduced beyond perception, and although it is possible to remove this limit by employing a stroboscopic technique, it was not used in this research.

While a deterministic vibration may produce holograms, a random vibration of any element in the equipment will degrade it. Therefore it is necessary to isolate the experimental apparatus from vibrations which may be transmitted by the surface upon which it rests. In setting up the holography laboratory which was used throughout this research the first important step was to provide such vibration isolation.

Four automobile inner tubes were inflated and a slate bed, made from an old snooker table, was placed upon these. Its mass of 250 kg. gave excellent vibration isolation, which was further improved when three optical benches, with a combined mass of 130 kg., were placed upon the table to provide a firm mounting system for the equipment. A B&K type 8306 accelerometer and the 2131 narrow band analyzer were

used to measure the acceleration levels on the concrete floor of the laboratory, and on the table. To provide sufficient low frequency ener-



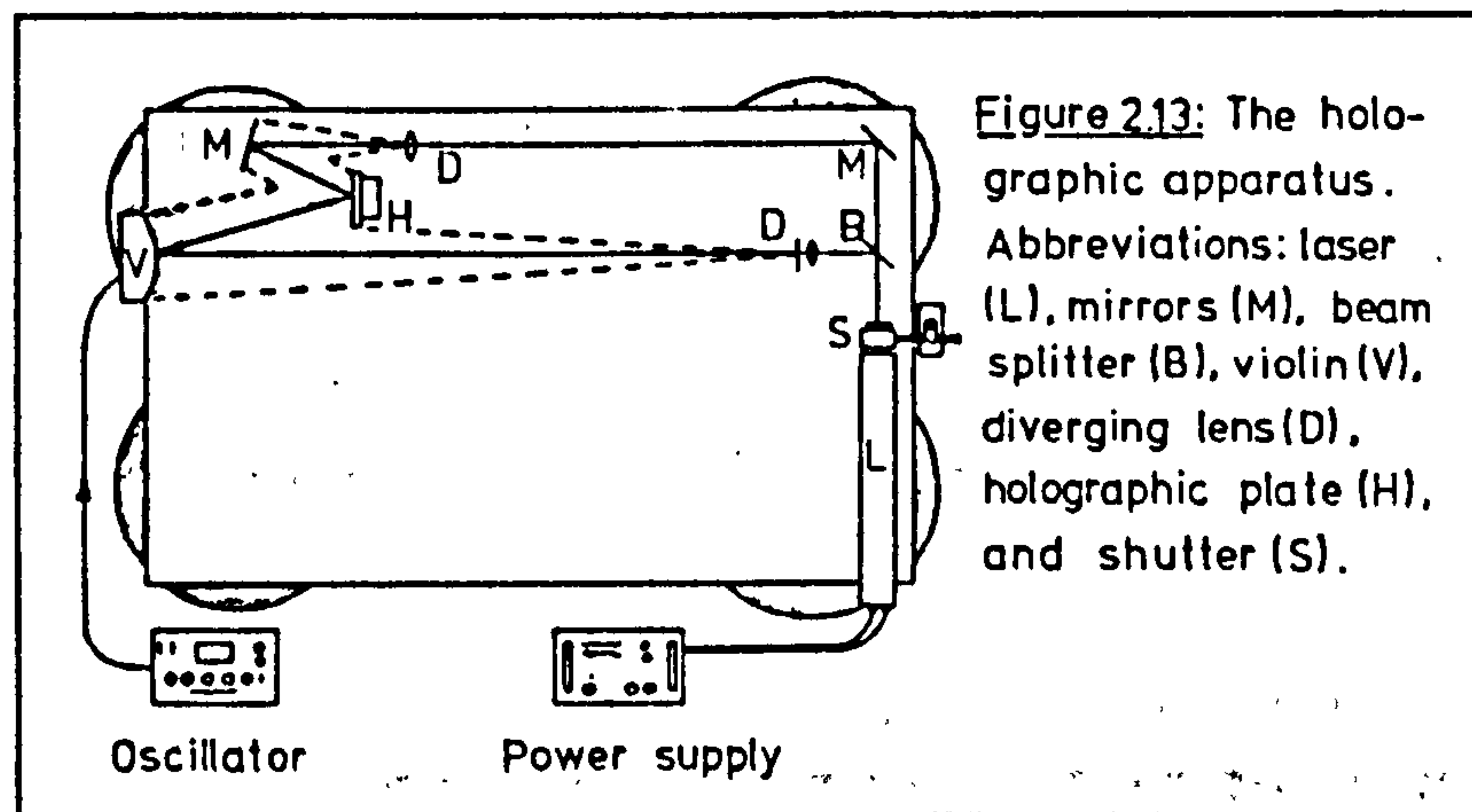
gy in the floor, such as would be caused by lorries passing by outside, several members of staff leapt about on piles of carpet tiles. The vibration isolation which was measured appears in figure 2.12.

A Scientifica Cook helium-neon laser, with a continuous power of 10 mW. and a wavelength of 633 nm. was used to make all of the holograms which appear in this work, although initially a 0.5 mW. model was used.

The laser had a separate power supply which, due to vibrations from its fan, was placed off of the table. A shutter was constructed using parts from an oscilloscope camera, and once again this was floor mounted to reduce vibrations.

The beam was split using a variable density silver-backed mirror which was specially mounted on a stand with an adjustment screw for moving it across the beam. This made it easy to adjust the relative strengths of the two beams which, when measured at the hologram's surface, should have a ratio of between 1:1 and 10:1, the reference beam being the stronger. One would expect the 1:1 ratio to be ideal. In fact, as the emulsion does not respond logarithmically to light at very low levels as it does at higher levels, a constant intensity needs

to be present to prevent complete destructive interference. In practice a ratio of about 4:1 is ideal [7].



Two mirrors, two lenses (25x and 10x microscope objectives), and a simple plate holder completed the initial

equipment, which is shown in figure 2.13.

A pinhole and an apparatus to mount both it and a lens greatly improved the quality of holograms by eliminating spatial noise from the object beam. Another major improvement was made by incorporating a light meter into the plate holder so that the intensities of the two beams could easily be measured [8]. Previously a hand-held meter had been used. Another seemingly trivial addition was of great use. As a small degree of divergence is present in the laser beam, it is important to keep the path lengths of the two beams within a few centimeters of each other. Small loops attached to each component made it easy to compare the path lengths with a piece of thread.

As already stated, the frame which held the violin and transducer could be transferred from the anechoic room to the holography lab and bolted directly to an optical bench. With this change in environment it was necessary to allow the violin to adjust to the new ambient conditions. Once it had settled down and the Muirhead Decade Oscillator had been adjusted to drive the violin at resonance, all was ready for exposing the plate.

Any stray light which could reach the plate would of course

partially expose it and degrade the hologram. Shades were placed on the table to shield the plate from stray laser light, and a black-out curtain was used to form both a canopy over the apparatus and a curtain for the lab's windows.

A squeeze-bulb and electronic stop-watch were used to control the shutter opening and, after a series of trial exposures with Agfa-Gervaert Scientia 10E75 plates, ten to fifteen seconds was found to produce a good image with a five minute developing time in Kodak D163 developer. Fixing in a bath of Kodak Kodafix solution and a final

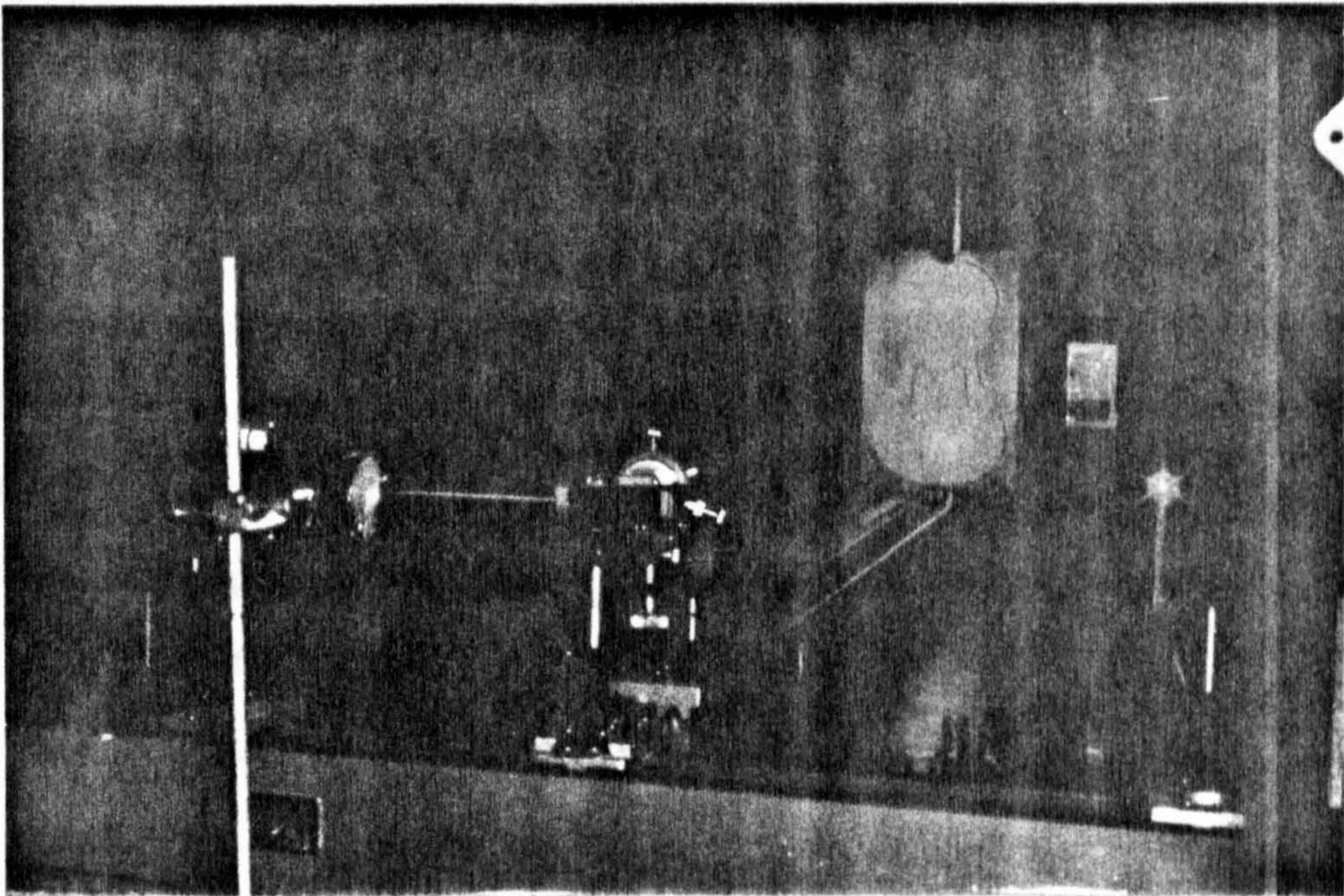


Figure 2.14: The holographic apparatus.

rinse in water with a few drops of Agfa Agepon wetting agent completed the processing. When using the 0.5 mW. laser and Kodak 649F plates exposure times were around five to ten minutes. At one point an additional bath was used to bleach the developed plates but the improvement in image quality was unnoticable.

Reconstruction of the image was usually done by holding the plate by hand in the object beam with the blackout curtain obscuring the

violin. Photographing any hologram of interest merely required a holder for the plate and an SLR camera to produce the photos which may be seen throughout this text.

### The Green's Function Technique.

The Green's Function Technique, in which a system is treated as a series of orthogonal functions which together make up a basis, is very useful in dealing with the vibrations of a violin. By determining a linear system's response to a point input it is possible to find the output from any form of continuous input simply by integration. This is exactly what occurs when the convolution integral, the Fourier transform, and the impulse response are used to describe a system in the time domain, but there is no reason that the space domain cannot be similarly treated! In the remarks which follow, the possibilities which this technique present will be applied to vibrating systems and later used to model the violin.

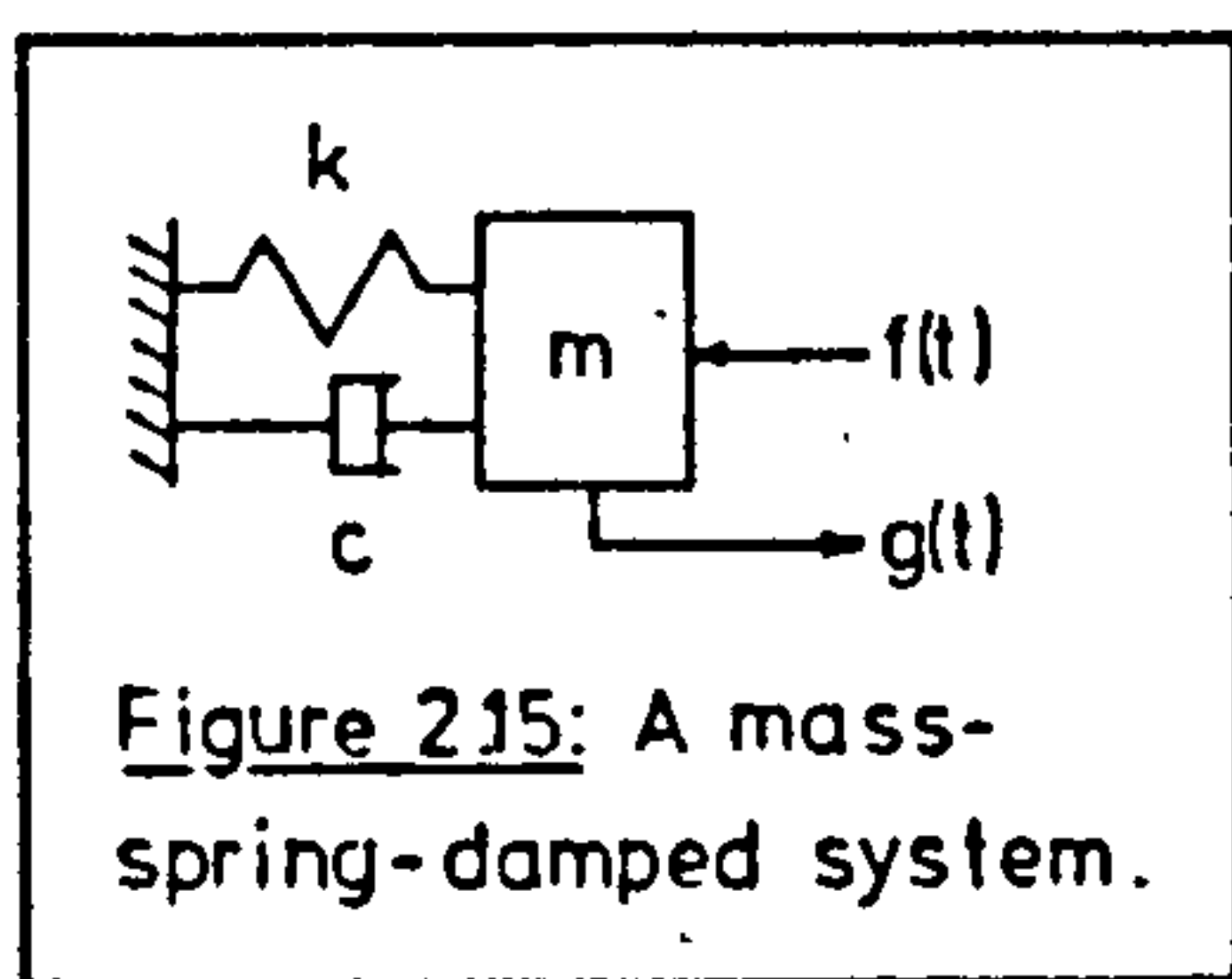
The convolution of two functions is defined mathematically as

$$(2.5) \quad g(t) = \int_{-\infty}^{+\infty} f(\tau)h(t-\tau)d\tau = f(t) \otimes h(t),$$

which defines the output in the time domain of a linear filter in terms of the input and the impulse response. The impulse response may be measured or it may be calculated from the system impedance. Then, in order to find the function  $g(t)$ , the convolution theorem is used. This theorem states that

$$(2.6) \quad G(w) = F(w)H(w) \text{ where } H(w) = \mathcal{F}\{h(t)\}, \text{ etc.}$$

The convolution integral is reduced to a product by the use of the Fourier transform and the output is easily determined for any input function. An example of this may be helpful: take the single degree of freedom system which appears in figure 2.15. The equation of motion



is  $m\ddot{g} + c\dot{g} + kg = f$ , with the functional notation dropped. To find the impulse response let  $f = \delta(t)$  and  $g = h(t)$  from equation (2.5). Multiplying by  $\exp(-j\omega t)$  and integrating over all  $t$  yields

$H(\omega) = 1/(k + j\omega c - \omega^2 m)$ , the impulse response.

In an example with lumped parameters like this one, only the time and frequency dependence is important. But with a continuous system the problem is more complex. The input will now be a function of both time and position,  $f(\hat{r}_0, t)$ , where  $\hat{r}$  is the vector representation of the input point in the system. The output will be in terms of  $\hat{r}$  and  $t$ ,  $g(\hat{r}, t)$ . To find the system response to a point input at  $\hat{r}_0$ , which is the Green's function, requires virtually the same steps as before. The equation of motion of a continuous system is often of the form

$$(2.7) \quad \frac{\partial^m}{\partial t^m} g(\hat{r}, t) + A \frac{\partial^n}{\partial t^n} g(\hat{r}, t) = B f(\hat{r}_0, t)$$

By substituting a delta function for  $f(\hat{r}_0, t)$  the Green's function is obtained, represented here by  $g(\hat{r}_0, t)$ , which conforms with the symbols in general use [9].

When working with a continuous vibrating system one important fact about  $g(\hat{r}_0, t)$  is already known; it may be separable into functions of time and space so that the partial derivatives in equation (2.7) become ordinary differentials. For a simple system it would then be possible to relate  $\hat{r}_0$ ,  $\hat{r}$ ,  $t_0$ , and  $t$ , by using the Fourier transform in both

time and space. The violin is not, however, a simple system, which makes it much more difficult to find a closed form solution to equation (2.7). When dealing with complex systems it is much easier to ignore the time dependence and only calculate the steady-state response. It is then, of course, impossible to determine the transients, but in this instance they are of no concern.

The use of the Green's function is, for most applications, similar. First the equation of motion is written in the form of equation (2.7). Next the terms  $g(\hat{r},t)$  are expanded as a series of orthogonal functions which together make up a basis. This is similar to a Fourier series:  $g(\hat{r},t) = \exp(j\omega t) \sum_I a_i \phi_i(\hat{r})$  with the terms  $a_i$  complex. Equation (2.7) may then be written as

$$(2.8) \quad (j\omega)^m \sum_I a_i \phi_i(\hat{r}) + A \sum_I a_i \partial^n \phi_i(\hat{r}) / \partial \hat{r}^n = B f(\hat{r}) \delta(\hat{r} - \hat{r}_0)$$

with the time dependant terms eliminated. Next let  $\frac{\partial^n \phi_i(\hat{r})}{\partial \hat{r}^n} = \gamma_i^n \phi_i(\hat{r})$  and combine terms in equation (2.8) to yield

$$(2.9) \quad \sum_I [(j\omega)^m + A \gamma_i^n] a_i \phi_i(\hat{r}) = B f(\hat{r}) \delta(\hat{r} - \hat{r}_0)$$

Each side of this equation should then be multiplied by  $\sum_j \phi_j(\hat{r})$  and integrated, making full use of the properties of orthogonal functions, namely  $\int_V \phi_i \phi_j dv = 0$  if  $i \neq j$ . This gives

$$(2.10) \quad \sum_I [(j\omega)^m + A \gamma_i^n] a_i \int \phi_i^2(\hat{r}) d\hat{r} = \sum_I B f(\hat{r}_0) \phi_i(\hat{r}_0)$$

Multiplying this by  $\phi_i(\hat{r})$  and rearranging gives once again the Green's function

$$(2.11) \quad g(\hat{r}_0, t) = \sum_i a_i \phi_i e^{j\omega t} = B \sum_i \frac{f(\hat{r}_0) \phi(\hat{r}) \phi(\hat{r}_0)}{\Lambda_i [(j\omega)^m + A\gamma_i^m]}$$

where  $\Lambda_i = \int_V \phi_i^2(\hat{r}) dV$ .

It then only remains to impose the boundary conditions to determine the response of the system to the point source at  $\hat{r}_0$ .

Before examples are cited, it will be useful to show that any number of waves with the same spatial frequency may be combined into a single wave with complex amplitude and phase. At any time  $t$  there may be an infinite number of waves travelling in one direction:

$$(2.12) \quad \Psi(x, t) = \sum_n [a_n \cos(\omega t + kx + \phi_n) + b_n \sin(\omega t + kx + \theta_n)]$$

Rewriting this using Euler's equation and factoring out the time dependent term leaves

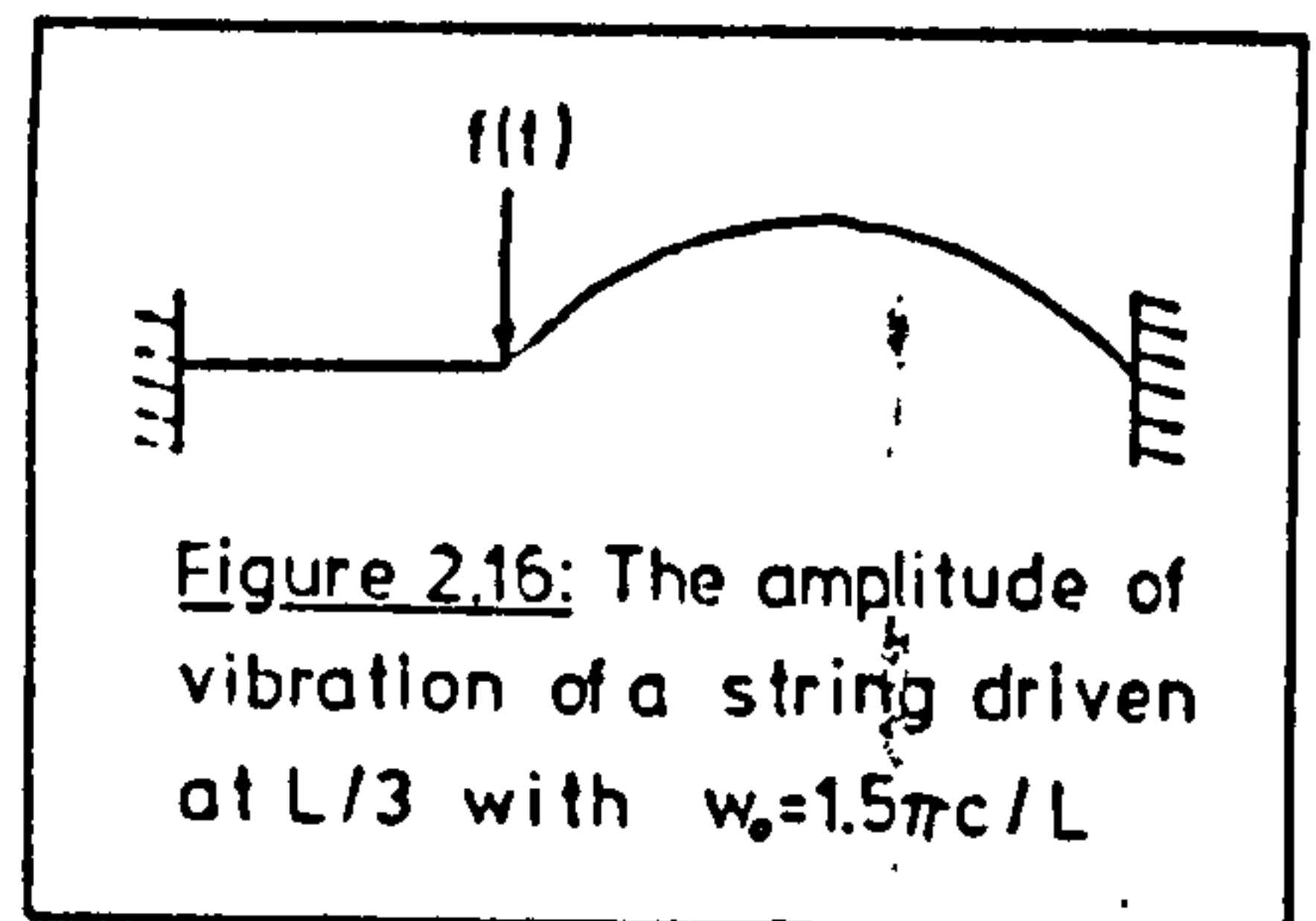
$$(2.13) \quad \frac{1}{2} \sum_n \left\{ e^{j\omega t} [a_n e^{j(kx + \phi_n)} + b_n e^{j(kx + \theta_n)}] + e^{-j\omega t} [a_n e^{-j(kx + \phi_n)} - b_n e^{-j(kx + \theta_n)}] \right\}$$

By factoring out the  $\exp(jkx)$  and  $\exp(-jkx)$  terms, and redefining  $a$  as  $a = \sum_n a_n \exp(j\phi_n)$ , this becomes

$$(2.14) \quad a e^{j(\omega t + kx)} + b e^{-j(\omega t + kx)} \quad \text{or} \quad a \cos(\omega t + kx + \phi),$$

with the proper choice of phase  $\phi$ .

The string in figure 2.16, driven by a force at a point one third of its length, with a frequency  $\omega = 1.5\pi c/L$ , makes a good example. In this case  $c$



is the wave velocity in the string. The equation of motion for a string may be written as

$$(2.15) \quad \epsilon \frac{\partial^2 g}{\partial t^2} + T \frac{\partial^2 g}{\partial x^2} = f(x,t) \delta(x-x_0) \quad ,$$

with  $\epsilon$  the mass per unit length and  $T$  the tension. The Green's function equation of motion may then be written directly from equation (2.12) as

$$(2.16) \quad g(x,t) = \sum_i \frac{\phi_i(x) \phi_i(x_0)}{\Lambda_i \epsilon (c^2 \gamma_i^2 - \omega^2)} \quad \text{for unit force, with } c^2 = T/\epsilon \quad .$$

Now a set of orthogonal functions which fit the boundary conditions are  $\phi_i = \sin(\pi i x/L)$ , which gives  $\gamma_i^2 = (\pi i/L)^2$  and  $\Lambda_i = L$  when  $i=0$  or  $L/2$  when  $i>0$ . Substituting this series into equation (2.16), along with the values of  $x_0$  and  $\omega_0$ , produces a series of sinusoids whose amplitudes vary as  $\pi^2 T (i^2 - 2.25)/L$ . This produced the interesting waveform of figure 2.16, which shows that there is no motion from  $x=0$  to  $L/3$ , and that from this point to  $x=L$  the string amplitude is that of a sinusoid with a wave number of  $4L/3$ .

If the ends of the string had not been fixed, but held by impedances  $Z_1$  and  $Z_2$ , then the boundary conditions would have produced different shape functions  $\phi_i(x)$ . With the origin now at the center of the string the boundary conditions may be written as

$$(2.17a) \quad \frac{F(-L/2)}{Z_1} = \frac{d\phi(-L/2)}{dx} \frac{T}{Z_1} = \dot{\phi}(-L/2) = j\omega \phi(-L/2)$$

and

$$(2.17b) \quad \frac{-d\phi(L/2)}{dx} \frac{T}{Z_2} = j\omega \phi(L/2)$$

Now let  $\phi_i = \sin(qx + i\pi/2)$ , where the  $i\pi/2$  term allows both even and odd symmetry, and substitute this into the boundary conditions to give

$$(2.18a) \quad \frac{1}{Z_1} q \cos(-qL/2 + i\pi/2) = \frac{j\omega}{T} \sin(-qL/2 + \pi i/2)$$

and

$$(2.18b) \quad -\frac{1}{Z_2} q \cos(qL/2 + \pi i/2) = \frac{jw}{T} \sin(qL/2 + \pi i/2)$$

These may be combined and rearranged to form

$$(2.19) \quad q \left[ \frac{Z_1 + Z_2}{Z_1 Z_2} \right] = -\frac{2jw}{T} \tan(qL/2 + \pi i/2)$$

which, when  $Z_1$  and  $Z_2 \gg 1$  is

$$(2.20) \quad q = \frac{-\pi i}{\left[ L - \frac{jT}{w} \frac{(Z_1 + Z_2)}{Z_1 Z_2} \right]}$$

The effect of a compliant termination for the string can easily be demonstrated. A spring-like termination at one end with an impedance of  $-jk/w$  makes  $q = -i\pi/[L + (T/k)]$ . In effect the string's resonance frequencies are all lowered as the denominator in equation (2.16) is dependent on  $q$ . More complicated impedances are easily treated in this manner.

The great advantages of this type of analysis will make it possible to improve the model of the violin in chapter 5. With driving forces that are a function of  $\hat{r}$  it is possible to predict the reaction of a continuous system to any form of periodic excitation. And when it is impossible to calculate the mode shapes of an object they may be determined experimentally for use in the equations of motion.

- [1] C. Raman, "On the mechanical theory of vibrations of bowed strings", Indian Assoc. Cult. Bull., vol. 15, pp. 1- (1918).
- [2] F. Saunders, R. Watson, and W. Cunningham, "Improved techniques in the study of violins", JASA, vol. 12, pp. 399- 402, (1941).
- [3] C. Hutchins, "Instrumentation and methods for violin testing", Journal of the Audio Engineering Society, vol. 21, pp. 563- 570, (1972).
- [4] W. Reinicke and L. Cremer, "Application of holographic interferometry to vibrations of the bodies of string instruments", JASA, vol. 48, pp. 988- 992, (1970).
- [5] E. Jansson, N.-E. Molin, and H. Sundin, "Resonances of a violin body studied by hologram interferometry and acoustical methods", Physica Scripta, vol. 2, pp. 243- 256, (1970).
- [6] D. Gabor, "Microscopy by reconstructed wave-fronts", Proceedings of the Royal Society, series A, vol. 197, pp. 454- 487, (1949).
- [7] A. Porter and S. George, "An elementary introduction to practical holography", American Journal of Physics, vol. 43, pp. 954- 959, (1975).
- [8] My thanks to Roger Darlington who constructed this circuit.
- [9] Morse and Ingard, Theoretical Acoustics, McGraw-Hill Books, New York, (1968).

### The Bowed String.

Many people would consider the motion of the bowed string to be of little interest. At first glance it appears merely to be a variation of the plucked string, the sort of problem encountered in elementary differential equations. It would appear that the bow draws the string aside until static friction is overcome, leaving the string free to vibrate until it is once again captured by the bow. But what if the bow pressure (which is the term that string players use to describe the normal force acting between bow and string) is increased without an increase in bowing speed? It would then take a larger deflection to overcome friction. This would mean that the period of vibration is dependent on both bow pressure and speed, a conclusion which cannot be true! One has only to watch a 'cellist as he "leans" on the bow to produce a sforzando to see that, even over a wide range of bow pressure and speed, the pitch is unaffected. Clearly some dynamic consideration has been ignored.

Herman Helmholtz was the first to shed light on this problem [1]. He designed an optical instrument to study the motion of a white speck on a blackened string and from his experiments concluded that the motion of any point on the bowed string could be represented by a sawtooth wave, such as that shown in figure 3.1. The rising and falling portions are related to the distance between the observation point and the string's end, and to the string length. If the string is viewed as a whole then the wave form may be represented very well by two straight

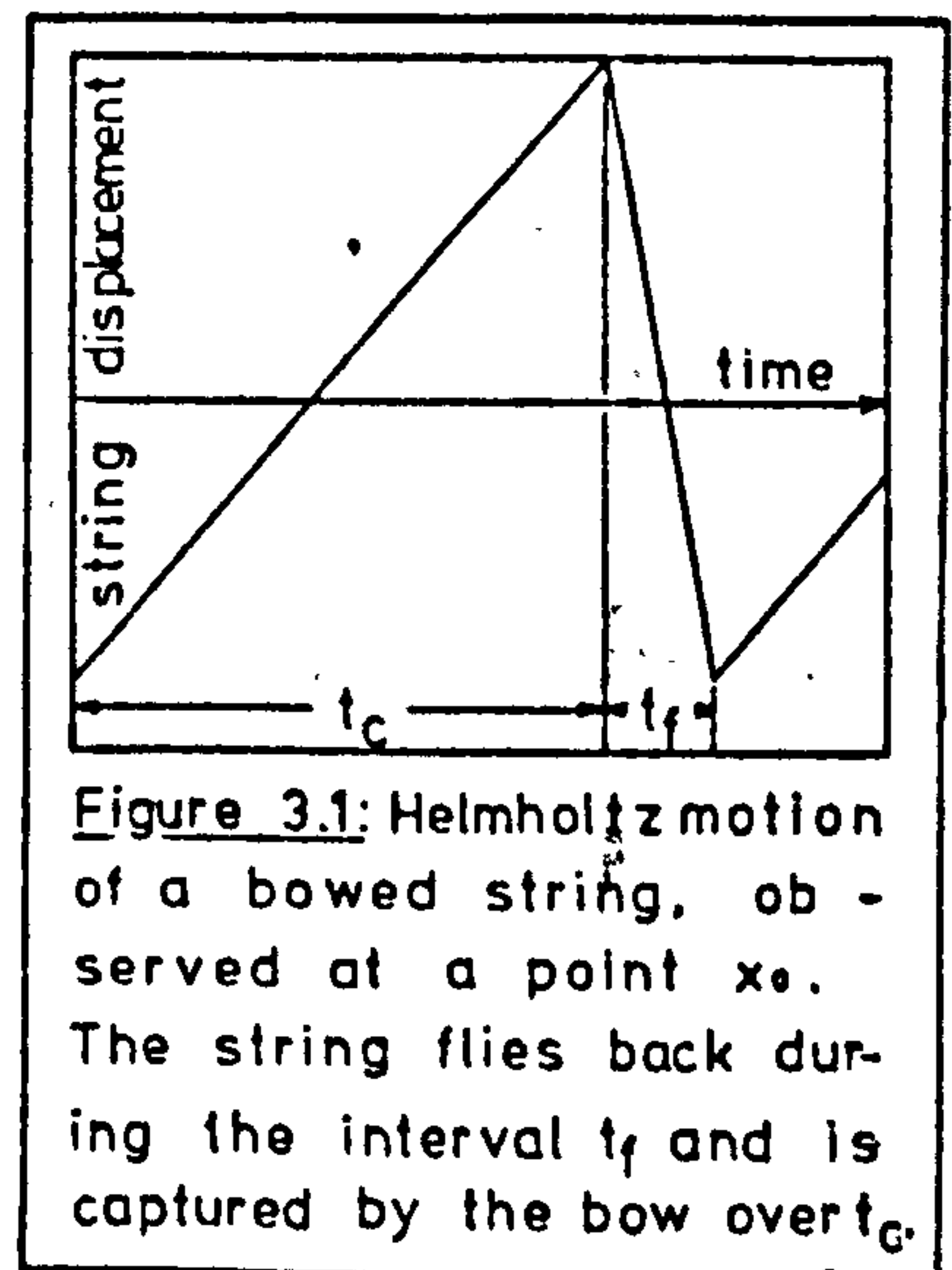


Figure 3.1: Helmholtz motion of a bowed string, observed at a point  $x_0$ . The string flies back during the interval  $t_f$  and is captured by the bow over  $t_c$ .

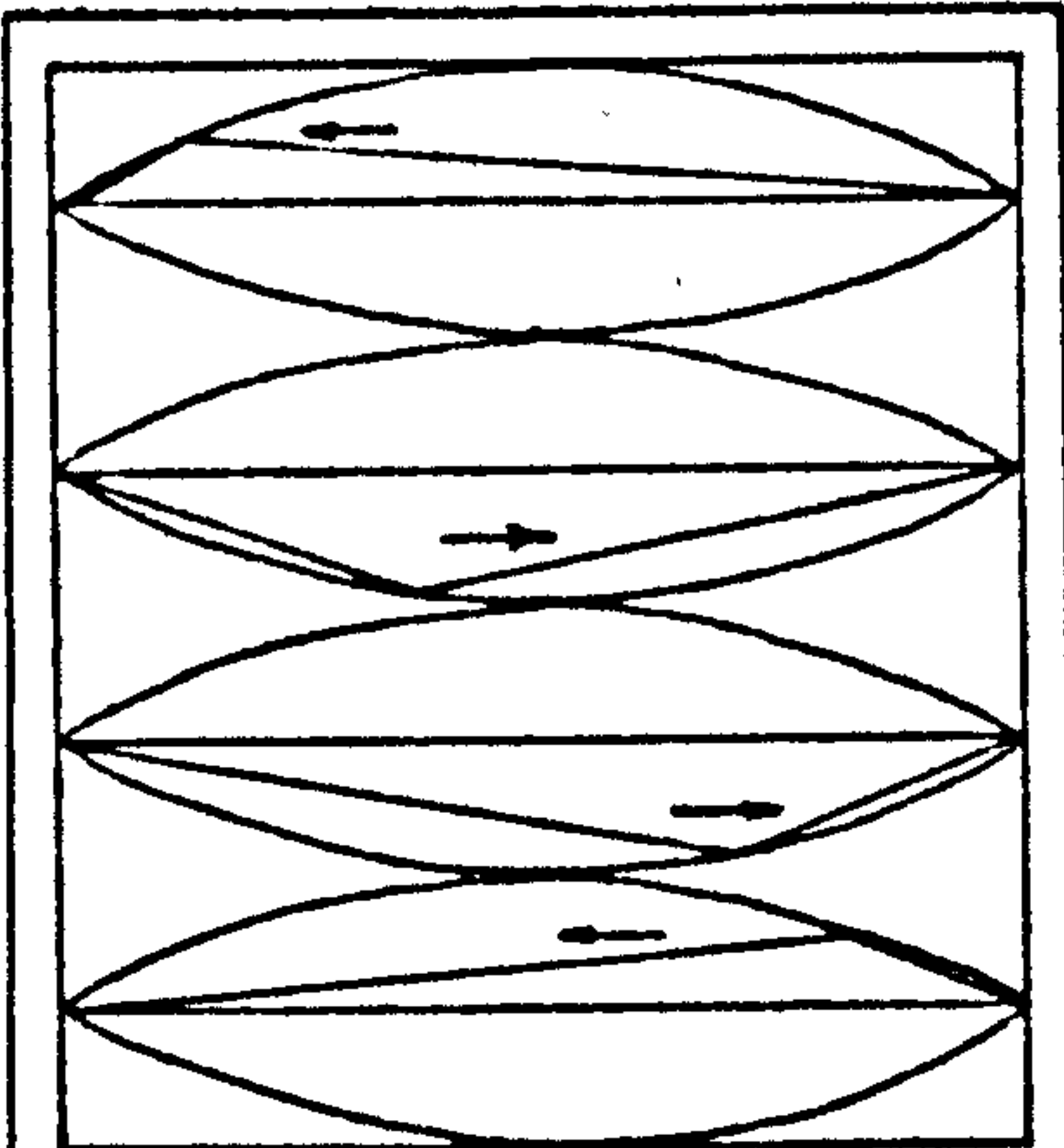


Figure 3.2: The slope discontinuity pictured above describes a parabolic curve as it travels around the bowed string.

lines with a discontinuity of slope which travels around the string on a parabolic envelope. It is this envelope which is seen when the string is bowed (figure 3.2).

The slope discontinuity produces velocity and acceleration discontinuities which also travel around the string. When the string is released from the bow the acceleration discontinuity travels towards the

bridge, reflects from it with nearly opposite phase, and as it passes the bowing point, initiates sticking. It then continues along the string, reflects from the nut (the string's termination at the end of the fingerboard), and initiates slipping when it once again reaches the bow. The release or capture by the bow is then precisely controlled by the time it takes for the wave to travel around the string. There are, of course, limitations to this model. Second order effects alter the wave-form slightly, but then so much in music depends on subtleties and cannot be ignored.

It is easy to see how a musician can control the dynamic level using the Helmholtz model of string motion. The force at the bridge from each string mode is proportional to its amplitude. An increase in bow speed or a change in position will change the amplitude by altering the distance the string moves in the time interval between capture and release. Some other factors of string motion are not, however, so easily described using the Helmholtz model.

Nearly fifty years later, C. V. Raman began a detailed study of bowed strings [2]. He used velocity waves to describe the string

motion and went into far greater detail than did his predecessor. By using the simple two state friction model (a coefficient of sliding friction  $\mu_d$  acting when there is a non-zero velocity between two objects and a coefficient of static friction  $\mu_s$  when they are not moving) and assuming equal damping of string modes, he confirmed Helmholtz's experimental work and firmly established the basic principles of the bowed string.

At this point it will be of interest to look at the Fourier Series representation of Helmholtz motion.

$$(3.1) \quad y(x,t) = A \sum_{n=1}^{\infty} \frac{1}{n^2} \sin(n\pi x/L) \sin(\omega n t),$$

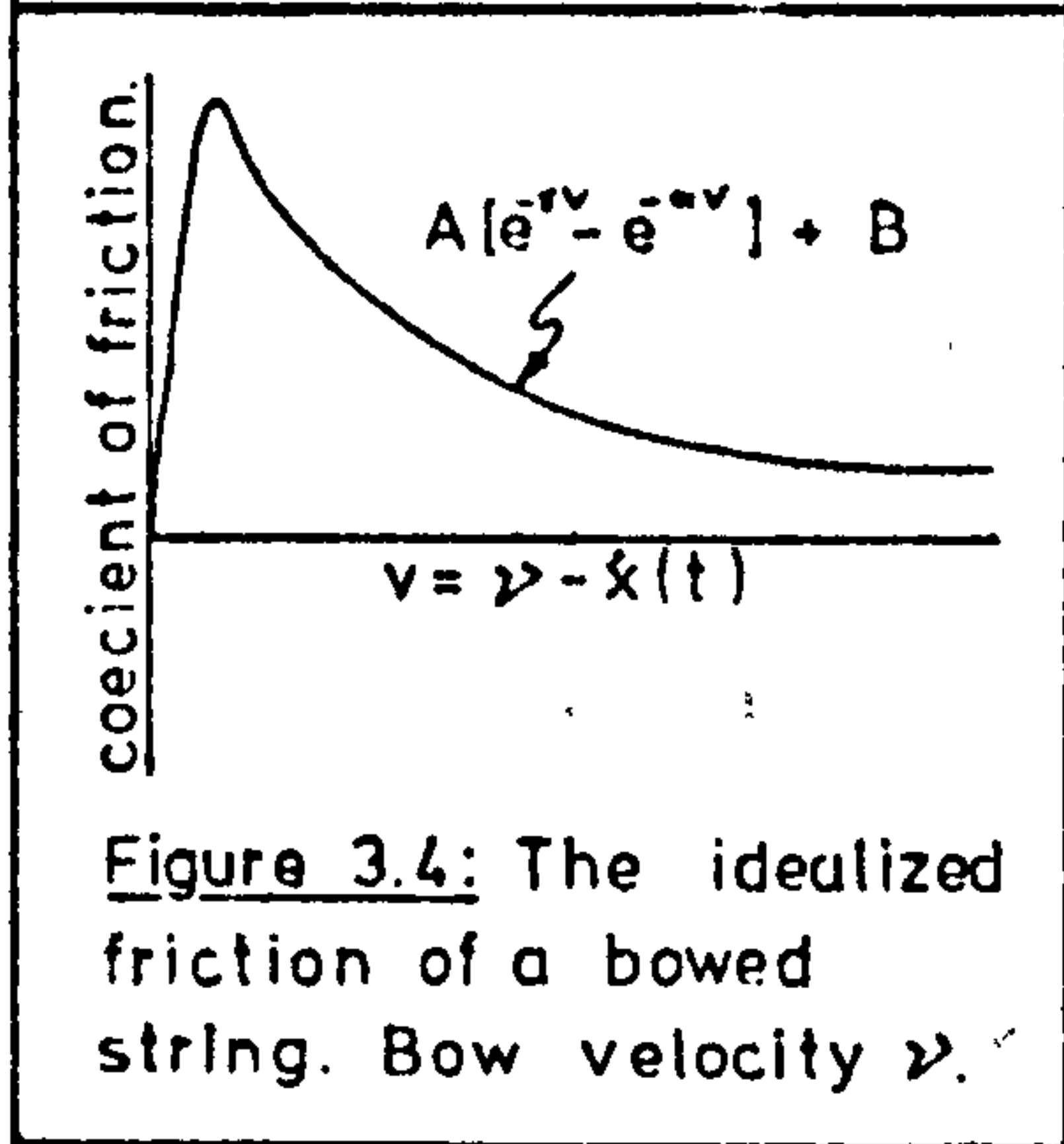
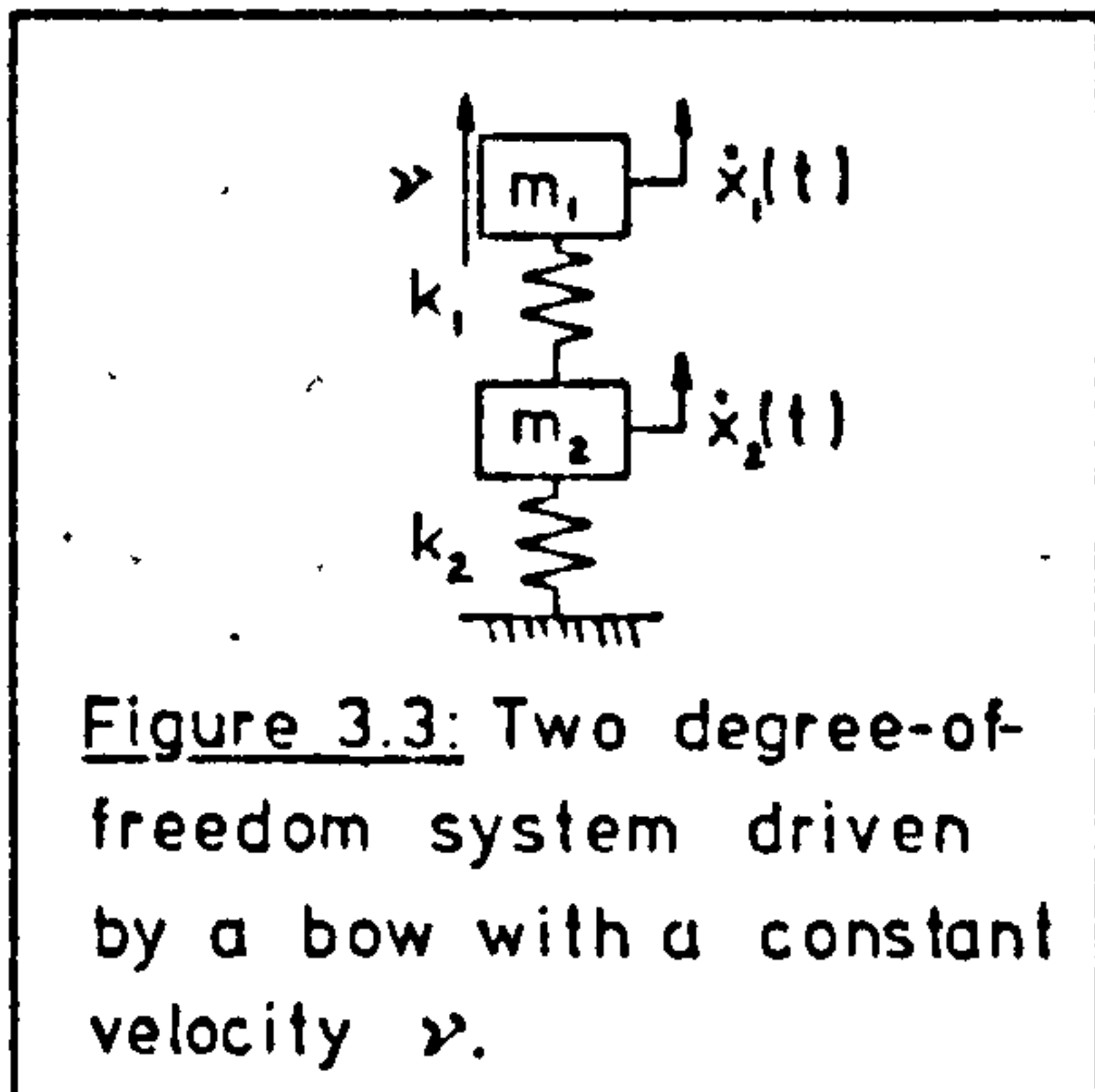
with  $\omega = c\pi/L$ ,  $c = \sqrt{T/\epsilon}$ ,  $\epsilon$  = lineal mass, and  $T$  = tension.

From this it is apparent that all of the string modes, even those with a node at the bowing point, have been excited, each with an amplitude of  $A/n^2$ . The force acting on the bridge is related to the slope of the string at that point so that, if the spatial derivative of equation (3.1) is taken, the force spectrum contains all harmonics with amplitudes proportional to  $1/n$ . It would then appear that the spectrum of forces acting on the violin body is independent of bowing position.

Practical experience shows that this is not the case as bowing nearer to the bridge, which requires a larger bow pressure, will produce a sound which the violinist considers to be "richer", a sound which has in fact many more high frequency components than would be produced when bowing at the finger board with a light stroke. Clearly something has failed to be accounted for in the Helmholtz model of the bowed string.

Arthur Benade suggests that the bowing process is highly non-linear and this lead seems a good one [3]. He states that

Helmholtz recognised the existence of harmonics in the string motion at points well away from the bowing point which should not have been excited when bowing at a node. Losses with each wave reflection and in



the string, and the non-zero width of the bow certainly help to excite these modes, but it is the non-linearity of the bowing process which is in fact primarily responsible for this phenomenon.

Before considering the bowed string a simpler system, such as the one in figure 3.3, may be profitably studied and will elucidate many of the principles of string motion. The mass in this system is being driven by a bow with constant speed  $v$  and a friction force  $N\mu(v)$ , whose characteristics are

like those in figure 3.4. As long as the relative velocity remains positive or very small, then the friction curve may be idealized as  $\mu = 0.5 [\exp(-v/10) - \exp(-v/100)] + 0.2$ , which fits the data available on string/bow friction [4]. The equation of motion of such a system may be written as

$$(3.2) \quad Z, \dot{x}(t) = N \left[ A \sum_{P=0}^{\infty} \frac{v^P}{P!} (\gamma^P - \alpha^P) (-1)^P \right] + NB$$

where  $\gamma = 1/10$  and  $\alpha = 1/100$ , with the expression for expanded into series form. It is possible to again use series expansions to change the right-hand side of equation (3.2) so that

$$(3.3) \quad Z, \dot{x}(t) = N \left\{ A \sum_{p=0}^{\infty} [\dot{x}(t)]^p [\gamma e^{-\gamma t} - \alpha e^{-\alpha t}] \right\} + NB$$

If  $\dot{x}(t)$  is thought of as being a single frequency term, then powers of  $\dot{x}(t)$  appear on the right hand side of equation (3.3). These powers introduce new frequencies into the equation so that  $\dot{x}(t)$  must equal zero, a trivial solution. Obviously  $\dot{x}(t)$  must include all of the possible frequency combinations which arise. With  $\dot{x}(t)$  represented as a Fourier Series,

$$(3.4) \quad \dot{x}(t) = \sum_{\eta=-\infty}^{+\infty} a_{\eta} e^{j\omega_{\eta} t}$$

so that it can take on any periodic form at all, the power series in equation (3.3) can be solved, although it becomes very lengthy. New frequencies appear in many different ways. When  $P=2$ ,

$$(3.5) \quad \dot{x}^2(t) = \sum_m \sum_{\eta} a_m a_{\eta} e^{j\omega(m+\eta)t}$$

and when  $P=3$ ,

$$(3.6) \quad \dot{x}^3(t) = \sum_m \sum_{\eta} \sum_p a_m a_{\eta} a_p e^{j\omega(m+\eta+p)t}$$

and so on. Physically this means that the system vibrates not only at some resonant frequency, but also at any multiple of that frequency or at any combination of two or more frequencies. Using equation (3.3) it is possible to work out the motion of the simple system, although the process is exceedingly tedious. Table 3.1 lists the simplest combinations of  $w$  and  $w$ , the two normal modes of the system, which occur with the parameters given in the table. The origin of the frequency components which Helmholtz observed in a string bowed at a

node should now be obvious: they were due to combination tones.

By including only terms up to third order in the table the number of possible frequencies has been considerably reduced, but even so the list is lengthy. What would happen if, rather than a two degree-of-freedom system a continuous one were dealt with? When the system has a series of harmonically related modes, as a string very nearly

Order of Coefficient	Radial Frequency	How it is obtained
1	170	
1	460	
2	290	460-170
2	340	2*170
2	630	460+170
2	920	2*460
3	120	290-170
		460-340
3	510	340+170
		3*170
3	750	920-170
		290+460
3	800	630+170
		340+460
3	1090	920+170
		630+460
3	1380	920+460
		3*460

Table 3.1: The simplest combination tones which arise in the bowed lumped parameter problem.

does, it is possible to use the same analysis as that applied to the simpler system, but such an approach is fraught with difficulties. By working in the time domain the problem may be more effectively analyzed, as recent work in this field has shown [5,6], but the frequency domain approach still yields some valuable information. It is quite easy to demonstrate how bow placement, speed, and pressure affect the tone quality of a bowed string. To begin, the equation of motion at the bowing point with second order terms may be written as

$$(3.7) \quad (Z_{\eta} - NA\Gamma) \sum_{\eta} a_{\eta} e^{j\omega t} = \frac{NA\Gamma^2}{2} \sum_{\eta} \sum_{\eta} a_{\eta} a_{\eta} e^{j\omega(m+\eta)t}$$

with  $Z_{\eta}$  the point impedance of the  $n$ th string mode, which may be determined using the Green's function approach, and where the operator  $\Gamma^{\eta}$  is defined as  $\Gamma^{\eta} = [\gamma^{\eta} \exp(-\gamma v) - \alpha^{\eta} \exp(-\alpha v)]$ . If the frequency terms

are equated, then the normal modes are defined by the series of equations

$$(3.8) \quad a_n = \frac{NA\Gamma^2}{2} \sum_m \sum_p a_m a_p / (Z_n - NA\Gamma),$$

for all values of n, with  $m+p = n$ . These can be solved by first assuming that all of the coefficients  $a_n$  are those predicted by the Helmholtz model of string motion, calculating a new set of coefficients with equation (3.8), scaling the terms to match the bow velocity, and iterating this process. Figure 3.5 demonstrates the change in the coefficients of the second harmonic when the bow force or velocity are altered.

It is immediately apparent that the coefficients  $a_n$  are influenced by the impedance Z, which for a string is dependant on the bowing position, and by speed and pressure through  $\gamma$  and N. It is easy to see that in a bowed string the amplitude of each harmonic is slightly changed due to the combination tones which arise and, as these depend on the way the string is bowed, the timbre will be altered. Increasing N or decreasing  $\gamma$  will mean that the combination tones

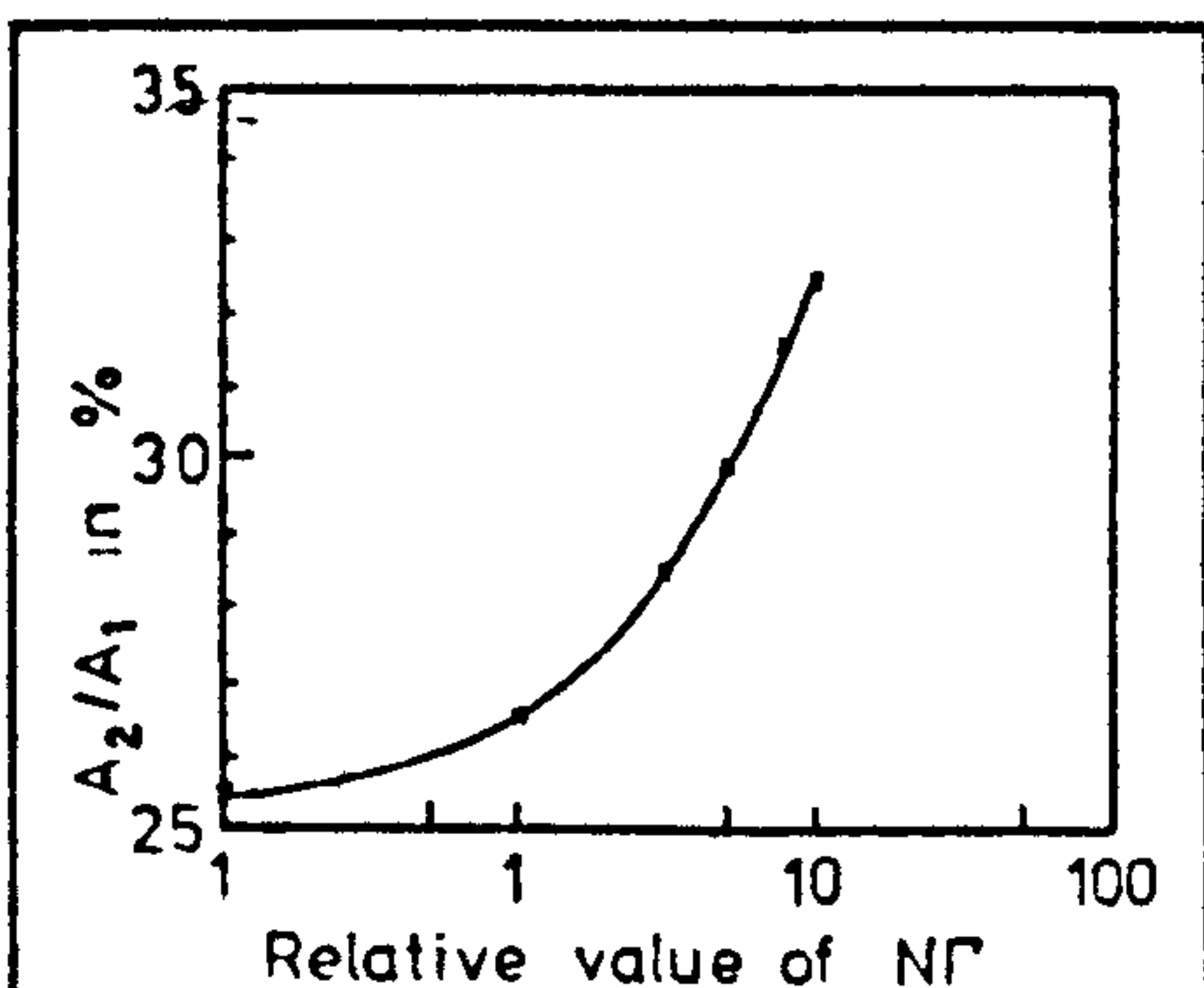
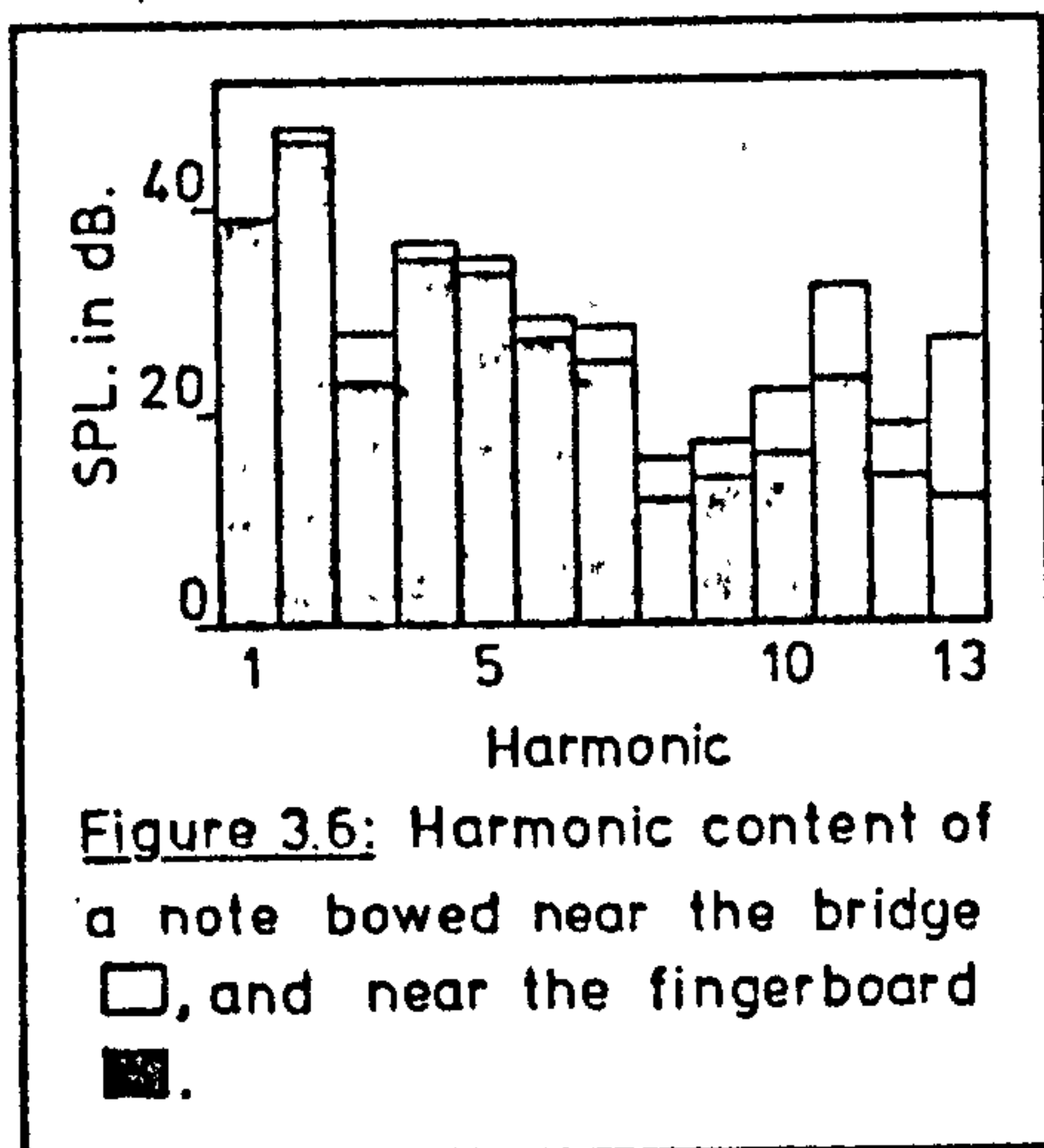


Figure 3.5: The way in which bow pressure and speed alter the amount of second harmonic present in the steady-state vibration.  $N\gamma^2 = N[\gamma e^{-\gamma} - \alpha e^{-\gamma}]$  with  $\gamma$  = bow velocity, N = pressure.

become more important, so that the player should hear more high frequency components, a phenomenon which has already been seen to occur.

From the discussion so far one would expect that with high bow speeds and low pressure the combination tones will exert little influence on the vibrating string, which will exhibit Helmholtz motion. As the term  $N\gamma^2$  is



increased the string motion will change significantly, as demonstrated in figure 3.6, where the frequency content of two notes bowed on a cello are plotted.

There are limits to the magnitude of  $N$  which allow an ordinary solution to equations (3.7). This becomes clear when second order terms in (3.8)

are ignored to produce equation (3.8a) below.

$$(3.8a) \quad Z_{\eta} - NA\Gamma = 0$$

As the  $NA\Gamma$  term is the only one which supplies energy to the system, through its "negative resistance", it must have a greater value than the losses in  $Z$ . Otherwise energy input cannot balance the losses. It is then the total negative resistance which controls how the oscillation builds up.

There is also a maximum value to  $NA\Gamma$  above which the solutions for  $w$  in equation (3.8) become purely imaginary and oscillations cannot occur.

Both of these phenomena occur in the bowed string, although the mechanism is somewhat different. Raman discussed the "minimum bow force" (the minimum value of  $NA\Gamma$ ) in his book [2] and J. Schelleng summarises work on this area in his excellent paper, "The Bowed String and the Player" [7].

The maximum bow force is reached when the Helmholtz discontinuity can no longer dislodge the string from the bow's grasp. When this occurs a rasping growl ensues. If the flyback portion of the Helmholtz

wave lasts only  $x_0/L$  of the cycle with  $x_0$  the distance between the bow and the bridge, its velocity must be  $vL/x_0$  during that interval. The magnitude of the force discontinuity is then  $Z_c vL/x_0$ , with  $Z_c = \sqrt{TE} = ce$  the characteristic impedance of a string. The condition for maximum bow pressure is then

$$(3.9) \quad N_{\max} = Z_c vL / (\mu_s - \mu_d) .$$

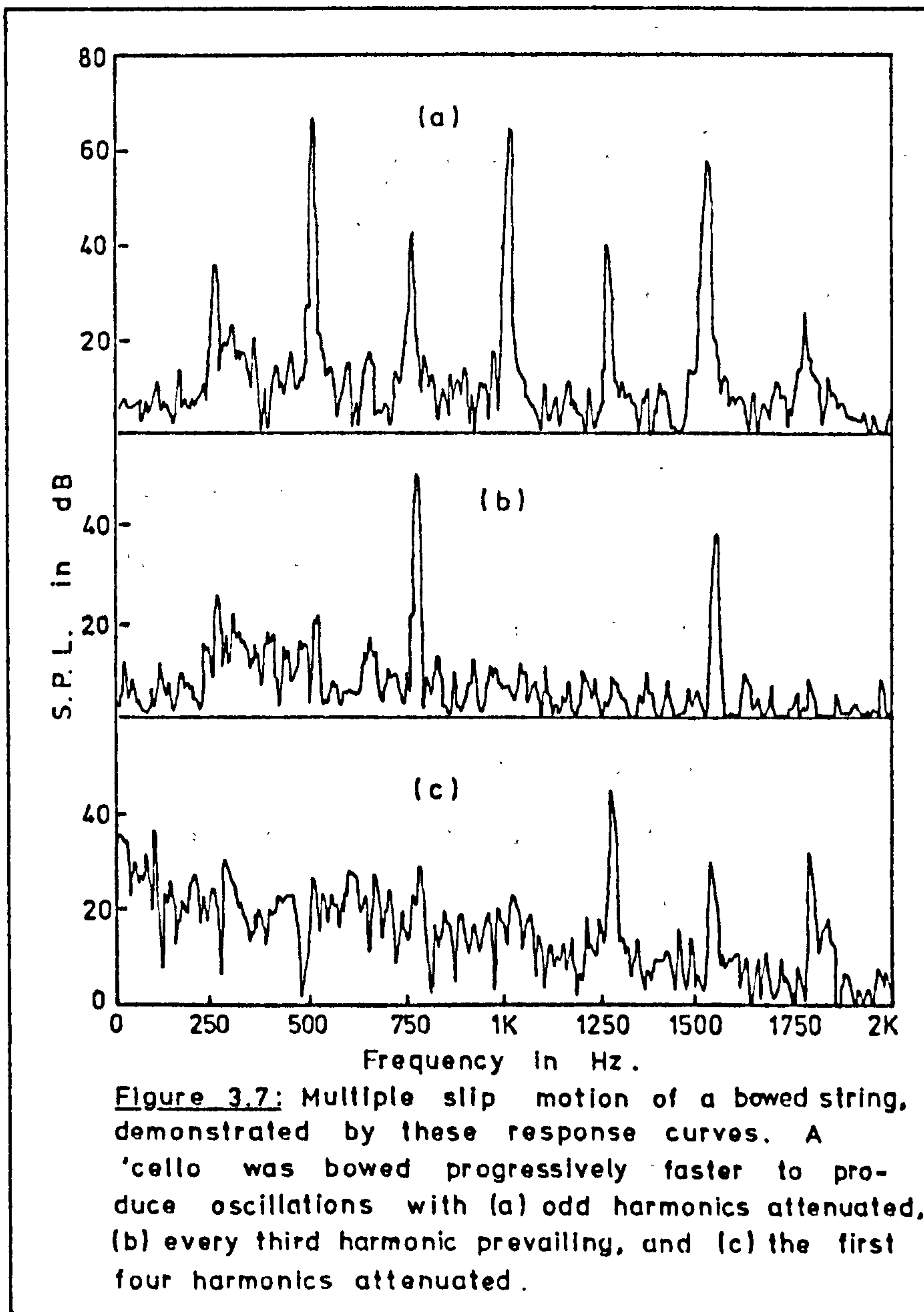
The minimum bow force occurs when the discontinuity just has sufficient time to return to the bow and release the string before friction is overcome. At lesser forces the string is released before the discontinuity reaches the bow and another wave is sent out. As there are now two, or more, discontinuities on the string, the fundamental jumps to a multiple of the fingered note and the time-keeping function of the Helmholtz wave is restored. Schelleng derives the value for minimum bow pressure, which is dependent on the impedance of the bridge and body [7]

$$(3.10) \quad N_{\min} = Z_c^2 vL^2 / 2r(\mu_s - \mu_d)x_0^2 ,$$

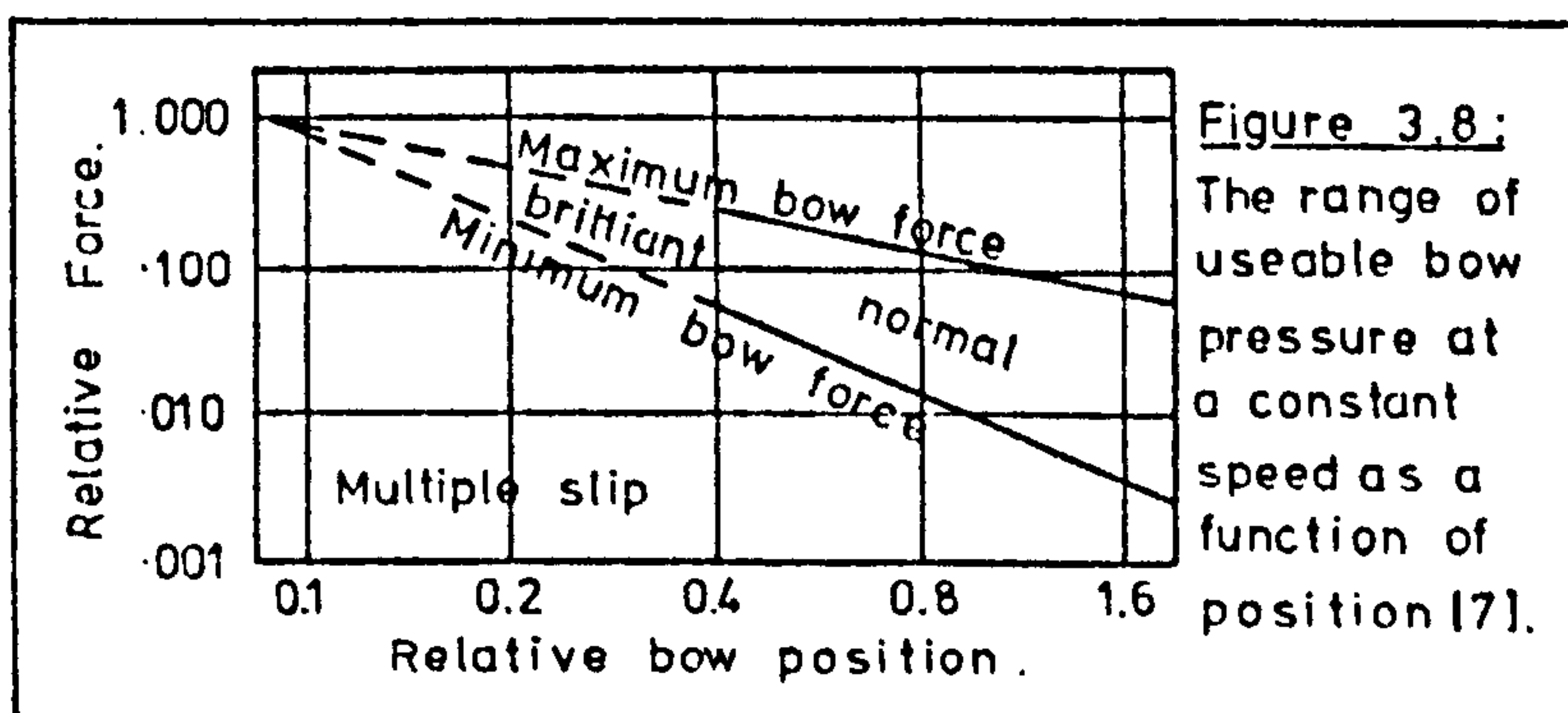
with  $r$  defined as the loss term for the first string mode. This estimate of  $N_{\min}$  is only good to an order of magnitude.

Examples of the frequency content of waveforms which exhibit the limits of bow parameters, along with the cases when these limits have been exceeded, are shown in figures (3.7) and (3.8).

The limits on  $N_{\max}$  and  $N_{\min}$  differ in their dependence on bow placement so that the range of pressures and speeds which may be used increases as the bow is moved away from the bridge. These results are illustrated in figure (3.8) where the range of pressures, for a given



bow speed, are plotted against bow position. From this figure it may be seen that at some point very near the bridge the two lines meet. With such a high pressure necessary at this point one would obtain a



brilliant sound due to the large amount of combination tones produced.

Only the very best string players can make use of the very narrow limits on the bowing process which permit such rich and beautiful tones! Lesser musicians play nearer the fingerboard and so reduce their range of expression, but also avoid the disastrous consequences of exceeding the bowing limits.

The bowing parameters may affect the sound in some other ways too. Equation (3.8) shows that if the real part of  $NA\Gamma$  is significant then  $w$  will be complex and the peak in frequency response will be shifted. This may easily be observed with strings by bowing heavily and slowly on the lowest string of a violin or 'cello. Schumacher observes that this effect is somewhat counteracted by the importance of high harmonics under these same conditions, which tend to be a bit sharp due to string stiffness, thus shifting the listener's perception of the pitch. The discussion of this effect in the time domain is extremely interesting [5,6].

There are many other factors which influence the vibrations of the bowed string. Stiffness must be the most important of these for it causes the partials of the string to deviate from the natural harmonic series, the effect being increasingly important as the wavelength decreases. It is the simple relationship between harmonic resonances which makes it possible for combination tones to become so important. With an inharmonic series the generated tones fail to reinforce the partials and so "brilliance" is lost.

Except in the case of wolf-notes, which will be discussed shortly, a very small amount of the string's energy is transmitted to the body. To maximize this transfer the impedance match between bridge and string must be as good as possible. This requires the mass of the string, and consequently its tension, to be as large as possible. Mass and string

Material	$E/10^{11}$ , Dynes/cm <sup>2</sup>	Density, gm/cm <sup>3</sup>	Inharmonicity /10 <sup>10</sup> $E/\rho^2$
Silver	7.5	10.5	0.68
Brass	9.2	8.6	1.24
German Silver	10.8	8.4	1.53
Gut	0.39	1.37	2.1
Steel	19.0	7.8	3.1
Aluminium	7.0	2.7	9.6

Table 3.2: Inharmonicity of various material used for strings [7].

String type	frequency perturbation $B \times 10^3 / n^2$	$n_{min}$
Violin E, steel	0.02	28
Violin D, gut	0.25	13
Violin G, gut	1.3	7
Violin D, wound gut	0.12	16
Violin G, wound gut	0.08	19
Cello G, wound gut	0.05	22
Cello C, wound gut	0.13	16
Cello C, on steel	0.23	28
Acceptable value	0.06	21

Table 3.3: Inharmonicity of various wound and solid strings using Young's expression for inharmonicity [7],[8].

stiffness are then the parameters to be considered when evaluating materials for strings. Several materials commonly used for strings are listed in table 3.2 along with their density and Young's Modulus, upon which the stiffness depends. Young

showed that it is the ratio of  $E/\rho^2$  which in part defines the degree of inharmonicity. This ratio forms the basis for evaluating solid strings and also appears in table 3.2. Clearly silver is the best material, aluminium the worst, and gut and steel about equal for solid strings. Unfortunately silver has a very low tensile strength and so cannot be used for solid strings.

By wrapping a core with a dense wire the mass increases without greatly affecting the stiffness. Table 3.3 compares various wound and solid strings using Young's expression for string inharmonicity [8],

$$(3.11) \quad f_n / n f_0 = 1 + B n^2$$

with  $f_n$  the frequency of the  $n$ th harmonic, and  $B$  defined for a particular string as in the table. The value  $n_{min}$  in table 3.3 is the number of the partial which falls about halfway between two of the natural harmonics. Combination tones cannot exert any noticeable effect at such frequencies, and the reinforcement which usually occurs in the bowed string cannot occur in such a case. The tone for a string like this is quite dull, as may be heard from a violin gut G-string, whose response falls off rapidly above the sixth harmonic.

Torsional vibrations certainly occur in a bowed string too. The transverse velocity can only match the bow when it has frequency components as dictated by Helmholtz motion, unless the contact point is allowed to roll. Thus coupling between torsional and transverse modes allows waveforms modified by combination frequencies to exist while the sliding velocity remains zero over much of the cycle.

The motion of the bow hairs has an effect on the string similar to that of torsional vibrations. Both of these phenomena have been treated in the time domain, although their musical effects have not been evaluated [5,6]. Obviously they will be least important at  $N_{min}$  for then the transverse waveform is most closely associated with Helmholtz motion.

#### The wolf-note.

Torsional vibration of the string makes it possible for it to exhibit forms of motion which, at times, are vastly different from Helmholtz motion and yet still remain in contact with the bow over part of its cycle. Vibrations such as these, unpleasant in the extreme, are known as wolf-notes, and although there are many possible forms for

them to take these all owe their origin to the same phenomenon.

A single string mode and its coupling to the bridge and plate is analogous to the simple lumped parameter system which was used earlier. If the impedances are quite similar a doublet will be formed between the two subsystems with two possible resonant frequencies. When bowed, both the two-mass system and the single string mode vibrate at both of these frequencies simultaneously if the impedance match is close. Of course other frequencies are present in the bowed string too but these are generally unaffected by the coupling between string and body.

As was demonstrated in equation (3.7), each frequency which is excited in a bowed string forms a harmonic series due to the non-linearities of the bowing process. If two of these frequencies exist where only a single mode would ordinarily be excited, as happens when a doublet is formed, then the impedances of the harmonics formed by

	Order		
1st	2nd	3rd	
98	4	2	
102	100	94	
200	198	96	
300	202	104	
	298	106	
		194	
		196	
		204	
		206	
		294	

Table 3.4: The highest order combination tones below 300 Hz. generated by a bowed string with a wolf-note at its fundamental.

combination tones are low enough for them to be excited to an appreciable level. Beats occur between the inharmonically related frequencies and heterodyne action produces new combination tones which all add an unpleasant roughness to the tone. As an example take a string whose lowest three harmonics, starting at 100 Hz., are affected by the bridge impedance. The fundamental is then split and the new series, in column 1 of table 3.4 above, produces combination tones such as those in the second column. These new frequencies then combine with

the original list to produce additional ones, and so on.

It is an easy matter to observe these beats occurring by looking at the frequency domain recorded of an instrument playing a wolf-note. Figure 3.9 shows how these additional frequencies appear when a wolf is in action.

It is difficult to establish under just what conditions a wolf will appear in the bowed string. String resonances occur whenever

$$(3.12) \quad w = n\pi(L - jT/wZ)$$

with  $Z$  the impedance of the violin plate at the bridge. When the string and the plate are tuned to the same frequency there are always three distinct, real roots to this equation. With the two tuned slightly differently there may be one, two, or three distinct solutions to (3.12). To determine whether or not a wolf occurs the equation which defines the resonant frequencies is rewritten

$$(3.13) \quad w^3 - \frac{w^2 n\pi c}{L} - \frac{w(kL + T)}{mL} + \frac{cn\pi k}{mL} = 0$$

Then, defining  $P = -n\pi c/L$ ,  $Q = -(Lk + t)/Lm$ , and  $R = cn\pi k/Lm$ , and with  $A = L/3(3Q - P^2)$  and  $B = L/27(2P^3 - 9PQ + 27R)$ , the nature of the solutions to equation (3.12) are given by

one real root if  $B/4 + A/27 > 0$

three real, unequal roots if  $B/4 + A/27 < 0$ .

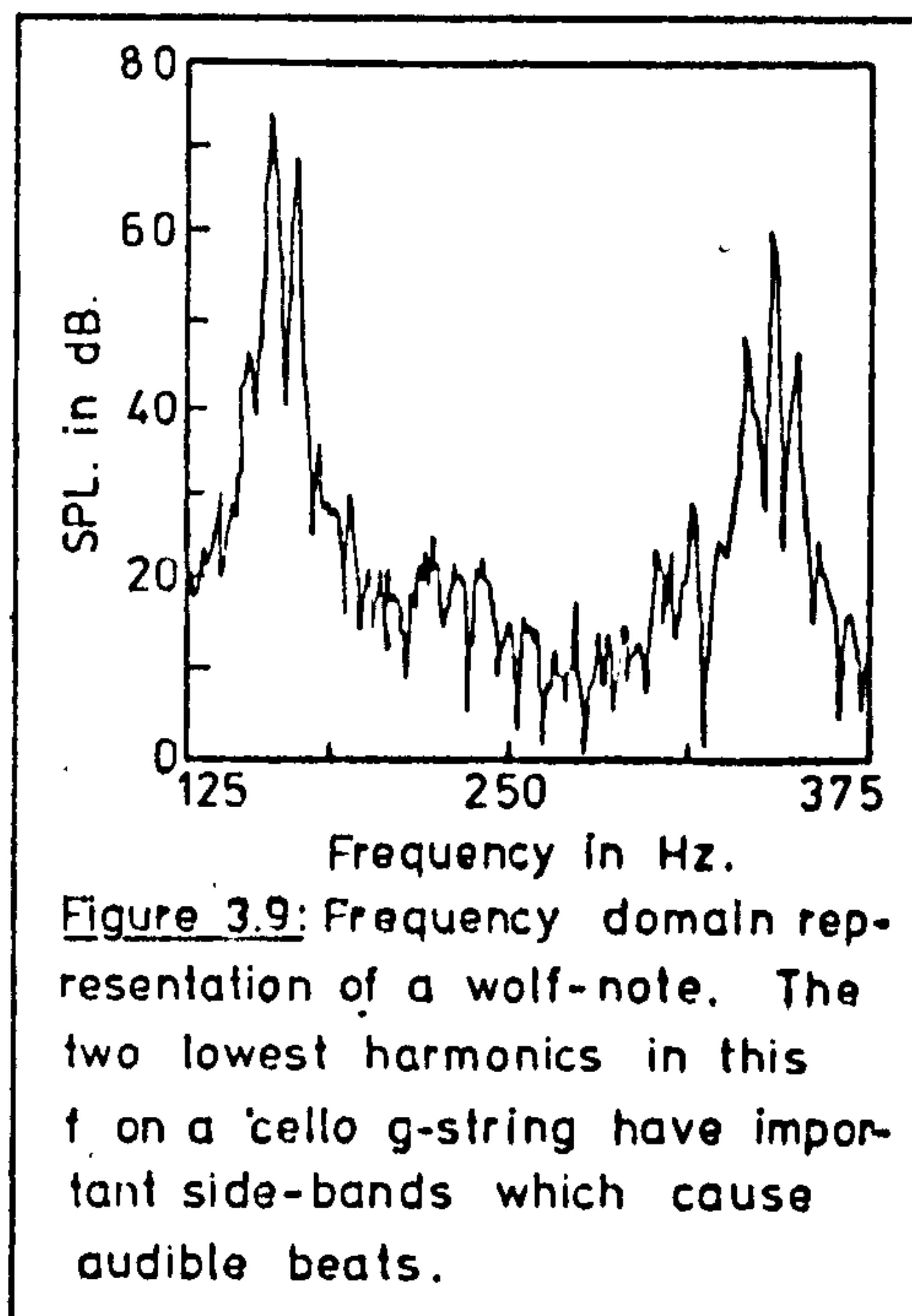


Figure 3.9: Frequency domain representation of a wolf-note. The two lowest harmonics in this  $f$  on a cello g-string have important side-bands which cause audible beats.

If the string and plate are tuned to exactly  $w$ , then invariably the three roots are  $<0$ :

$$(3.14) \quad -[\alpha w_0^4 48/27 + 13w_0^2 \alpha^2 / 108 + \alpha^3 / 27] < 0, \quad \alpha = T/Lm$$

This does not mean that a wolf-note is heard, for as equation (3.14) approaches zero the roots move more closely together until the effect disappears. This suggests several remedies for avoiding wolf-notes in string instruments, all of which are in use.

Increasing the plate impedance will reduce  $\alpha$  and the influence of the wolf considerably. Unfortunately, the response of the plate will be reduced at all frequencies if this action is taken so it does not appear to be a useful solution. The same could be said for reducing the string tension, for while  $\alpha$  is again decreased, such an action would reduce the force which a vibrating string can apply to the plate.

Some violin-makers go to extreme lengths to ensure that the wolf-note occurs at a frequency between two equal-tempered notes, so that it need never be excited. This is successful only if the violin (or 'cello, in which the wolf is a much more pernicious problem) is tuned properly, and even then changes in humidity or strings, or even age can displace the plate resonance enough to bring the wolf-note back into action. Clearly another solution must be sought.

The performer has recourse to one method for removing the wolf. As the string length helps to determine  $\alpha$  playing the note on another string will have a remarkable effect. The A-string on a violin has a length of about 32 cm. Playing the A(440), which is commonly the wolf in violins, on the D-string leaves only a string length of 21.3 cm.,

while on the G-string a mere 14 cm. of string vibrates at this frequency. The lowest of the strings is by far the most susceptible to the wolf-note, as equation (3.14) suggests. Playing this note on a higher string will often cause the wolf to disappear but unfortunately it is often musically or technically essential to use these upper positions on the G and D-strings.

What would happen if a tuned vibration absorber were attached to the bridge as is commonly done with 'cellos? The bridge impedance then has two resonance peaks, with a vibrating mass that is much larger than that of the bridge and violin plate alone at these frequencies. If this vibration absorber has significant damping, the resistive mis-match between the string and the bridge at the absorber's resonance frequency may be great enough to eliminate the wolf-note.

Often a mass is attached to one of the short sections of string between the bridge and the tailpiece, and positioned so that it acts as just such a vibration absorber. It is an excellent remedy that may be applied by the performer without sacrificing the instrument's response at other frequencies.

Wolf-notes may occur at other frequencies besides that of the lowest front plate mode, but this is the most troublesome. A minimum value for  $\alpha$  to avoid this problem has not been determined for some work must be done on the perception of wolf-notes before this is possible. Schelleng has, however, published a guideline for predicting the onset of wolf-notes which is of considerable value [9].

Although the causes of the wolf-note have been described there remains much to learn about this phenomenon. Bowing angle seems to have an effect on its presence, possibly due to the polarization of transverse waves on a string and its interaction with the bow. Those waves polarized at  $90^\circ$  to the bridge motion see a near-infinite

impedance at the bridge and the single frequency they vibrate at may help to set up a stable regime of oscillation. Those waves polarized with the same direction of motion as the bridge not only may possess a triple root because of the interaction of string and its termination, but they couple with torsional modes at the bow which may suppress or enhance them. Many other types of wolf-notes exist, which could be studied with time domain modelling of the complete process. Future work may reveal much more about the mechanics of this complex process, and about the perception of complex tones. The bowed string is certainly not the simple system it first appeared to be!

[1] H. Helmholtz, On the Sensations of Tone, Translated by Alex. Ellis, reprint edition, Dover Books, New York, (1954).

[2] C. Raman, On the Mechanical Theory of Strings. This book, long out of print is referred to second-hand.

[3] A. Benade, Fundamentals of Musical Acoustics, Oxford University Press, New York, (1976).

[4] H. Lazarus, Thesis, Technical University of Berlin, 1973. Also reported in L. Cremer, "Die Einfluss des 'Bogendruks' auf selbsterregten Schwingungen der Gestrichenen Saite", *Acustica*, vol. 30, pp. 119-136, (1974).

[5] M. McIntyre and J. Woodhouse, "On the fundamentals of bowed string dynamics", *Acustica*, vol. 43, pp. 91-108, (1979).

[6] R. Schumacher, "Self-sustained oscillations of the bowed string", *Acustica*, vol. 43, pp. 109-120, (1979).

[7] J. Schelleng, "The bowed string and the player", *JASA*, vol. 53, pp. 26-41, (1973).

[8] R. Young, "Inharmonicity of plain wire piano strings", *JASA*, VOL. 24, PP. 267-273, (1952).

[9] J. Schelleng, "The violin as a circuit", *JASA*, vol. 35, pp. 326-338, (1963).

The Violin's Design.

It was shown in the previous chapter that, except for the special case of the wolf-note, the force acting on the bridge due to the transverse string motion is dependant on the bowing procedure alone. It is therefore possible to deal with the remainder of the violin, its bridge and body, in isolation to learn exactly how it converts the energy of the string into acoustic radiation. In this chapter the design of the violin will be examined and the action of several subsystems, the air-cavity, the back and front plates, and the bridge, is studied in detail. All of the parts referred to are illustrated in figure 1.3.

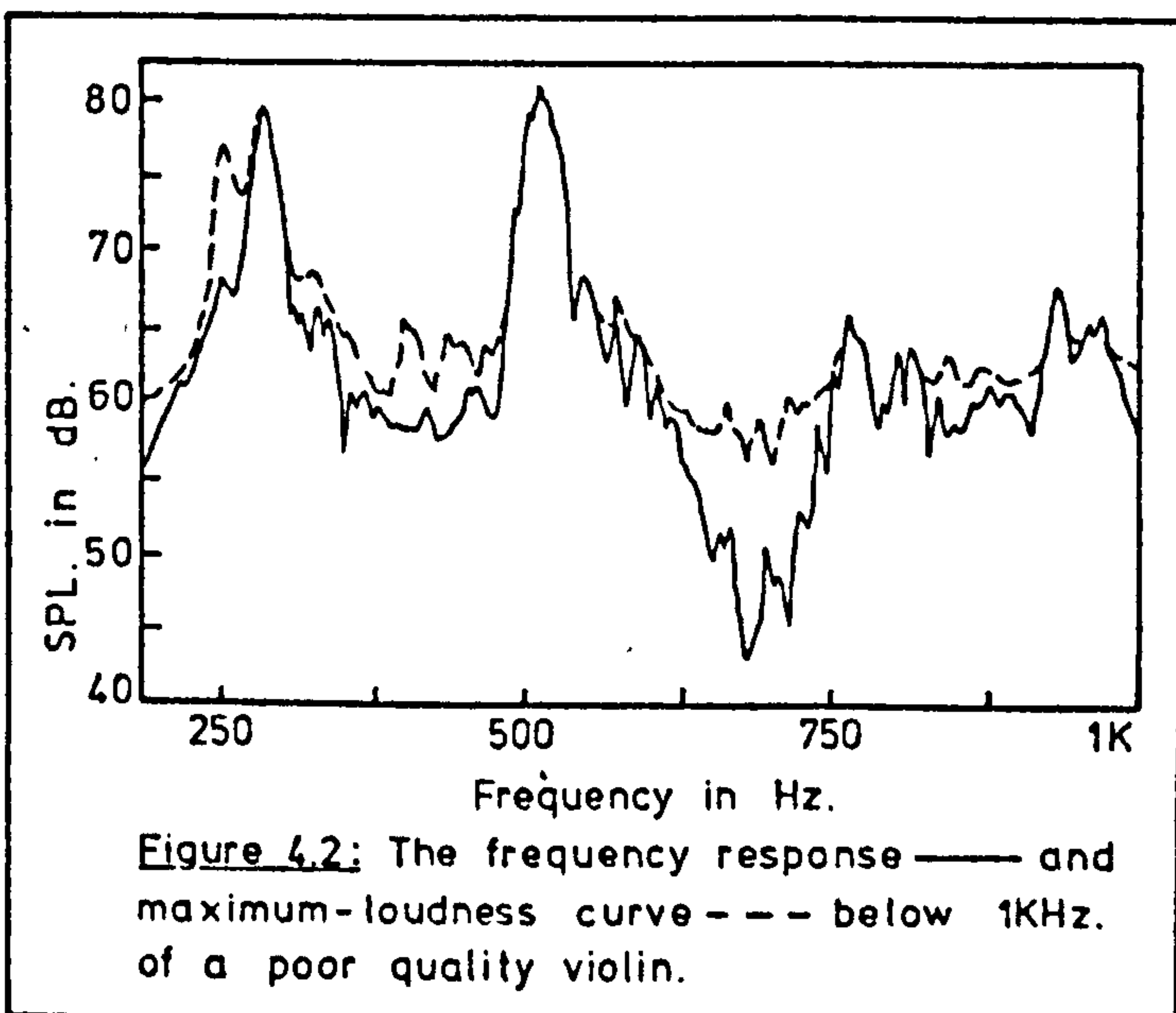
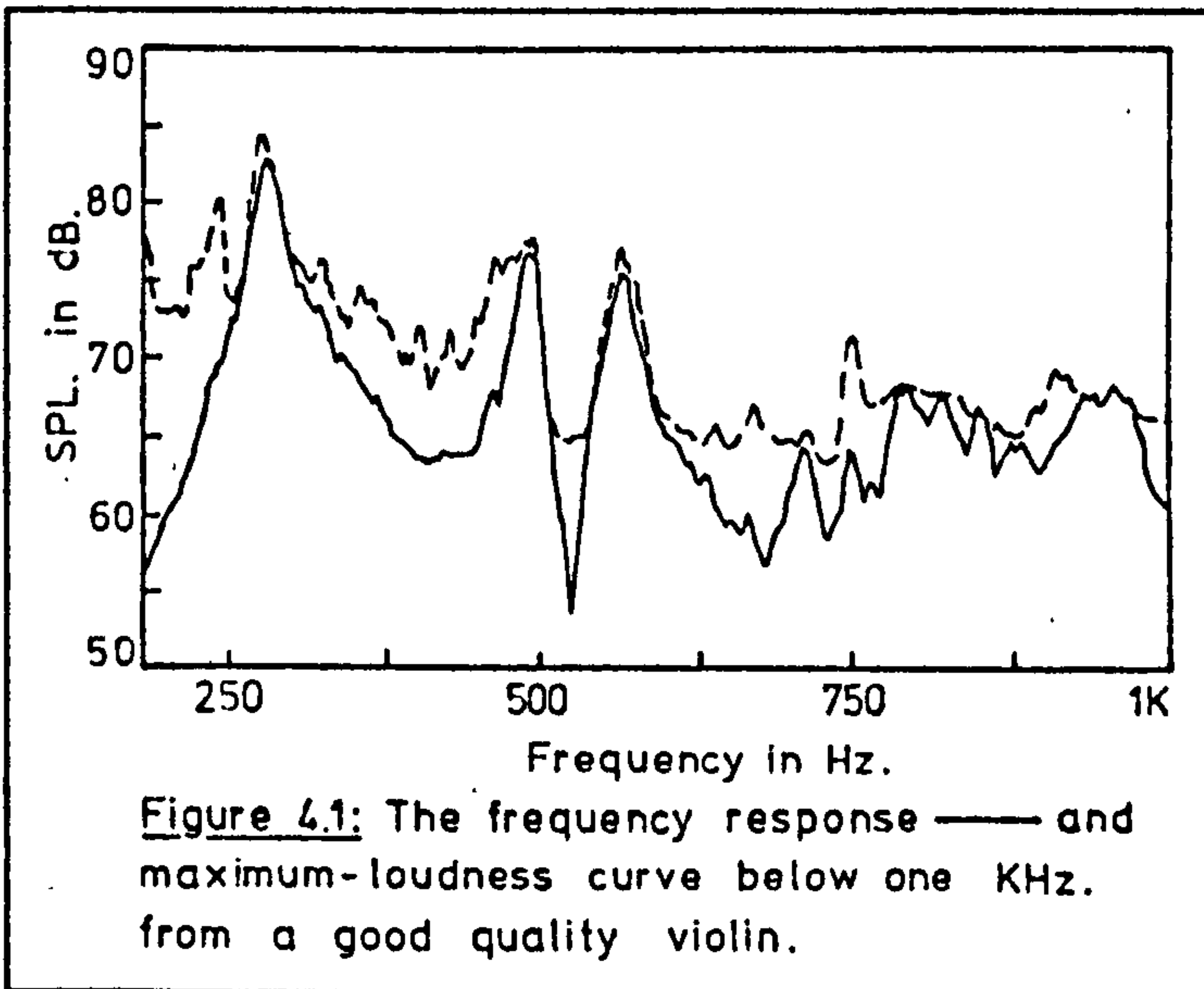
To understand the reasons which underlie the violin's complex design one must keep in mind the ideal frequency response which was described in chapter 1 [1]. Briefly, the violin's frequency response should be as large as possible up to 1200 Hz., quite low from this point to about 2 KHz., once again large up to 4KHz., and fall off rapidly at frequencies above this. The gap between 1.2 and 2 KHz. coincides with the second vocal formant responsible for the irritating nasal sound in m, n, and ng, and its presence in the violin's tone is described by the musician as contributing to a nasal sound. Unlike the loudspeaker, where efficiency is not of prime importance and uniform response is obtained by eliminating resonances, a violin should convert as much as is possible of its input into acoustic energy. This is accomplished by designing the violin to have a modal behavior. Except at low frequencies, this objective is met.

If pure tones were used as an input this would be an unsatisfactory solution as the output level would vary wildly with different notes, but the properties of the bowed string and the human

ear make possible a "quasi-uniform" response.

It's well known that if some components of a harmonic series are missing the ear still assigns a pitch to these frequencies very near to that of the fundamental. This is true even if the fundamental itself is missing. Since a complete harmonic series is present in the bowed string the ear will assign the correct pitch even if the fundamental lies between two resonances and very little sound is radiated at this frequency. The loudness of such a note will be that due to the summation of each harmonic's output so that even though the fundamental

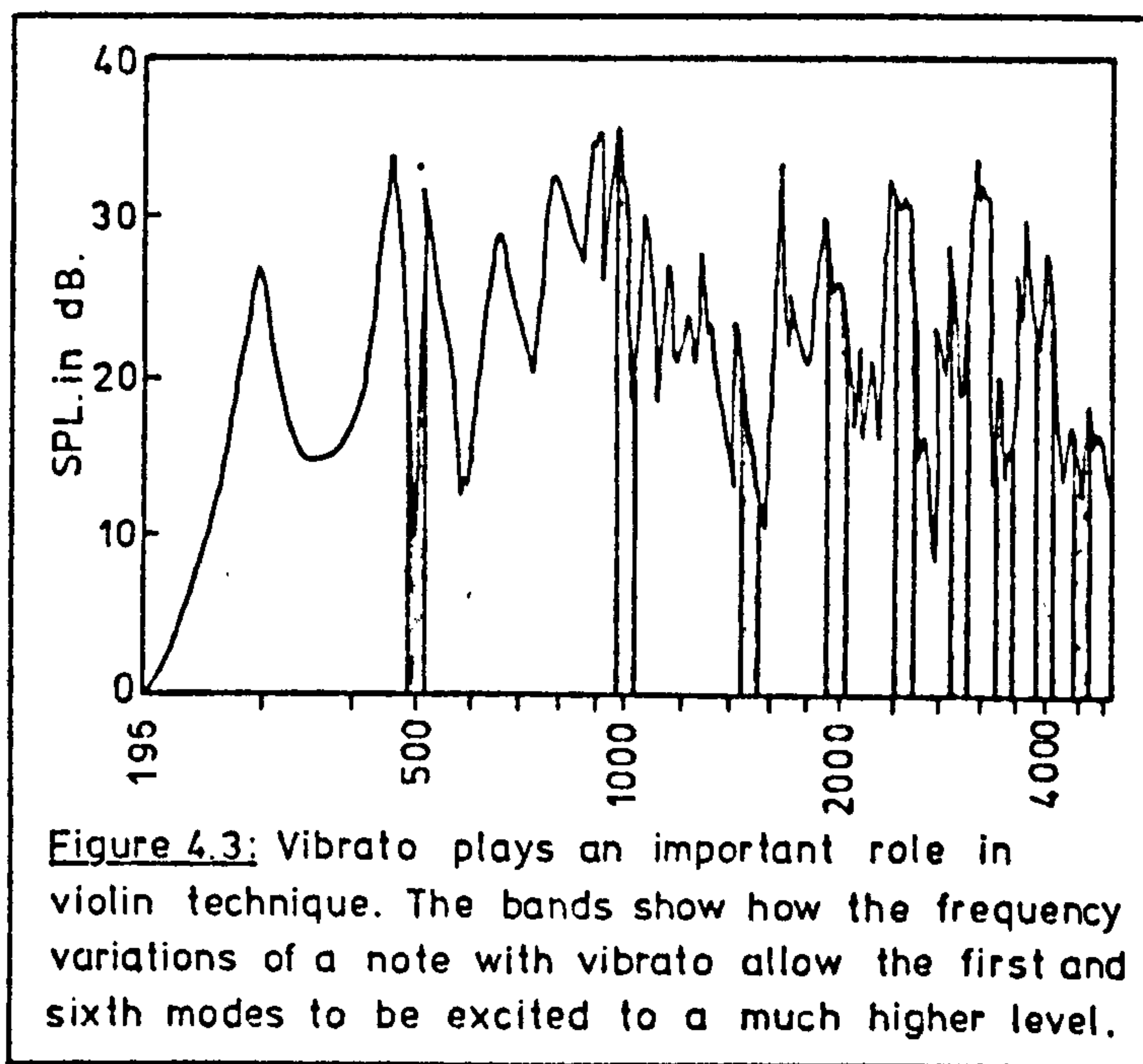
is unimportant, the second or third harmonic may coincide with one of the violin's resonances and produce a loud tone. The importance of this phenomenon is illustrated in figure 4.1 where both the frequency response and maximum loudness curves are plotted. Below the lowest resonance frequency very little sound is radiated although the notes in this region sound quite loud when the violin is bowed.



Curves of this type are obtained by bowing at the maximum bowing force, a definite limit which has been shown to give reproducible results [3].

The spacing of resonances in this example proved to be ideal. In figure 4.2 there are similar curves for a violin whose lowest two resonances are not so favorably spaced. The maximum loudness curve in this case does not show the same degree of uniformity below 300 Hz. as did the previous example. The spacing of these lower resonances is indeed critical, as a comparison of figures 4.1 and 4.2 will prove. This conclusion is not unanticipated for the LTAS tests described in Chapter 1 showed a correlation between the low frequency response and violin sound quality [1].

Violin technique also is well adapted to exploit the modal response. Vibrato, besides contributing to the transient portion of the string's cycle, also ensures that more resonance peaks are included in the



oscillating regime. The frequency variation of high string modes is often large enough to excite a particular violin mode when a steady tone would fall between adjacent resonances. This property is demonstrated in figure 4.3.

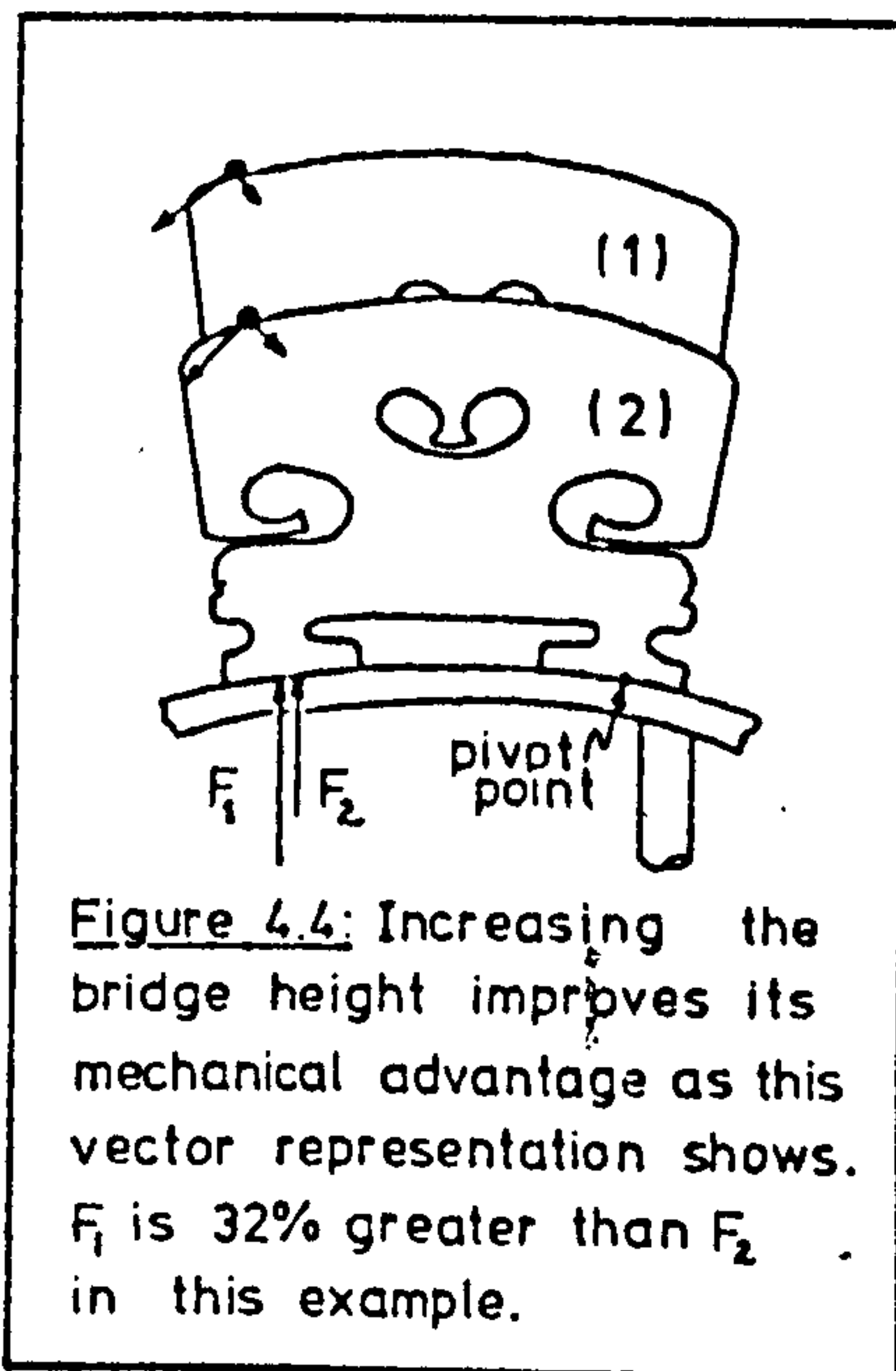
Building a violin without regard for its structural requirements would result in an instrument which collapsed the first time it was strung up. The design must always remain a compromise between the

static and dynamic requirements. The master craftsman is always seeking the optimum.

It is immediately obvious that the violin must be essentially a sounding-board mounted on a load-bearing frame. This is the only construction which can withstand the string tension, about 250 Newtons on a modern instrument, and yet retain a large surface which is light enough to be driven into resonance by the motion of the strings. Another consequence of string tension is the down-bearing force of the bridge. This force is proportional to the angle of the string between the bridge and the nut. There are two ways to reduce this downwards force: reduce the string tension or lower the bridge, and each may have dire consequences.

The force which a vibrating string may exert on the bridge is proportional to its tension and so a compromise between the driving and static forces on the plate must be reached.

Lowering the bridge reduces the string's ability to drive the violin due to the loss of the mechanical advantage which the bridge enjoys. Figure 4.4 will help to make this point clear. Below about 3 KHz. the bridge behaves essentially as a rigid body which pivots about some point near to the treble foot [4]. A high bridge, as shown in the figure, has only a very small component of the dynamic string force directed through the pivot point, ensuring that most of the energy goes into vibrating the plate. When the bridge height is reduced a larger component is directed through the pivot. A compromise between



the bridge's mechanical advantage and the down-bearing force of the strings must be sought.

It is the arching which allows the violin to withstand such a great down-bearing force. Viols, with their flat plates, had to have much smaller string tensions and consequently lacked the power of their arched cousins. The total eclipse of the viol family (except the double-bass) by the violins indicates the importance of string and bridge design and the benefits of arched plates. There is, however, a limit to the amount of arching which can be used. The resonant frequencies of many modes are increased by the arch, as may be the damping. The range of arching which has been used by luthiers is vast, but the extremes in design have never produced results comparable to the beautifully shaped plates of the Italian masters.

---

Usable materials	$E_{-10}$ *10	$E_{-10}$ *10	$\rho$	Structure	$D_{x-8}$ *10 <sup>8</sup>	$D_{y-8}$ *10 <sup>8</sup>	$\delta$ gm/cm
Spruce selected by violinmakers	11.0	.33	.44	anisotropic sheet	1.4	4.2	~.13
Urea-formaldehyde	10.3	10.3	1.5	ribbed	1.4	8.6	.20
Graphite-Epoxy sandwich	40.	31	>.4	2 sheets of composite on a core	1.4	721	.12
maple	5.8		.56	Table 4.1: Materials which may be considered for violin making. $D_x$ and $D_y$ are the orthogonal stiffnesses.			
sycamore	5.6		.56				
poplar	12.7		.55				
white pine	12.0		.50				
Aluminum	69.		2.7				
magnesium	45.		1.7				
fiberglass	69.		1.9				

---

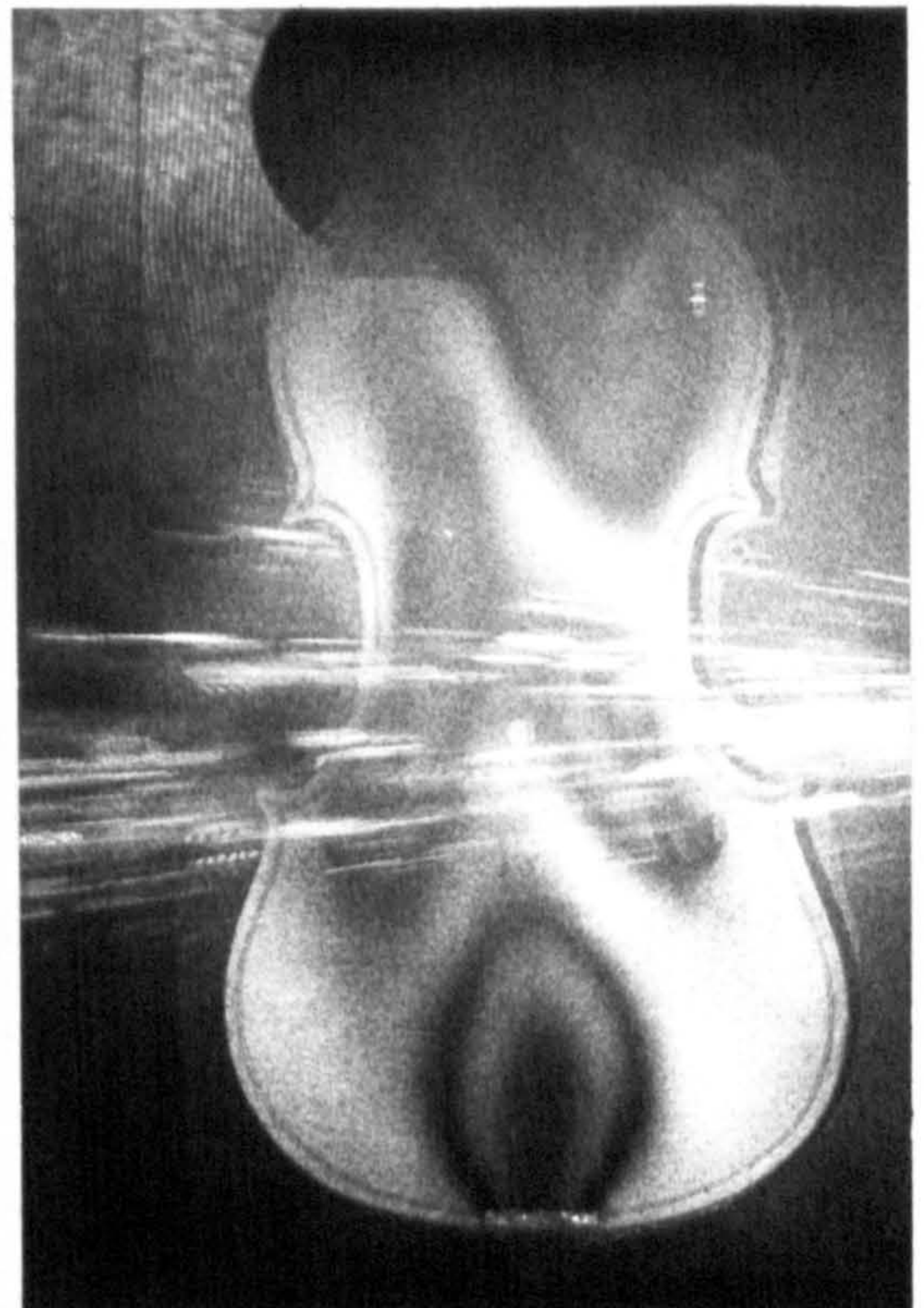
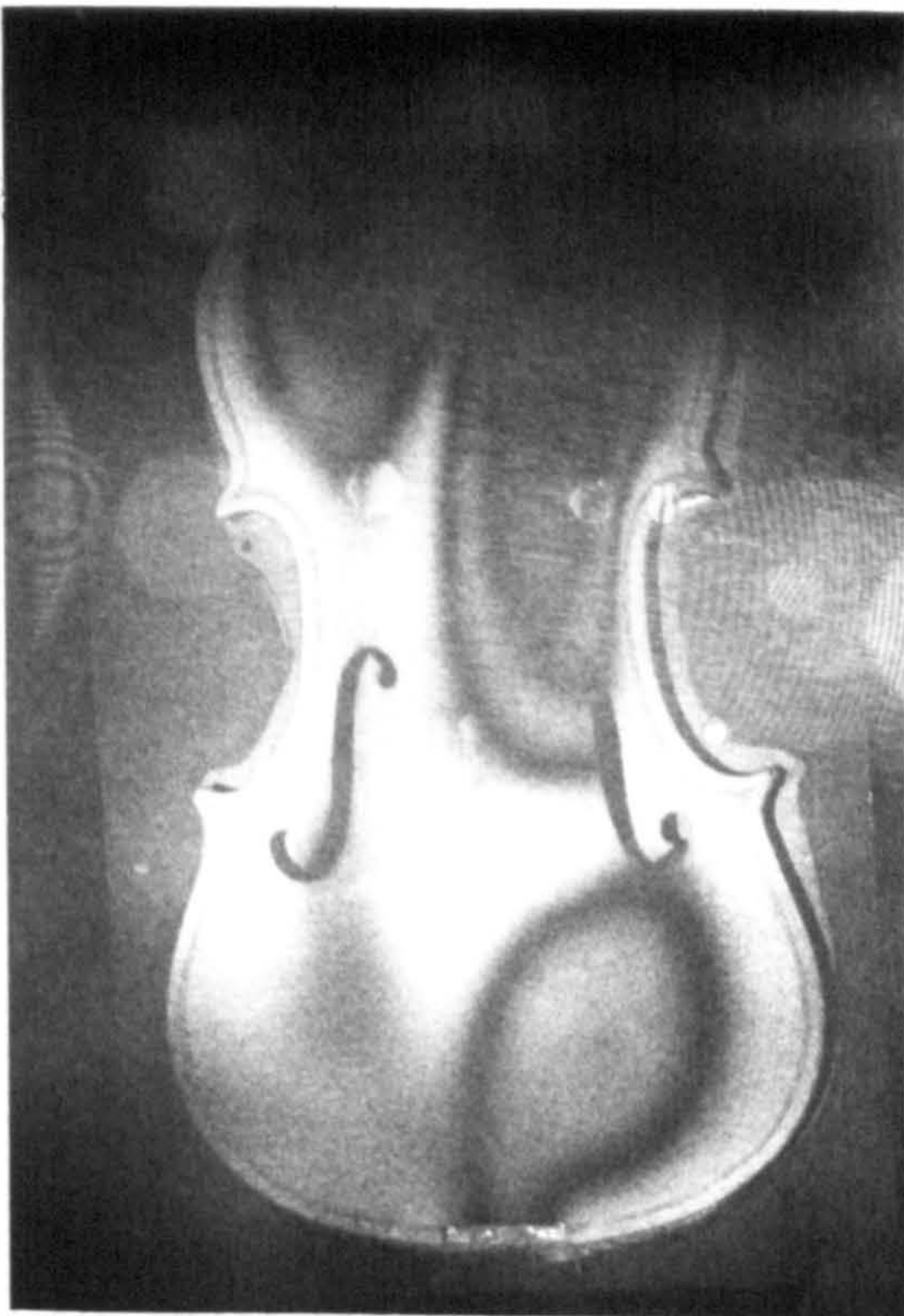
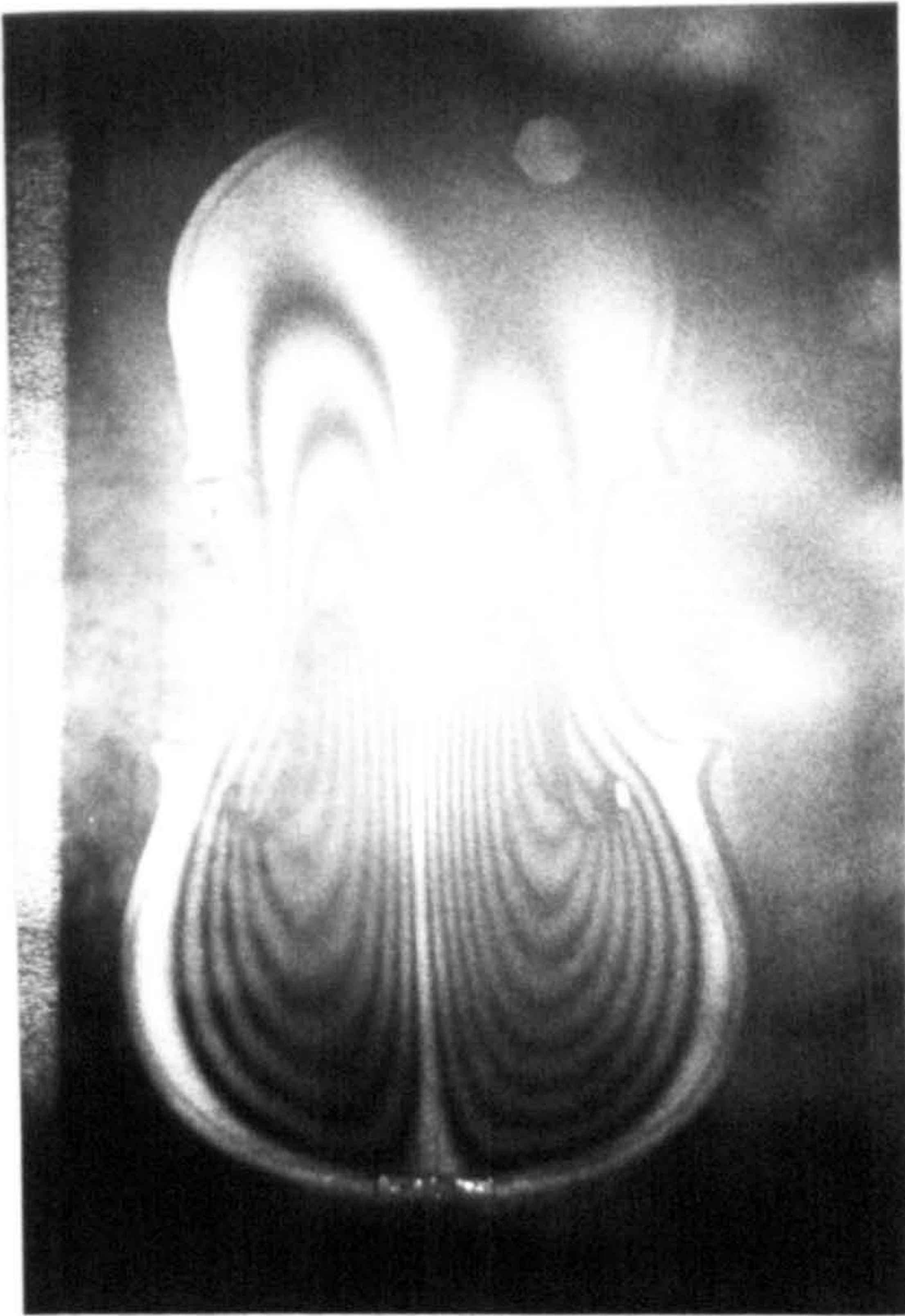
One area in which the luthier need not compromise is in the selection of a suitable material for the belly. The two main requirements, a low density and extremely high stiffness, are met in only a handful of materials. Add to this the benefits of having different wave velocities along perpendicular axes and the most

suitable natural material must be spruce. Mechanical properties for several types of wood, and for some man-made materials which have been used to make violins, are listed in table 4.1.

It may not be clear why these traits are desirable in making violin plates. A plate with low mass will generally vibrate with a larger amplitude than a more massive one. High stiffness is essential to resist the down-bearing force over a long period of time. It also allows the luthier to use a larger plate. The third point is rather more obscure.

Any bowed instrument must be designed so that the strings can be reached one at a time. It is for this reason that the top of the bridge is curved. This also means that the body must be rather narrow so that the highest and lowest strings may be bowed- thus the narrow waist of the violin. The kit, or dancing master's fiddle, was narrow for its entire length. One of the reasons for its sudden disappearance was its small radiating surface which emitted a feeble sound when compared to the violin.

An additional advantage of the narrow-waisted plates is their ability to divide into separate vibrating areas, each with its own series of resonances. A noticeable increase in the modal density is made possible by the sudden change in wave impedance at the top and bottom of the waist. The vibration holograms of figure 4.5 clearly demonstrate this point (plate orientation and mode numbers are shown in figure 4.5- the number 2,1 indicates that there are two antiresonances along the violin's length and one across it). But what has this to do with the wave velocities in wood? It all becomes clear when one notices that the plate's second resonance has two anti-nodes across the plate rather than along it! This surprising result is explained by the difference in the stiffness of wood across and along the grain. Since



Figures 4.5: Holograms of several of the front plate modes. [1,2] at 500 Hz., [2,1] at 635 Hz., [2,2] at 800 Hz., and [3,1] at 920 Hz.

plate is a dispersive medium, the low modulus across the grain in wood reduces the wave velocity considerably in that direction so that the [1,2] resonance occurs at a frequency much closer to the [1,1] mode. Holograms from figure 4.5 show that this is much closer to the [1,1] mode. These two resonances would normally be about two octaves apart in a uniform plate with the mean dimensions of a violin. When using spruce the [1,2] mode can be used to increase the modal density in the violin's weak, low frequency range, giving a more uniform response in the assembled instrument.

Table 4.1 lists some structures which have different wave velocities in the x and y directions. The ribbed assemblies prove to be more massive than spruce but the composites, when used in a sandwich construction, compare favorably. These composite materials are a relatively recent engineering advance. By embedding fibers with a high tensile strength and modulus in an epoxy matrix the material takes on some of the properties of each. Fiber-glass is the most widely known example of this. Glass has a high tensile strength but is of course very brittle. Glass-fiber is extremely flexible, however, and when imbedded in a matrix of epoxy a light, flexible, yet strong composite is formed. Graphite and Boron fibers are also used, but their advantage in terms of stiffness and strength is somewhat offset by their cost. Both of these materials are usually used with the fibers running unidirectionally which gives a material with essentially the same properties as of the matrix alone when measured across the "grain". In this form it has been used with great success for golf-clubs, bicycle frames, turbine blades, even violins [5]!

When the stiffness to mass ratio is important, as it is in violins, two layers of composite are used to form a sandwich around a light-weight core. On bending this core is subject to a considerable

compressive force normal to its surface yet many light materials are able to withstand such a force. Cardboard has been successfully used as a core for violin plates [5].

In one area graphite-epoxy sandwiches have a distinct advantage over spruce: the material will not vary greatly from piece to piece as do samples of wood. Add to this the potential to adjust the damping through the selection of core material and it would appear that an ideal substitute is available for wood. Yet any commercial exploitation of this material has so far met with little success. This is not entirely surprising for a violin is usually valued as much for its aesthetic qualities, the figuring of the wood and depth of finish, as for its acoustic attributes.

Once the material for the plate has been selected, it needs to be fashioned into the size and shape which will produce the greatest amount of acoustic energy and yet still resist the force of the strings. Increasing the plate size may well lower the [1,1] resonant frequency, which is a great advantage, and increase the radiating area too, but these are offset by an increase in bending moment. The plate thickness must then be increased, which raises the resonant frequency and increases the vibrating mass. A viola, which has its [1,1] resonance much nearer to the bottom of a violin's range, sounds nothing like a violin when strung to the same pitch- its tone color lacks the higher harmonics and power because of the large plate size.

There is still another way to increase the output of the [1,1] resonance without sacrificing a great deal of strength. Cutting the f-holes, the long slots near the middle bouts, changes the plate's boundary conditions considerably. With the free edges along the central vibrating area the volume of air displaced by the vibrating plate is greatly increased. A rectangular plate, clamped on all four

sides, displaces almost twice as much air when two of these boundaries are removed, and a violin benefits similarly.

Strength is retained by using the sound-post near the treble bridge foot and the bass-bar beneath the bass foot to spread the load.

If the front plate was designed so that its lowest mode was near the bottom of the violin's compass it would be handicapped by a very high mass and its output thereby significantly reduced. Instead, this mode is usually located somewhere about an octave above this at 440 Hz., where the second harmonic of these low notes will excite it strongly. The large gap in between 220 and 440 Hz. is filled in an entirely different manner.

When an opening is made into a cavity, such as the f-holes of a violin or the rose of a guitar or lute, a Helmholtz resonator is formed with the enclosed volume of air driven by the motion of the plates. This is analogous to a base excited, one degree of freedom mechanical system. The resonance frequency may be adjusted by changing either the cavity volume or the hole area. In the violin it is best located between 220 and 440 Hz., 290 Hz. having been shown to produce the best results [6].

Already it may be seen that the design of a violin is a compromise between several conflicting and interacting factors. These are most easily summarized in tabular form (see table 4.2 below).

The greatest violin-makers, Stradavarius, Stainer, the Amatis, and the Guarneris, experimented throughout their lives on violins with greatly varying shapes and sizes. Each developed a characteristic style, a unique solution to the infinitely varied possibilities of violin design. Those instruments which have the best combination of acoustic and aesthetic values have been copied for well over two and a half centuries. It is a fitting tribute to their work.

---

Action	Desireable Consequences	Indesireable Consequences
Increase plate thickness	-Better able to resist the bridge force	-Increases vibrating mass -Raises resonance freqs.
Increase plate dimensions	-Lower resonance freqs. -Increase radiating area	-Increases vibrating mass -Increases bending moment
Raise bridge	-Better mech. advantage -More bow clearance	-Increases down-bearing force of the strings
Reduce string tension	-Decreases down-bearing force of the strings	-Less force to drive the violin
Increase the arching	-Better able to resist the bridge force	-Increase damping -Raise resonance freqs.
Cut f-holes	-Helmholtz resonance -Lower resonance freqs. -Greater radiating surface	-Weakens plate

---

Table 4.2: A summary of the contradictory requirements which determine the design of the violin, especially of its front plate.

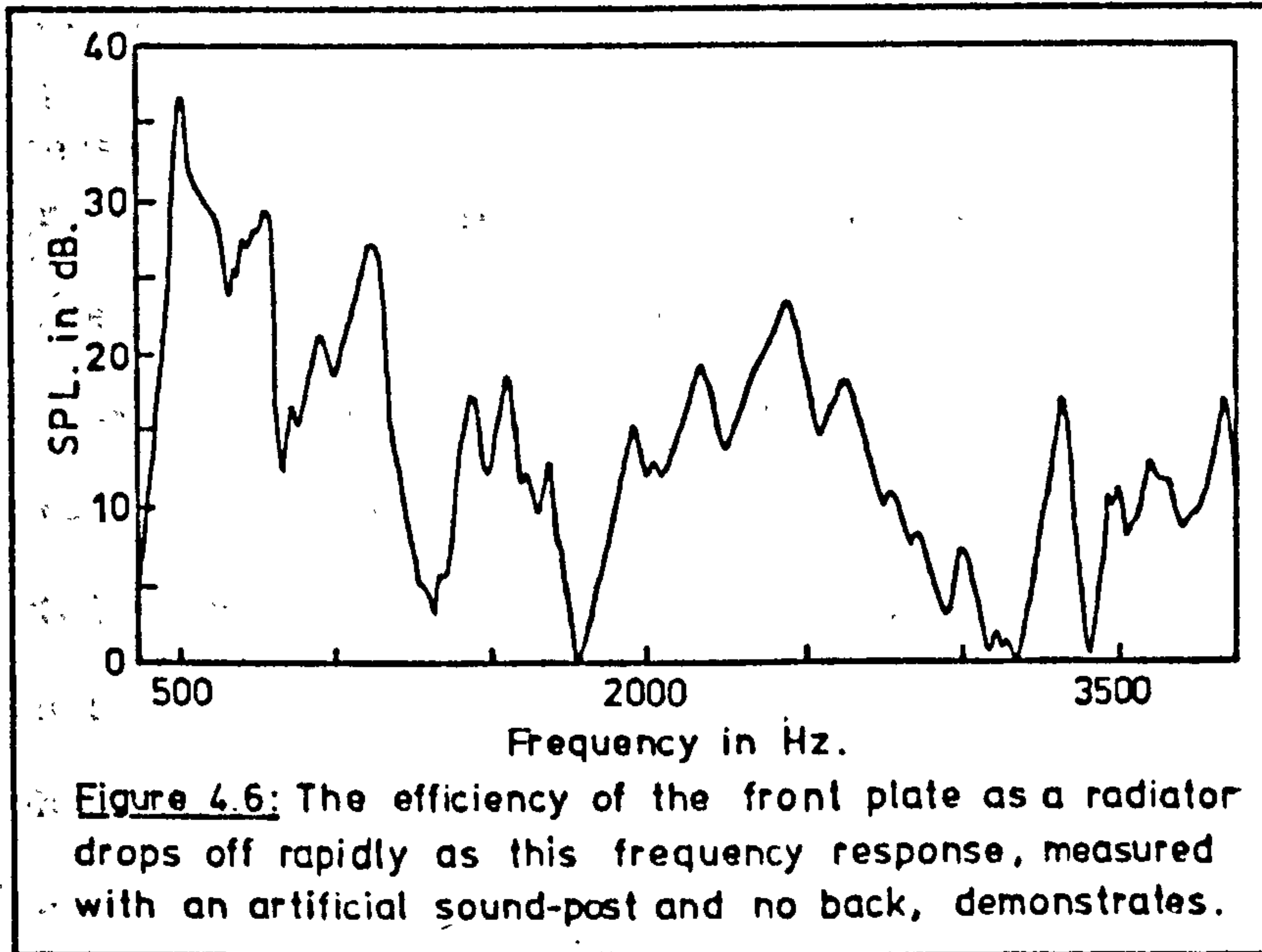
---

#### The Bridge as a Transmission Element.

Whereas the spacing of resonances is critical at low frequencies, above about 1 KHz. the modal density is high enough so that the violin-maker need only be interested in the trend of the frequency response, not the particulars.

As the frequency of excitation increases the plate must divide into more vibrating regions, each with smaller and smaller area. This may easily be seen in figure 4.5. At, say, 800 Hz., where one would expect the front plate to be divided into four regions across the lower portion, the wavelength in air is much larger than the regions themselves and a major portion of energy remains in the near field shuttling from one area to another. The radiation efficiency drops quite quickly as the plate divides into more vibrating regions. A

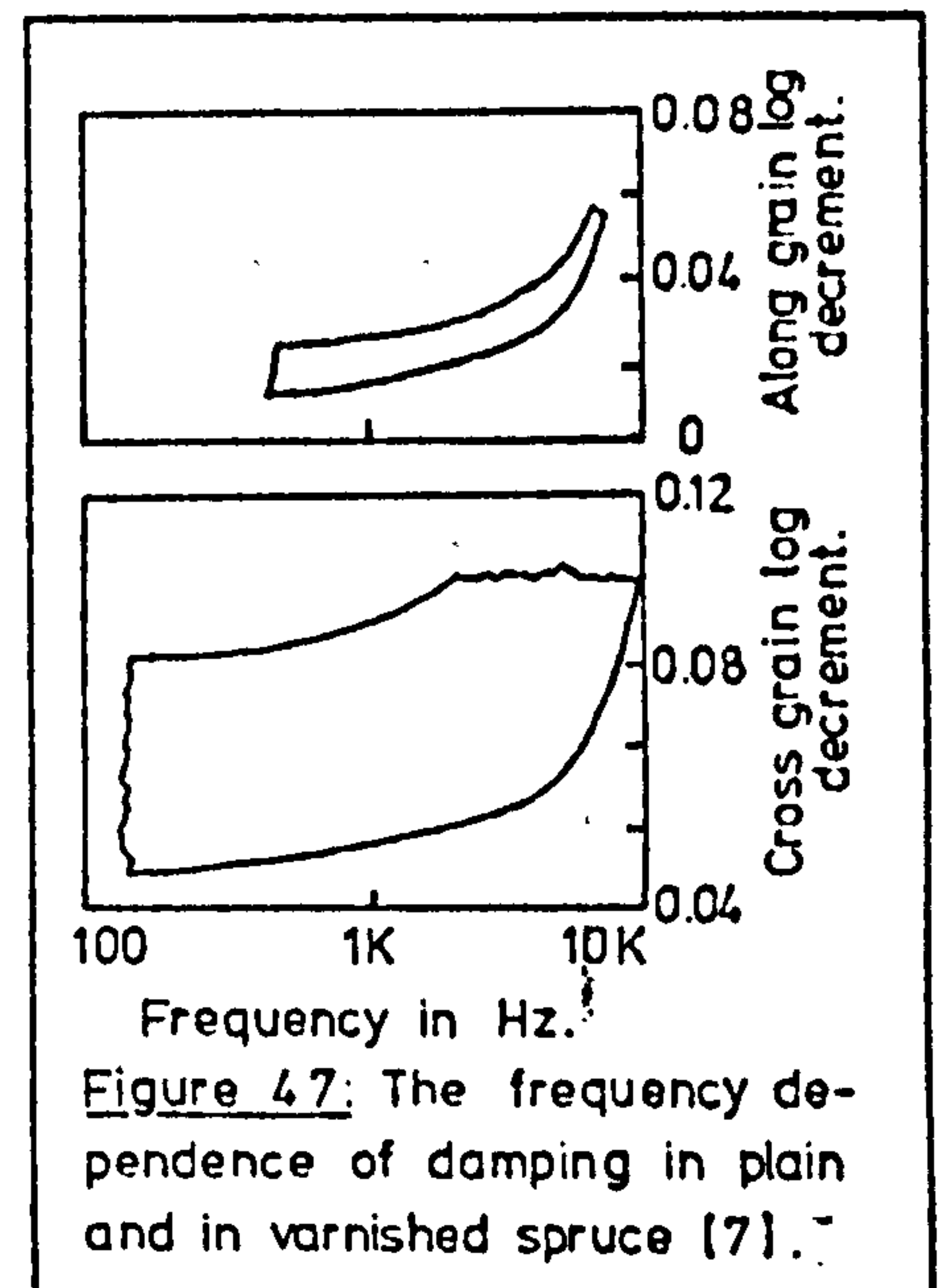
trend towards reduced acoustic output with increasing frequency should be expected, which may be verified by the frequency response curve of an assembled violin without strings or bridge, in figure 4.6 below. The increased damping with frequency exhibited by spruce also contributes to this trend.



The skilled luthier can make use of this reduced output to eliminate the irritating nasal sound which occurs with acoustic output around 1200

Hz., but how then is it possible to obtain the peak in response from 2 to 4 KHz. which the LTAS tests showed were so important in a good violin? It is the unique design of the bridge and its action as a single degree of freedom transmission element which gives a significant response over this range. A noble violin needs an expertly made bridge to reach its full potential.

A glance at figure 4.7 shows that a violin bridge consists essentially of a solid base with a mass connected to it by a narrow section which acts



as a stiffness element. This simple system is constrained from translational motion and so possesses three degrees of freedom, of which two may be dismissed as lying normal to the plane in which the string forces act. Those modes which occur because of the continuous nature of the bridge are at a much higher frequency than these "lumped parameter" modes.

The characteristics of such a transmission element are simple and appear in figure 4.8. With the bridge adjusted properly so that the transmission peak is at about 3 KHz. the violin should display an increased output in the important 2 to 4 KHz. region, which may be observed in the frequency response curve of figure 4.10. A relatively broad peak in transmission is desirable if output is to be enhanced throughout this region.

The response of the bridge can have a dramatic effect on a violin's tone

quality. Take, for example, two bridges with their resonances at 3 kHz., but with greatly different values of mass and stiffness. The lighter bridge would produce the higher response at 3 kHz., but while this would make a violin sound bright, nasality would inevitably be increased. Such a tone is favored by soloists as it stands out well against an orchestral background, but is unsuitable for the subtleties of chamber music. The more massive bridge, with a "darker" sound caused by a decrease in output around 3 kHz., would probably be the choice in such a case. The number of possibilities which this presents

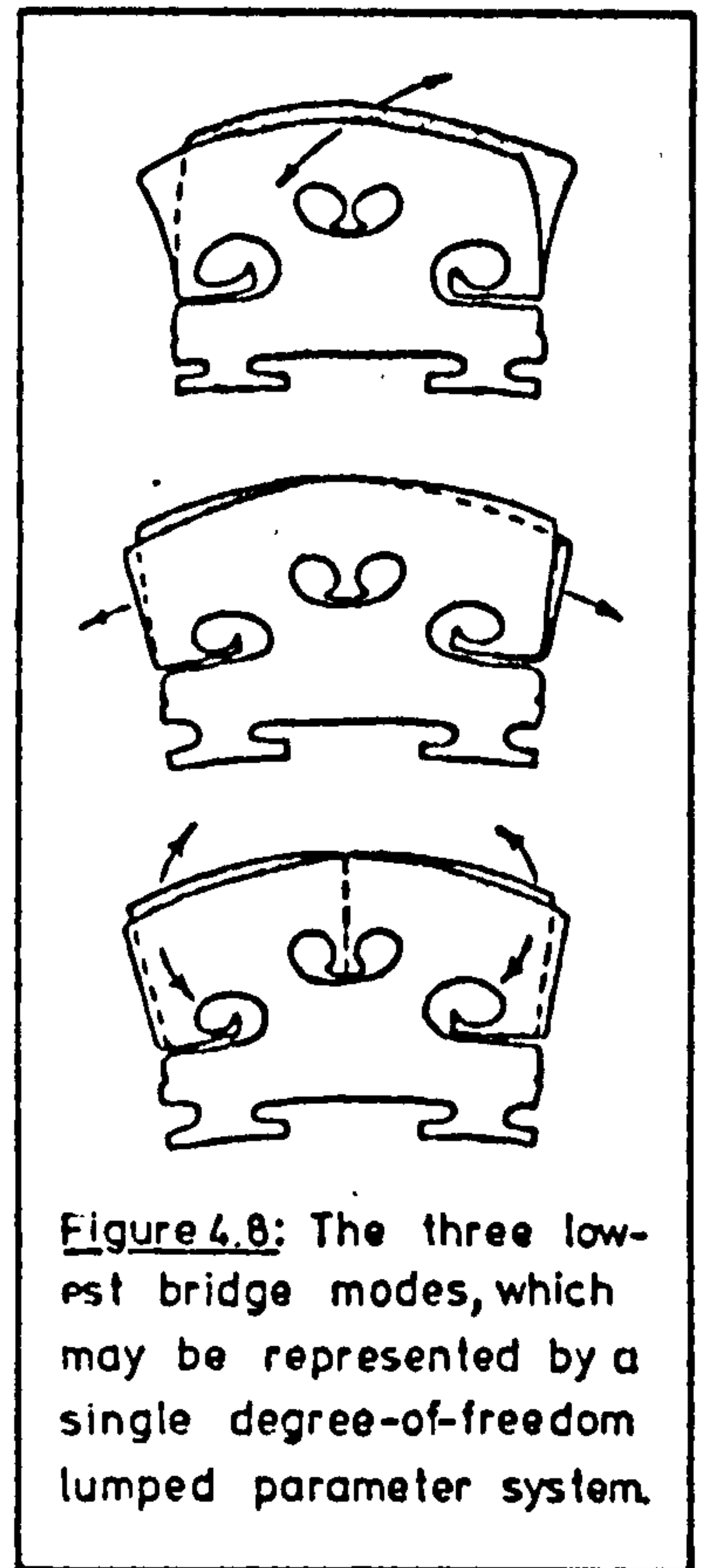
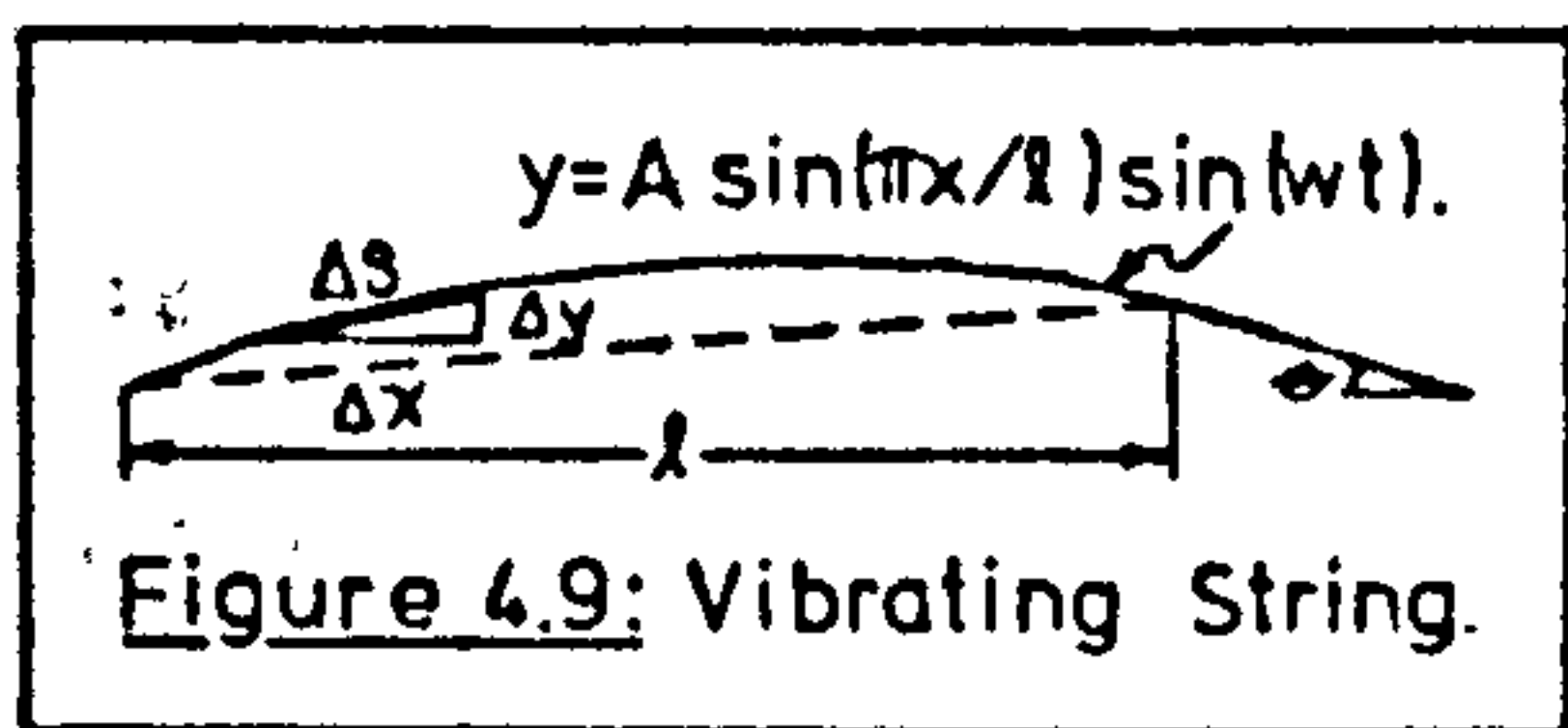


Figure 4.8: The three lowest bridge modes, which may be represented by a single degree-of-freedom lumped parameter system.



explains the great variety of shapes in which the bridge is found [8].

Thus far it has been assumed that the motion of the bridge occurs only in its own plane. In the analysis of string motion it was assumed that changes of string tension are only of second order and may be ignored however, Arthur Benade, in his excellent book Musical Acoustics, maintains that these changes in tension produce an "indirect force" which acts on the violin. He states that this force plays an important, perhaps even dominant, role when playing fortissimo passages [9]. The argument is straightforward. There is in figure 4.9 a string vibrating in its lowest mode with an amplitude of A. The differential length  $\Delta S$  is

$$(4.1) \quad \Delta S = \sqrt{\Delta x^2 + \Delta y^2} = \Delta x \sqrt{1 + (\Delta y/\Delta x)^2} .$$

As  $\Delta x, \Delta y \rightarrow 0$  this becomes a differential which, using the binomial expansion, is

$$(4.2) \quad dS = 1 + (dy/dx)^2/2 .$$

On integration this yields

$$(4.3) \quad S = L + \frac{A^2 \pi^2}{4L} \sin^2(\omega t)$$

The change in length is related to the tension by Young's Modulus and the component of dynamic force directed downwards is

$$(4.4) \quad f(t) = \pi r^2 E (A \pi / 2L)^2 \sin(\theta) \sin^2(\omega t) .$$

For a typical violin E-string  $L=32.5$  cm.,  $r=0.014$  cm.,  $\theta=6^\circ$ ,  $E=1.9 \times 10^{12}$ , and  $F(t)=2.5 \times 10^5 A^2 \sin^2(\omega t)$ . It is interesting to note that this form of excitation occurs at a frequency of  $2\omega$ :

$$(4.5) \quad f(t) = \frac{\pi r^2 E (A\pi/2L)^2 \sin(\theta) \cos(2\omega t)}{2}.$$

This indirect force may be compared with the second harmonic of the direct excitation applied by the string as both have the same frequency. If the Helmholtz approximation for string motion and the same E-string with a tension of  $7.6 \times 10^6$  Dynes are used, then the magnitude of the second harmonic direct force is about  $7.3 \times 10^5$  A Newtons. For all amplitudes likely to be encountered, (the approximations break-down with large amplitudes in any case), this direct force is at least an order of magnitude larger than the indirect force. One should not, however, assume that there is no musical importance of this phenomenon. It would be of value for someone to explore, both mathematically and experimentally, this indirect form of excitation and to compare it with the musical consequences of the bowing process which, though small, have already been shown to be of importance.

#### The Function of the Sound-post and the Back Plate.

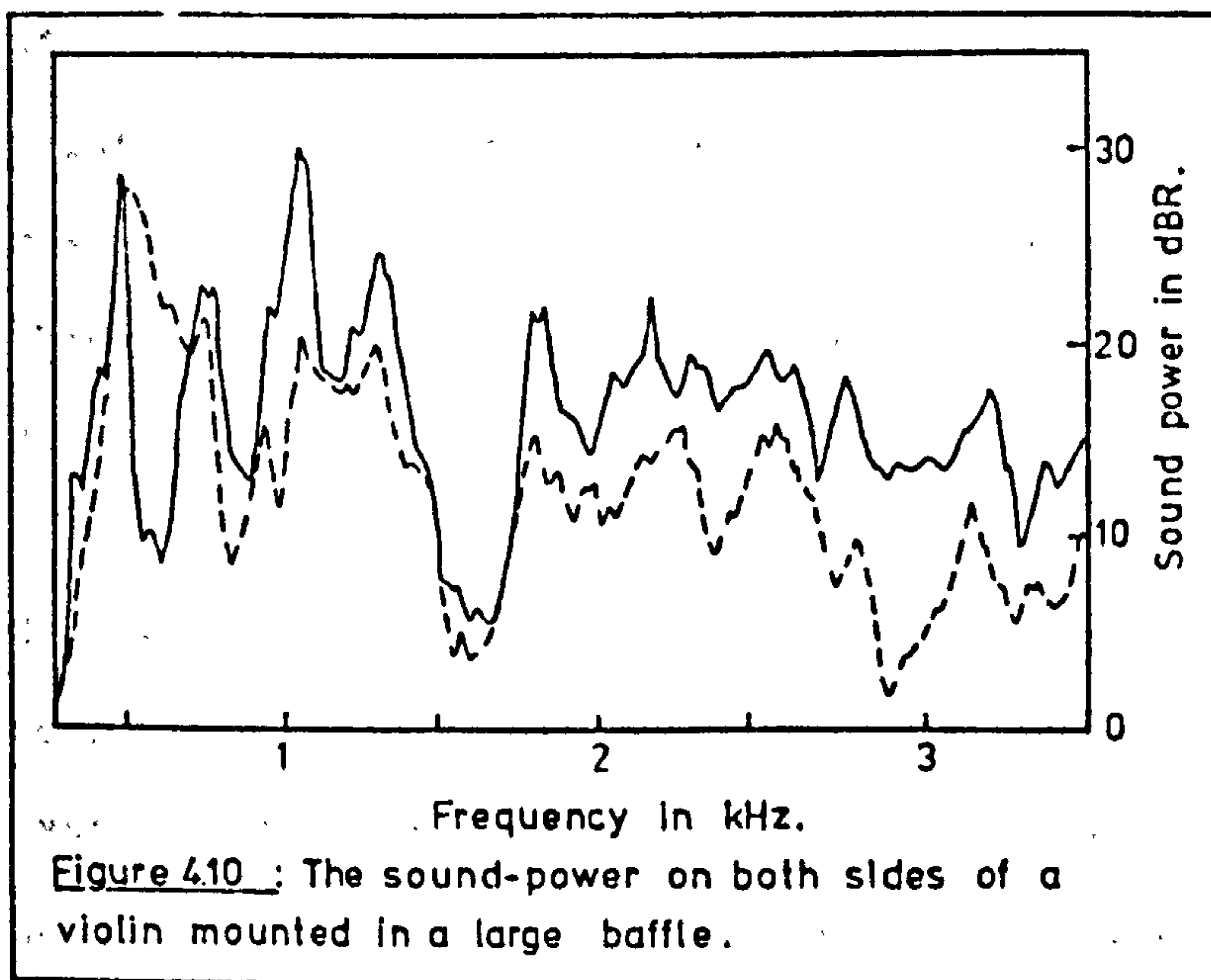
It has already been said that the sound-post serves not only to help support the belly against the down-bearing force, but also acts as a pivot for the bridge. (See figure 4.4) The post is made of spruce but its properties and even dimensions vary considerably from one to another. It is held in place by a jam fit between the plates which is

quite secure (unless the strings are loosened). Its importance as a resonator may be ignored for its lowest longitudinal mode occurs at about 20 KHz., but as a direct coupling between the plates its location is of extreme concern. Replacing the post or moving it slightly may entirely alter the character of an instrument. Such is its importance that the French refer to it as "l'ame", the soul of the violin. Obviously the sound-post will alter the stiffness of the belly and so play an important part in determining its resonance frequencies. What, ideally, is its function and how does it improve the violin's response? If not for the sound-post and bass-bar, the impedance of the plate at each bridge foot would be similar and the bridge would rock about its center of gravity when driven by the string. With the feet moving equally but in opposite phase excitation of the second plate mode (figure 4.5) would be very efficient but the first mode would hardly be excited at all. With one foot constrained the first mode can be driven much more effectively. Fixing the treble bridge foot has an advantage as the leverage is increased for the lower strings in the critical low frequency range. Unfortunately the second mode would be suppressed if one foot remained stationary. If, however, the post presented an impedance to the belly which was very high at the [1,1] resonance frequency, yet matched the plate's impedance at the [1,2] resonance frequency, both modes could be efficiently driven by the bridge. This simple view of the sound-post's function is of course far from ideal, but it does demonstrate that the impedance which it presents to the front plate is crucial to the violin's performance.

Whatever impedance characteristics the post has arises from its contact with the back plate. Thus one would expect that the back is designed not solely as an efficient radiator but as an impedance device as well. The fact that the back is made from maple, which is much more

dense than spruce, lends support to this idea. It would be interesting to measure the proportion of sound radiated from the back plates of some of the best violins, but such a project is beyond the scope of this work. Instead, a good factory-made violin of the 1920's was tested with some interesting results [10].

In this experiment the violin's front plate was removed and the ribs, with the back still in place, were fitted into an outside mould, such as used by some luthiers for constructing the bouts. Caulking compound was used to seal any air gaps and then the front was glued back into place. The mould, with the violin sealed into it, was then attached to an 8'x 8' baffle and placed in an anechoic room. Seventeen microphone positions on each side of the baffle were used to measure the sound power of the violin, with the sound-post in place. These re-



sults appear in figure 4.10, and suggest that the back plate radiation is about 5 dB less than that of the front plate, except at the back's [1,1]

resonance. Clearly a balance must be struck between the two requirements of the back at low frequencies and this is an area which could benefit from further study. The radiation of the back plate in the test violin was not of great significance and supports the view that its main function is as an impedance device, although in the best instruments its acoustic contribution may be a noticeable one.

The action of the other internal component, the bass-bar, is less fully understood. It is generally assumed that its main dynamic role is in transferring vibrational energy to the upper and lower portions of the belly, but there is still a great deal to be learned about it. Is it possible that it provides a smooth change in impedance across the end of the f-holes? This is yet another area to which study should be applied.

#### Modelling the Helmholtz and Front Plate Modes.

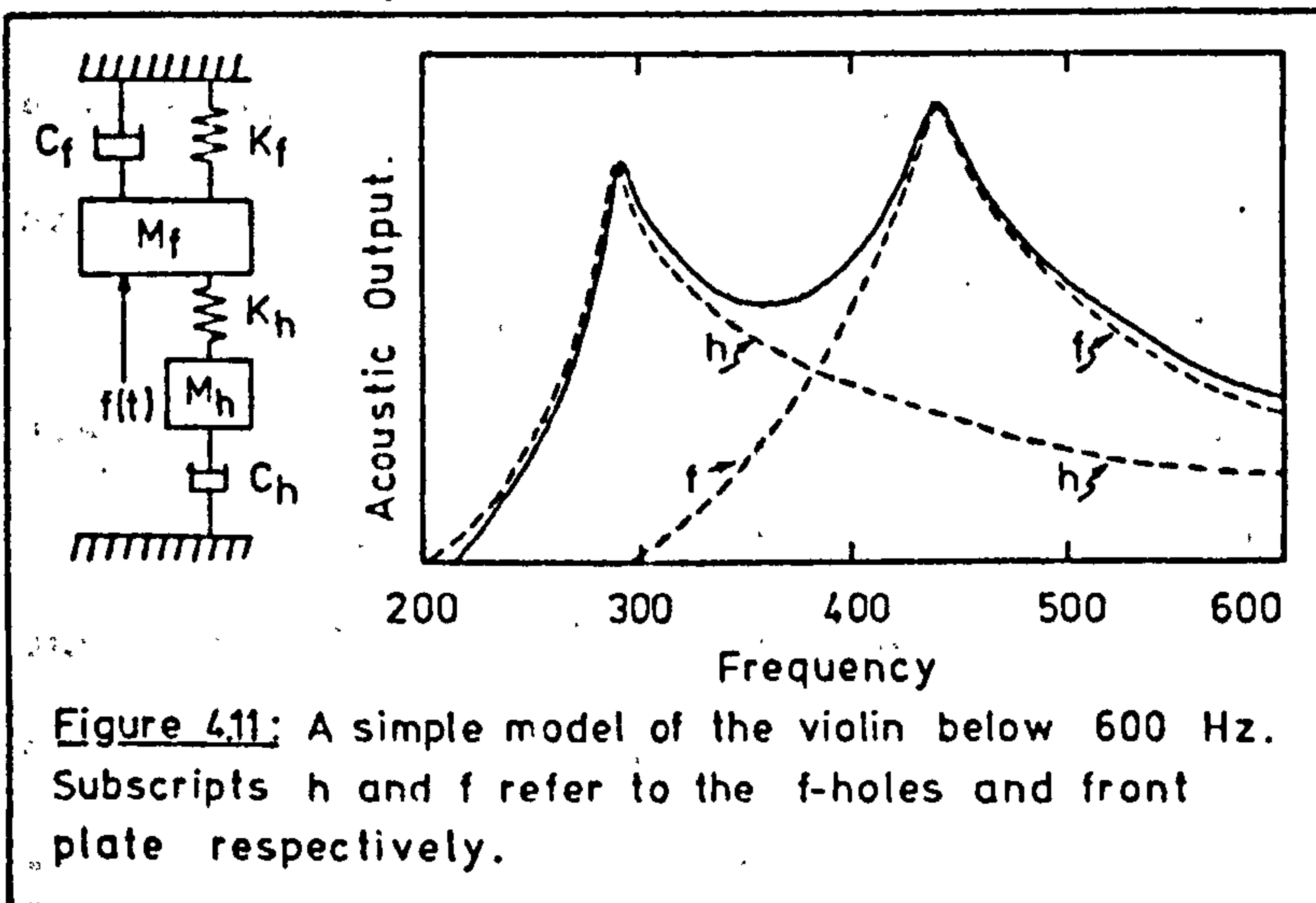
The importance of the sound-post, and the difficulties involved in modelling the coupling between the two plates, has led researchers to include it implicitly in their models. John Schelleng made the first significant contribution to the understanding of the violin's action by treating the [1,1] front plate and Helmholtz air modes as coupled resonators [11]. Electric analogues were used in his work, however, throughout this thesis a mixture of mechanical and acoustic analogues are used.

Schelleng limited the frequency range in his model to below 600 Hz. so that of all the belly's resonances only the lowest one needed to be considered. This mode may be represented as a lumped parameter system with appropriate values of equivalent mass, stiffness, and damping. To determine these values for the front plate Schelleng added a small mass to the region of maximum acceleration and measured the shift in the plate's resonant frequency. (Adding the mass at another point with a smaller acceleration would have had a smaller effect on the resonant frequency.) From this data and the half-power points it is possible to determine all of the equivalent parameters for the plate. As this data was obtained from an assembled violin, the effects

of the sound-post, back plate, radiation impedance, and any coupling to the cavity's air modes were intrinsic properties.

The Helmholtz resonator may be treated in the usual way: since the dimensions of the holes are much less than the wavelength of sound in air throughout the frequency range of interest their shape is unimportant and an equivalent piston with the same area may be used to represent each hole. Radiation impedance accounts for most of the reactive loading and is usually calculated by allowing two end correction terms on each f-hole. The mass found in this manner may be lumped into one component of the model.

It is the change in cavity volume which takes place as the plate vibrates that drives the air mode. This is analogous to a base excited mechanical system, such as that shown in figure 4.11.



Schelleng's electrical analogue produced frequency response curves similar to the broken line in the figure for each mode's vel-

ocity. Using the mechanical analogue and a digital computer it is possible to duplicate his results. The total acoustic output is not, however, simply the sum of these two curves which must first be converted to sound pressure levels. The phase relationship between the two sources must be considered before it is possible to understand the way in which these modes interact. Since the radiators are much smaller than the wavelength of sound in air their exact shapes are not

critical. If it was possible to find an equivalent area such that it displaces the same amount of air when it moves with the velocity of the f-holes or the plate at its driving point, it would be simple to estimate the SPL. It is convenient to make this estimate at a point along the axis normal to the violin plate at its center.

For the f-holes it may be assumed that the air moves through them as a uniform mass. The volume flow is then the product of the area and velocity. To determine the volume flow (the product of the equivalent area and the velocity) of the front plate one needs information about the mode shape which is readily available from vibration holograms. Graphical integration performed initially by hand and later by computer gave an equivalent area for the test violin of  $150 \text{ cm}^2$  in its [1,1] mode. Each f-hole had an area of  $6.3 \text{ cm}^2$ . The broken lines in figure 4.11 represent the SPL at one meter on axis calculated for the f-holes and the plate.

At frequencies well below the Helmholtz resonance the air mass displacement will be in phase with its excitation. When the plate moves inwards to compress the air in the cavity, the air mass will move outwards. The radiation from these two sources will then be  $180^\circ$  out of phase so that most of the energy will remain in the near field. Air will shuttle back and forth between the plate and f-holes with very little radiation taking place. One could also say that the force and particle velocity are in quadrature so that the work done is very small.

At frequencies well above the Helmholtz resonance the air mass displacement is  $180^\circ$  out of phase with its forcing function, so that when the plate moves inwards, compressing the enclosed air, so too does the air mass. Radiation from the two areas is then in phase and the output will be approximately that of the sum of curves "h" and "p" in

figure 4.11.

The phase difference between the two resonators at frequencies close to the Helmholtz resonance passes through  $90^\circ$  and the two have little effect on each other.

There can be no doubt that this form of coupling is of benefit. Output is greatly increased, as in the figure, between the two resonances, far beyond either one considered in isolation. Below the air resonance the radiation is reduced but it is almost impossible to produce any significant output in this range in any case. Strong excitation of upper harmonics, especially the second, will produce sufficient output at pitches below the Helmholtz resonance frequency.

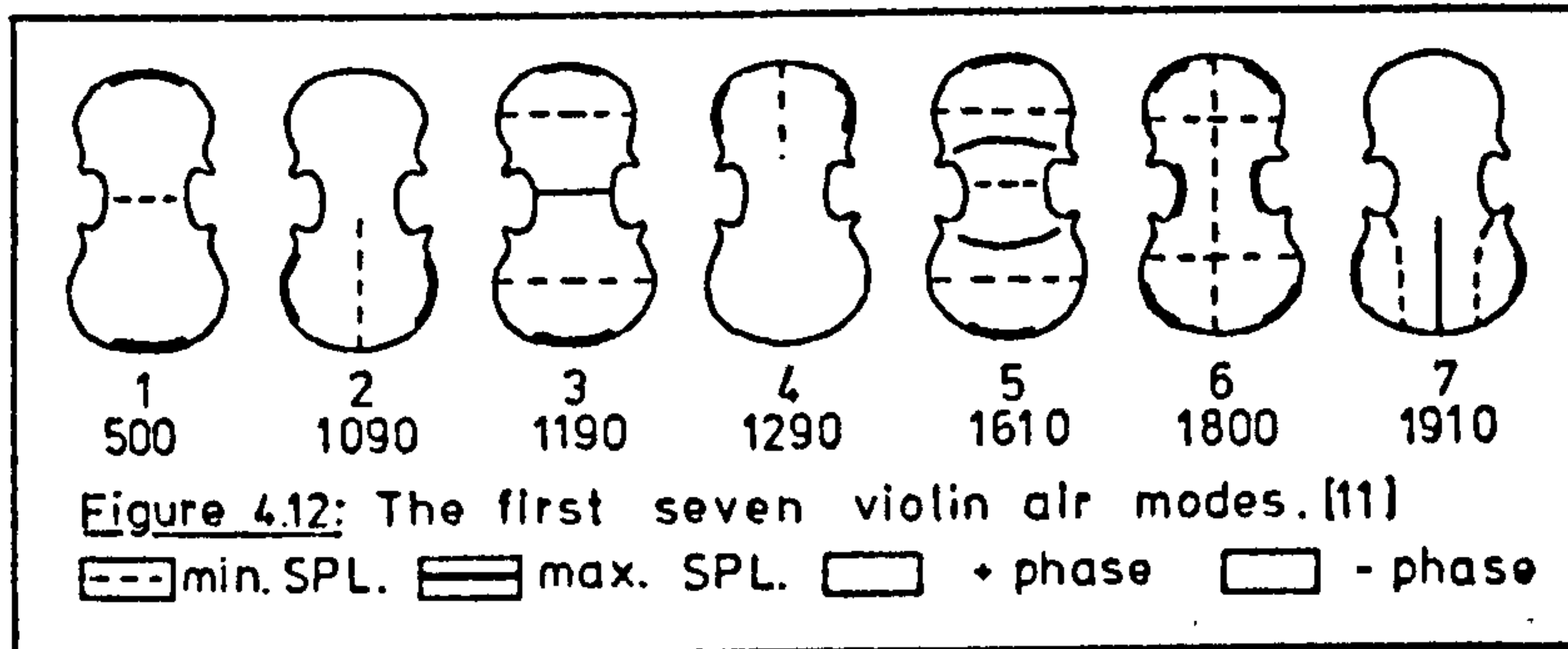
Schelleng's work on this subject was most important as it revealed so much about the violin's action at low frequencies, but in simplifying it to such a degree many important aspects were ignored. The mutual radiation impedance of vibrating surfaces as close together as are the f-holes and the plate is undoubtedly of significance, while the effect of the cavity air resonances and the coupling to the back plate are certainly of major importance. To be of real use for investigating the action of the violin, a model must incorporate at least the second of these features.

#### Other Air Modes in the Violin Cavity.

The unique shape of the belly makes it possible for many more resonances to occur than those that would be present in a rectangular plate. It is not surprising that the air cavity too has many more modes than simpler enclosures.

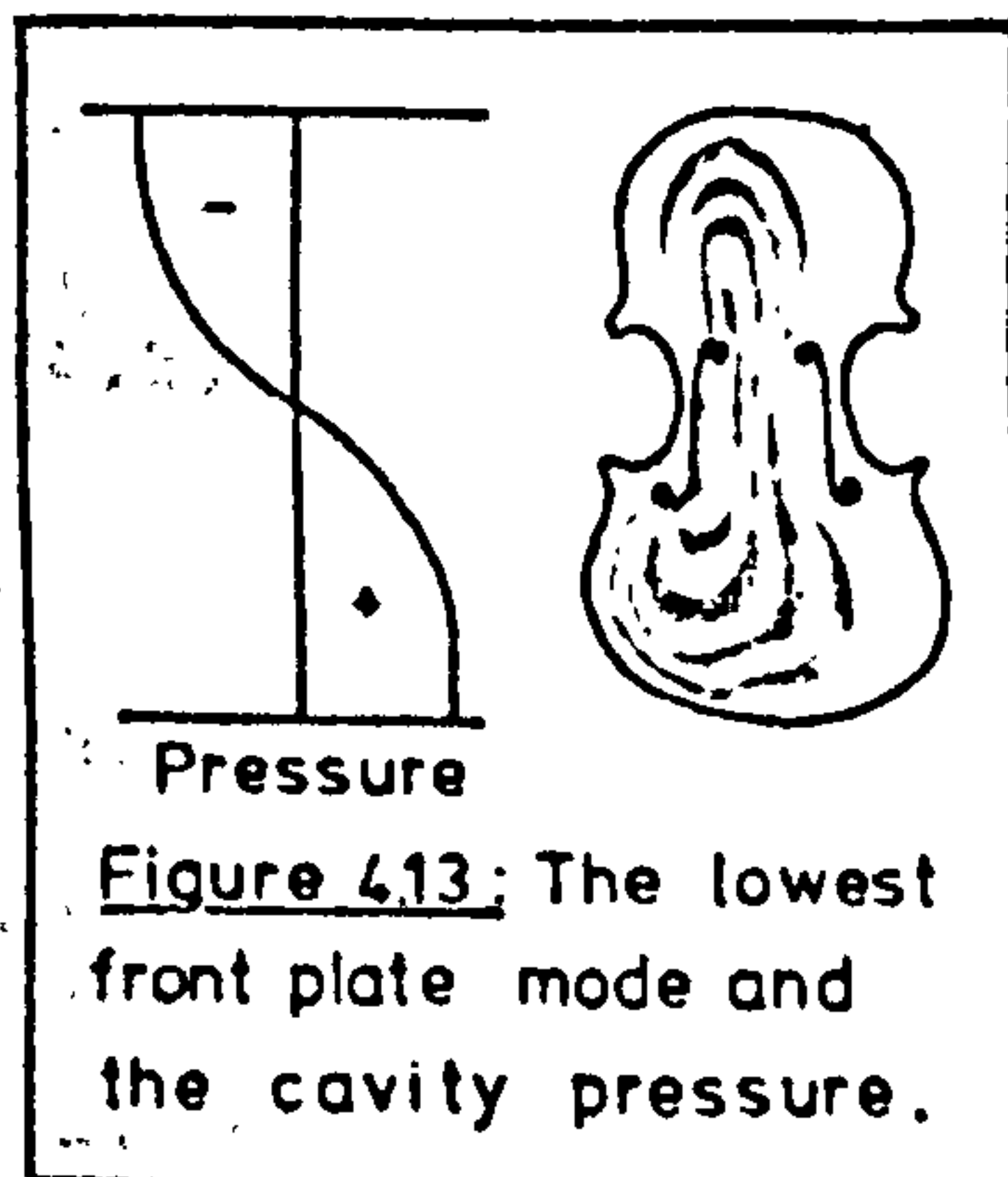
It is not very difficult to imagine what these lowest few modes should be: it turns out that the first, third, fifth, and sixth modes

are similar to the  $[1,0,0]$ ,  $[2,0,0]$ ,  $[3,0,0]$ , and  $[2,1,0]$  rectangular room resonances, while the second and fourth are the lowest modes of the upper and lower subsections [12]. The first seven modes appear in figure 4.12 below.



Of these modes only the third radiates much sound. The first and fifth modes have a node at the center of the f-holes while the second and fourth modes have very little energy in the standing wave close to the f-holes. Saunders reports that body air resonances can be detected at 1300, 2600, and 3660 Hz., which confirms that most of these air modes do not radiate directly to the outside environment [13]. This does not mean that these modes are unimportant!

It is the first of these which is of most interest as it lies in the important low frequency range and couples very strongly to the  $[1,1]$  plate mode. Figure 4.13 will help to show why these modes couple so strongly. Consider each point on the plate to be a point source, just as one would when using the Green's function approach (see chapter



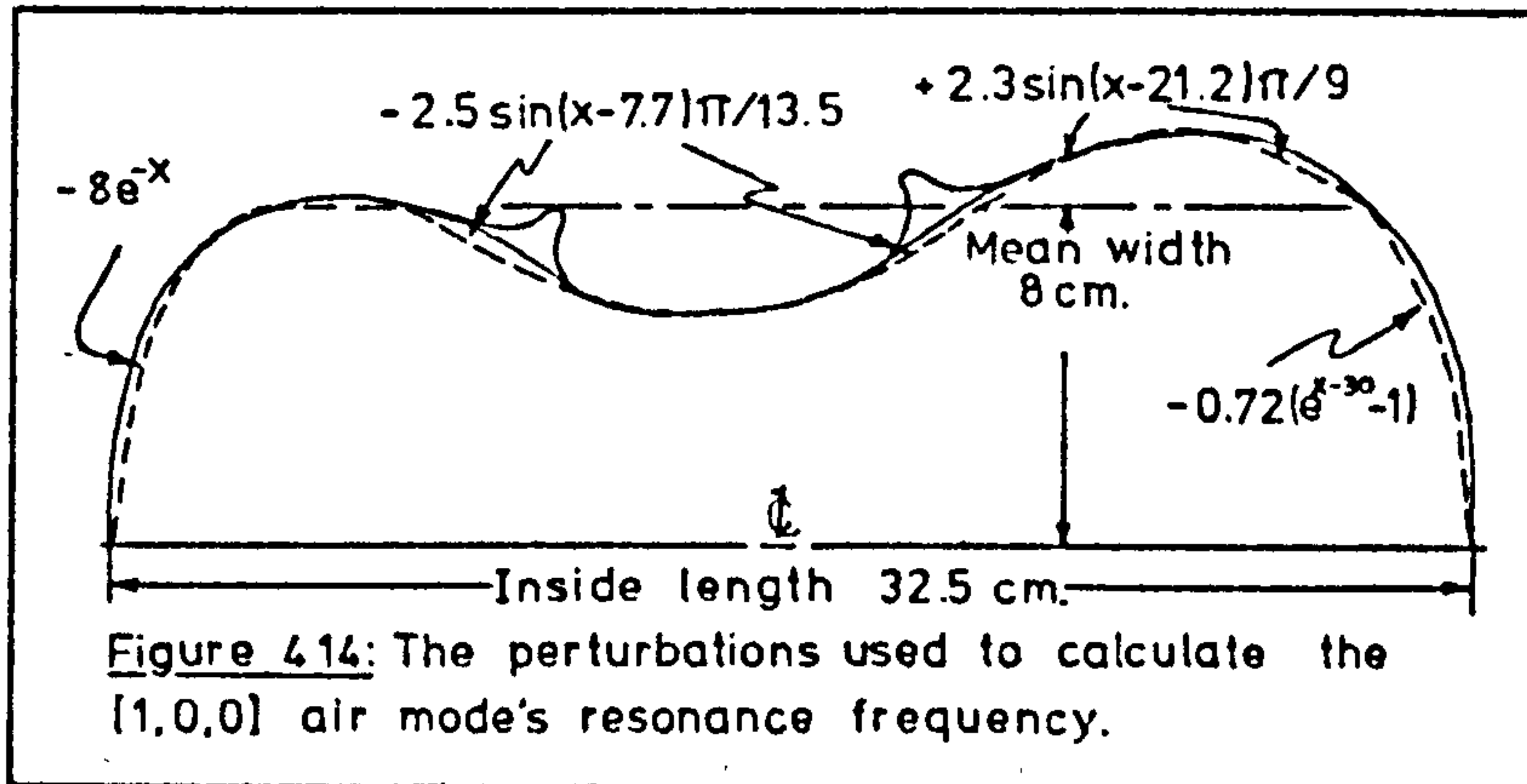
2). A point at a pressure node would not drive the air mode at all, while those at either end of the plate would drive it with opposite phase. If the velocity distribution across the plate was symmetric about the midpoint then the air mode would not be driven at all for the contribution by

the upper half of the plate would be opposed to that of the lower half. Of course this is not the case: the lower half of the plate drives the air mode much more strongly, as a glance at the figure reveals. It is possible to define an equivalent piston area which, when vibrating with the same velocity as the driving point on the front plate, represents the total effective volume velocity which drives this air mode. It may be found by integrating the product of differential area, plate amplitude, and pressure magnitude at a point, over the entire surface. This graphical integration gave an effective area of  $54 \text{ cm}^2$  for the test violin's front plate, and  $17 \text{ cm}^2$  for the back. When dealing with the violin plates it is necessary to use both of the effective areas which have been described, one for the interaction with the Helmholtz mode and another for the  $[1,0,0]$  air mode. These will be designated  $S_{m_0}$  for the former and  $S_{m_1}$  for the latter, with the first subscript indicating the plate and the second the air mode with which it interacts.

When modelling the interaction with the  $[1,0,0]$  air mode some account of the cavity's shape and the way in which it affects the air mode must be made. Jansson [12] outlines a method using the perturbation technique of Rayleigh [14] to deal with this problem. A first estimate of the resonant frequency may be made by using the maximum internal dimension. For the test violin the resonant frequency based on this measurement was 522 Hz. The perturbation equation is

$$(4.8) \quad \Delta f/f = \frac{-1}{L} \int_0^L \frac{\Delta S}{S_0} \cos(2\pi x/L) dx$$

where  $S_0$  is the mean cross-sectional area. Rayleigh developed this equation for tubes of almost constant cross-section, but Jansson's work has demonstrated that the method gives good results when applied to the



violin. The perturbations used in finding the effective length of the test violin are shown in figure 4.14 and table 4.3. The air resonance frequency predicted using the perturbation method, 516 Hz., cannot be compared directly with the experimental value for this is greatly altered by the compliance of the plates, but using the effective length improves the accuracy of the model, as will become apparent when the completed model is evaluated.

	Perturbation	limits	$\Delta f/f$ in %
1	$-8\text{Exp}[-x]$	0 to 5	+2.9
2	$-2.5 \text{Sin} \frac{(x-7.7)\pi}{13.5}$	7.7 to 21.2	-6.6
3	$+2.3 \text{Sin} \frac{(x-21.2)\pi}{9}$	21.2 to 30	-1.2
4	$-0.72[\text{Exp}(x-30) - 1]$	30 to 32.5	+3.0
<u>Total change</u>			<u>-1.9%</u>

Table 4.3: The change in the [1,0,0] resonance frequency due to the cavity shape.

It will also be useful to be able to estimate the losses of this mode. This was no problem with the Helmholtz mode as radiation accounted for the largest portion, but here local absorption by the walls, thermal losses, etc. may be significant. Jansson calculates the thermal and viscous losses but finds them to be much smaller than those due to the absorption by the wood [12 and 16]. If the cavity is

treated as a rectangular room, this absorption should be given by

$$(4.9) \quad P_w = \frac{1}{2} \int_S \frac{P^2 \alpha_w}{8\rho c} dS$$

where  $P_w$  is the power lost to the walls,  $P^2$  is the pressure, and  $\alpha_w$  is the acoustic absorption coefficient.

The absorption coefficient is difficult to measure with small samples at 500 Hz. An impedance tube test proved to be impossible. Values for  $\alpha = 0.04$  were obtained from the literature [16]. The losses through the f-holes were ignored and the resistance was calculated in the form of a Q-value,  $Q=2\pi fW/P$ , with the stored energy  $W$  defined by

$$(4.10) \quad W = \frac{1}{2} \int_V \frac{1}{\rho c^2} P^2 dV .$$

The Q-value determined in this way may be compared to Jansson's experimental data for a violin cavity encased in plaster, which gives a value of 73. Considering the large range of  $\alpha_w$  between different samples of wood the agreement between the experimental value and the calculated Q of 54 is satisfactory.

Most of the information needed to model the violin below 600 Hz. is now at hand. The work of John Schelleng will be extended to include the coupling between the belly, [1,0,0] air mode, and the back plate. Even more important will be the way in which the sound-post is treated, for this makes it possible to accurately predict the response of the completed violin before it is assembled.

[1] A. Gabrielsson and E. Jansson, "Long-time average-spectra and rated quality of twenty-two violins", *Acustica*, vol. 42, pp. 47- 55, (1979).

[2] B. Yankovskii, "Objective appraisal of violin tone quality", *Soviet Physics, Acoustics*, vol. 11, pp. 231- 245, (1966).

[3] F. Saunders, "The mechanical action of violins", *JASA*, vol. 9, pp. 81- 98, (1937).

[4] W. Reinicke, "Übertragungseigenschaften de Streichinstrumentenstegs", *Catgut Acoust. Soc. Newsletter* 19, pp. 26-34, (1973).

[5] D. Haines and N. Chang, "Making better musical instruments from graphite composites", *Mechanical Engineering*, vol. 98, no. 3, pp. 25-27, (1976).

[6] C. Hutchins, "The physics of violins", *Scientific American*, vol. 138, pp. 73- 86, (1962).

[7] M. Minneart and C. Vlam, "The vibrations of the violin bridge", *Physica*, vol. 4, pp. 361- 372, (1937).

[8] For a further discussion of the dynamics of the violin bridge refer to M. Hacklinger, "Violin timbre and bridge frequency response", *Acustica*, vol. 39, pp. 323- 330, (1978).

[9] A. Benade, Fundamentals of Musical Acoustics, Oxford University Press, New York, (1976).

[10] E. Johnson, "Decoupling the back and front plates of a violin", *Applied Acoustics*, vol. 14, pp. 157- 161, (1981).

[11] J. Schelleng, "The violin as a circuit", *JASA*, vol. 35, pp. 326- 338, (1963).

[12] E. Jansson, "The acoustic properties of cavities", *Acustica*, vol. 37, pp. 211- 221, (1977).

[13] F. Saunders, "Recent work on violins", *JASA*, vol. 25, pp. 491- 498, (1953).

[14] Lord Rayleigh, Theory of Sound, second edition, Dover Books, New York, (1945).

[15] U. Ingard, "On the theory and design of acoustic resonators", *JASA*, vol. 25, pp. 1037- 1061, (1953).

[16] L. Beranek, Acoustics, McGraw-Hill, New York, (1954).

The Model.

Schelleng's model was important for it was a first step towards understanding the vibrations of the violin [1]. It elucidated the way in which the Helmholtz resonance, formed by the f-holes and the spring-like volume of air in the violin body, and the lowest front plate mode interact and form the two most important vibrational modes. There are of course many other factors which were not taken into account in his model and which lead to further insights when examined. It is now time to develop a more accurate model which more closely approximates the behavior of real violins.

The Helmholtz mode, which in the notation of chapter 4 is the  $[0,0,0]$  mode, is only one of the countless resonances which occur in the violin cavity. Every one of these couples with each of the front and back plate modes, and in some case with the f-holes as well. Including all of these in the model obviously gets extremely complicated, but from what was learned in chapter 1 it is the spacing of the  $[1,0]$  and  $[0,0,0]$  modes which is the critical factor at low frequencies and higher resonances are of far lesser importance. For this reason the same range as that chosen by Schelleng, 196 to 600 Hz., will be used. There is one additional resonance which always occurs in this range, the  $[1,0,0]$  air mode in which the length of the enclosure (and to a lesser extent its shape—see chapter 4) dictates the resonant frequency. It is quite easy to measure the pressure in a violin-shaped cavity with a short probe tube fitted into the walls, and an experiment of this nature will show that while the  $[1,0,0]$  mode is in resonance the acoustic output of the violin remains rather low. This may be observed in the frequency response curve of figure 5.1 where the contribution to the response by each mode has been indicated. Just

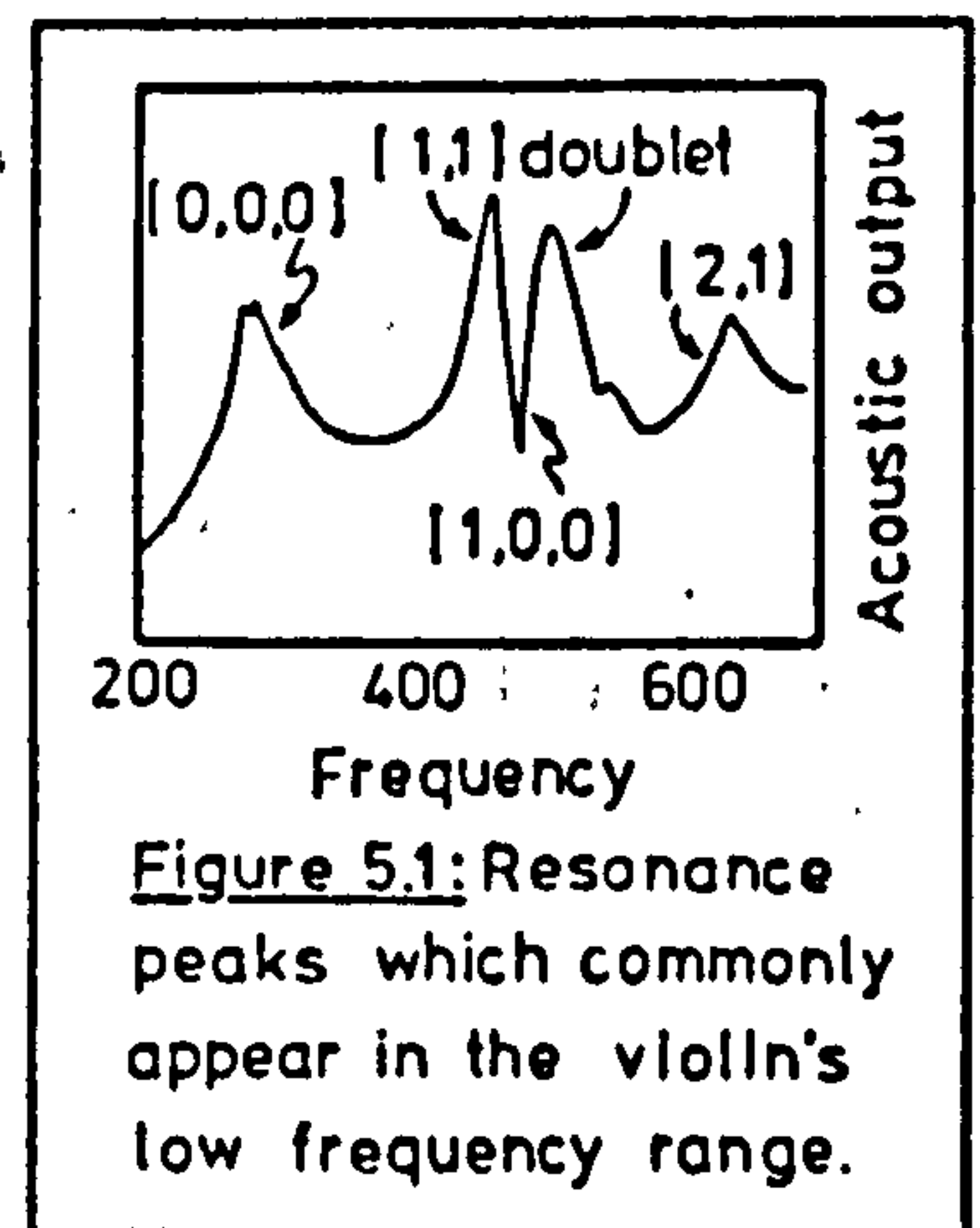
like a vibration absorber the air mode draws energy from the plate's vibration and causes a doublet to be formed. The acoustical consequences of this mode will be discussed in some detail later.

It sometimes happens that the back plate  $[1,1]$  resonance falls into this range as well, although ideally it should perhaps not do so. If the impedance match between the plates through the sound-post is good, this form of direct coupling will have to be included in the model, which will make the problem much more difficult. Fortunately, even if the imaginary parts of the impedances are equal, the different shapes and materials of the plates will insure that the real parts are quite different. Thus it is that the violin which in figure 5.1 proved to possess a back plate resonance at about

550 Hz. did not show any large degree of direct coupling. This can be judged in the vibration holograms which show that no motion occurred at the sound-post in either plate. One may conclude from this that only the air coupling need be considered between front and back plates over this

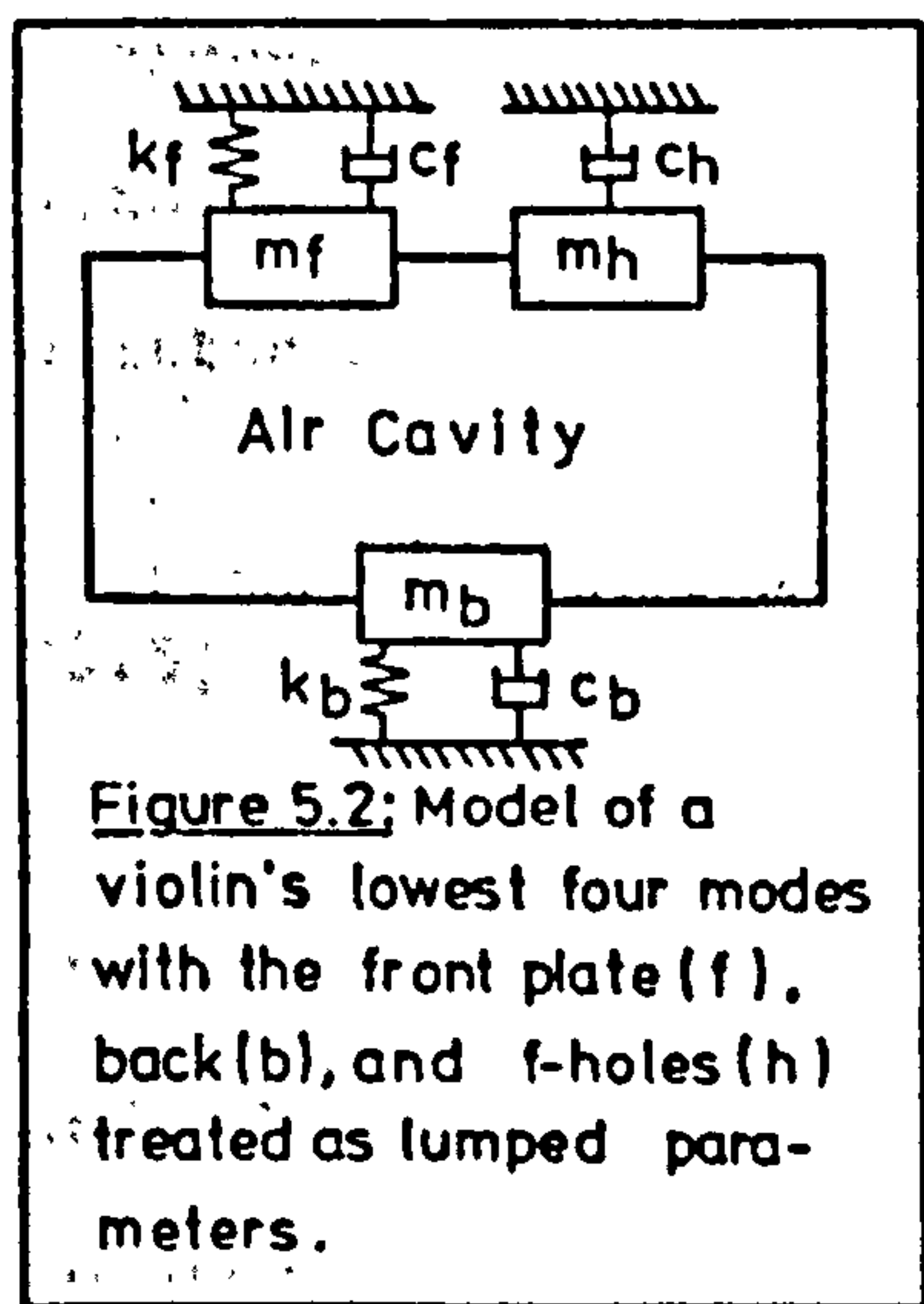
frequency range provided that the post's effect on the mode shapes and resonance frequencies is known.

There is another factor which should be considered before beginning to model the violin. Although the ribs will not have a resonance in the frequency range of interest, they will affect the boundary conditions of the plate and lower the stiffness of the air volume for the Helmholtz resonator. As with the sound-post, the effect of the ribs on the plates may be ignored, provided the way in which they change the plate's mode shapes and resonance frequencies are known. This will prove to be no obstacle. Their effect on the



Helmholtz resonance can be calculated by treating them as a spring-like boundary.

The analysis begins by including all of the elements mentioned thus far in an idealized violin, with a right-regular air cavity and pistons acting as models for the vibrating surfaces. Such a model is shown in figure 5.2. This strange mixture of mechanical and acoustic components is used as it is a more intuitive approach to the problem.



The green's function, equation (2.16), may be used to describe the pressure distribution throughout the cavity, but before this is possible the equation of motion for the standing wave must be developed. This is most easily done in one dimension and the results then extended to three.

Newton's law, when applied to a differential particle of air, may be written as

$$(5.1) \quad \frac{dP}{dx} dx S = \rho S dx \frac{d^2e}{dt^2} ,$$

with  $dP/dx$  the pressure gradient,  $S$  the cross sectional area, and  $e$  the particle displacement. From this the equation of motion may be written as

$$(5.2) \quad \frac{d^2e}{dt^2} - c^2 \frac{d^2e}{dx^2} = 0 ,$$

and the relationships between displacement, velocity and pressure as

$$(5.3) \quad u = j\omega e , \quad P = -j\rho c u , \quad \text{and} \quad \frac{dP}{dx} = j\omega \rho u .$$

Extended into three dimensions with the vector notation  $\hat{r} = x\hat{i} + y\hat{j} + z\hat{k}$ , the equation of motion with a point source at  $\hat{r}_0$  is

$$(5.4) \quad k^2 P(\hat{r}) + \frac{d^2 P(\hat{r})}{d\hat{r}^2} = -j \frac{w^2 \rho}{c} \delta(\hat{r} - \hat{r}_0) u(\hat{r}) dV,$$

using the relationships between displacement, velocity, and pressure in a standing wave. This equation is of the same form as equation (2.8) with  $A = c^2$  and  $B = jw^2 \rho c$ . The green's function may now be directly written from equation (2.12) as

$$(5.5) \quad g(\hat{r}, \hat{r}_0, w) = -j \frac{w^2 \rho}{c S} \sum_{\eta} \frac{\phi_{\eta}(\hat{r}) \phi_{\eta}(\hat{r}_0) u(\hat{r}_0) dV}{\Lambda_{\eta} (k^2 - K_{\eta}^2)}$$

In the violin there are, however, no internal sources; only the plates and f-holes drive, or are driven by, the air modes and these are located on the cavity boundaries. It is therefore possible to perform a surface integration over each plate and f-hole rather than the volume integral in the previous equation. This leaves

$$(5.6) \quad P(\hat{r}, \hat{r}_0, w) = -j \frac{w^2 \rho}{c S} \sum_{\eta} \frac{\phi_{\eta}(\hat{r}) \int_S \phi_{\eta}(\hat{r}_0) u(\hat{r}) dS}{\Lambda_{\eta} (k^2 - K_{\eta}^2)}$$

The integral  $\int_S \phi(\hat{r}_0) u(\hat{r}) dS$  is the total effective volume velocity of the plates and f-holes. The "equivalent" or "effective piston area" which was introduced in the last chapter is related to this integral, and may be obtained by dividing it by the velocity of a reference point on the vibrating surface. This point is one with maximum velocity. These areas depend on both the air mode  $\phi_{\eta}$  and the surface which drive them so it will be necessary to adopt some notation to describe them.

$S_{m\eta}$  is the equivalent area of the mth surface, either f, b, or h, which

drives or is driven by the  $n$ th air mode, either 0 or 1, eg.:  $S_{f0} = \int_S \phi(\hat{r}_f) u(\hat{r}_f) / u_f dS$ . Using this notation equation (5.6) may be expressed as

$$(5.7) \quad P(\hat{r}) = \frac{-j\omega^2 \rho}{cS} \sum_{\eta} \frac{\phi_{\eta}(\hat{r}) [u_f S_{f\eta} + u_b S_{b\eta} + u_h S_{h\eta}]}{\Lambda_{\eta} (k^2 - K_{\eta}^2)}$$

In order to determine  $K_{\eta}^2$  and the shape functions  $\phi_{\eta}(\hat{r})$ , the boundary conditions must be imposed on the problem. As the dimensions of the violin are much greater in the  $x$  direction (see figure 5.3 for orientation) than in either the  $y$  or  $z$  directions, the pressure distribution below 600 Hz. will be

essentially one dimensional. Waves which travel along the  $x$ -axis are affected by the impedances which they meet at each end,  $Z_0$  and  $Z_L$ . If these impedances are written in terms of pressure and particle velocity,

making use of the relationships in equations (5.3), then

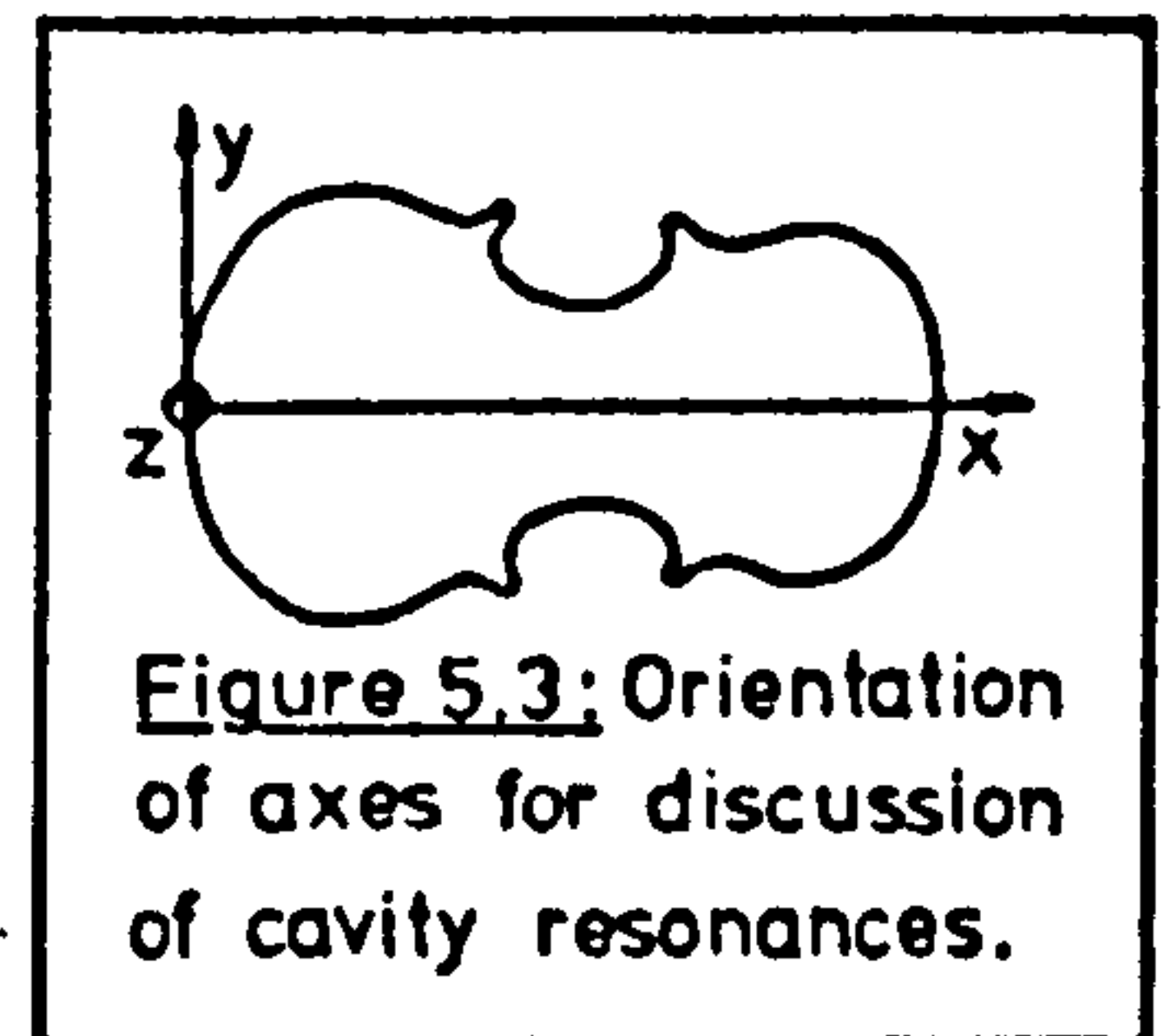


Figure 5.3: Orientation of axes for discussion of cavity resonances.

$$(5.8a) \quad \frac{dP(0)}{dx} = \frac{j\omega\rho P(0)S_0}{Z_0} \quad (5.8b) \quad \frac{dP(L)}{dx} = \frac{j\omega\rho P(L)S_L}{Z_L}$$

where  $S_0$  and  $S_L$  are the areas normal to the  $x$ -axis at  $x=0$  and  $x=L$ . The change in sign of equations (5.8) is due to geometrical considerations.

If the pressure is then written as  $P = a \cos(Kx + \phi)$ , in much the same way as was done in the case of the vibrating string of chapter 2, then equations (5.8) yield

$$(5.9a) \quad K \sin(\phi) = \frac{j\omega\rho}{Z_0} \cos(\phi) S_0$$

and

$$(5.9b) \quad -K \sin(\phi) = \frac{j\omega\rho}{Z_L} \cos(KL + \phi) S_L$$

Rearranging terms gives the equations

$$(5.10a) \quad K \tan(\phi) = j\omega\rho S_0 / Z_0$$

and

$$(5.10b) \quad K \tan(\phi + KL) = -j\omega\rho S_L / Z_L$$

As long as  $Z_0$  and  $Z_L \gg 1$ , as they will be in the case of a violin,  $\phi$  and  $j\omega\rho S_0 / Z_0$  will be  $\ll 1$  and the nature of the tan function makes it possible to express equation (5.10a) as  $\phi \approx j\omega\rho S_0 / Z_0 K$ . Using this relationship, substituting  $K = K + n\pi/L$ , and once again noting that  $Z_L \gg 1$ , the expressions for  $K_n$  are

$$(5.11a) \quad K_0^2 = -\frac{j\omega\rho}{L} \left[ \frac{S_0}{Z_0} + \frac{S_L}{Z_L} \right]$$

and

$$(5.11b) \quad K_n^2 = (n\pi/L)^2 - \frac{2j\omega\rho}{L} \left[ \frac{S_0}{Z_0} + \frac{S_L}{Z_L} \right]$$

Extending these results to three dimensions yields

$$(5.12a) \quad K_0^2 = -\frac{j\omega\rho}{V} \left[ \frac{S^2}{Z_s} + \frac{S_{f0}^2}{Z_f} + \frac{S_{b0}^2}{Z_b} + \frac{S_{h0}^2}{Z_h} \right]$$

and

$$(5.12b) \quad K_n^2 = (\pi/L)^2 - \frac{j\omega\rho 2}{V} \left[ \frac{S^2}{Z_s} + \frac{S_{f1}^2}{Z_f} + \frac{S_{b1}^2}{Z_b} + \frac{S_{h1}^2}{Z_h} \right]$$

where  $S$  is the total surface area of the cavity and  $Z_s$  the average over this area of the surface impedance of the wood, mostly due to absorption and the stiffness of the walls.

The bracketed terms in equations (5.12) are small so that the shape functions may be approximated as  $\phi_0(\hat{r}) = 1$  and  $\phi_n(\hat{r}) = \cos(n\pi x/L)$ , with  $L$  the effective length as defined in chapter 4. It's not possible to ignore the bracketed terms when  $K_0^2$  or  $K_n^2$

appear in the denominator of equation (5.7) as the imaginary part of this includes all of the loss terms in  $Z$ . The real part of  $K_0^2$  also is mostly due to the mass reactance of the f-holes and it is this term which represents the Helmholtz resonance.

Although the way in which the plates drive the air modes is now known, the reaction forces, and their effects on the plates and f-holes, still remain to be found. These may be calculated in much the same manner as were the pressure distributions, using the green's function approach.

Once again, the first step is to write the equation of motion, which for a plate is

$$(5.13) \quad \rho h \frac{\partial^2 \psi(\hat{r})}{\partial t^2} + \frac{Eh^3}{12(1-\nu^2)} \nabla^4 \phi(\hat{r}) = P(\hat{r}) \delta(\hat{r}-\hat{r}_0) + \frac{F}{dS} \delta(\hat{r}-\hat{r}_0)$$

where  $E$  = Young's Modulus,  $\nu$  = Poisson's Ratio, and  $P(\hat{r})$  is the pressure acting on the plate at a point  $\hat{r}$ . If equations (5.12) are differentiated, the plate velocity may be written in terms of the input force and the cavity pressure using the green's function:

$$(5.14) \quad u(\hat{r}) = \frac{j\omega}{\rho h} \sum_{\lambda} \frac{\psi_{\lambda}(\hat{r})}{\Lambda_{\lambda}(\omega_{\lambda}^2 - \omega^2)} \left[ \int_S \psi(\hat{r}_0) P(\hat{r}_0) dS + F \phi(\hat{r}_0) \right]$$

where  $u(\hat{r})$  must be obtained for each vibrating surface.

The velocity of surface  $m$  could be written as  $u(\hat{r}_m) = u_m \psi(\hat{r}_m)$ , with  $\psi(\hat{r}_m)$  normalized and the vector  $\hat{r}$  defining a point on this surface. Similarly, the pressure distribution on surface  $m$  may be expressed as  $P_{\eta}(\hat{r}_\eta) = P_{m\eta} \phi_{\eta}(\hat{r}_m)$ , with  $\eta$  indicating the air mode. It is then possible to rewrite the equivalent area as

$$(5.15) \quad S_{mn} = \int_S \phi_{\eta}(\hat{r}_m) \psi(\hat{r}_m) dS$$

which, due to the nature of orthogonal functions, demonstrates the property of reciprocity. This makes it possible to write equation (5.15) as

$$(5.16) \quad u_m(\hat{r}_m) = \frac{j\omega \psi(\hat{r}_m)}{\rho h S \Lambda(\omega_m^2 - \omega^2)} [P_{m_0} S_{m_0} + P_{m_1} S_{m_1} + F \psi(\hat{r})] ,$$

with only the single mode of interest shown for each surface  $m$ .

In deriving equation (5.7)  $K_n^2$  was obtained directly from the shape functions  $\phi$ . Here it is impossible to do this as the shape functions cannot be predicted, due to the complex design of the plates. Instead the term  $(\omega_n^2 - \omega^2)$  may be expressed as  $[(k/m - \omega^2) + (\omega\xi/m)^2]^{1/2}$ , with  $k$ ,  $m$ , and  $\xi$ , the equivalent values of stiffness, mass, and damping of the plate.

With the equations for  $u$  and  $P$  related in the way they are, some simultaneous equations must be solved before it is possible to write the piston velocities  $u$  explicitly. The algebra is extremely tedious but may be simplified if one considers the violin's action. Only one input force, at the treble bridge foot, need be considered, and the equivalent area  $S_{h1}$  is very nearly zero since the  $[1,0,0]$  air mode has a node at the center of the f-holes. With these simplifications the piston velocities are [2]:

$$(5.17a) \quad u_f = \beta_f F [1 - \beta_b (S_{b_0}^2 \alpha_0 + S_{b_1}^2 \alpha_1) - \beta_h S_{h_0}^2 \alpha_0 + \beta_b \beta_h (S_{h_0} S_{b_1})^2 \alpha_0 \alpha_1] / A$$

$$(5.17b) \quad u = \beta_b F [\beta_f (S_{f_0} S_{b_0} \alpha_0 + S_{f_1} S_{b_1} \alpha_1) - \beta_f \beta_h (S_{h_0}^2 S_{f_1} S_{b_1} \alpha_0 \alpha_1)] / A$$

and

$$(5.17c) \quad u_h = \beta_h F [\beta_f (S_{f_0} S_{h_0} \alpha_0) + \beta_f \beta_b (S_{b_0} S_{h_0} S_{f_1} S_{b_1} + S_{f_0} S_{h_0} S_{b_1}^2) \alpha_0 \alpha_1] / A$$

and where  $\beta_n = -j\omega(k_{eq} - \omega^2 m_{eq} + j\omega\xi) / \Lambda_n$ ;  $\alpha_n = -j\omega^2 \rho / [cS\Lambda_n(k^2 - K_n^2)]$ ;

and  $\Lambda_n = 1/2$  when  $n \in \{1, b, f\}$  or  $= 1$  when  $n \in \{0, h\}$ ,

$$(5.18) \quad A = 1 - \beta_f (S_{f_0}^2 \alpha_0 + S_{f_1}^2 \alpha_1) - \beta_b (S_{b_0}^2 \alpha_0 + S_{b_1}^2 \alpha_1) + \beta_f \beta_b (S_{f_0} S_{b_1} - S_{b_0} S_{f_1})^2 \alpha_0 \alpha_1 \\ - \beta_h S_{h_0}^2 \alpha_0 - \beta_f \beta_h (S_{f_0} S_{h_1})^2 \alpha_0 \alpha_1 - \beta_b \beta_h (S_{b_0} S_{h_1})^2 \alpha_0 \alpha_1$$

### Evaluating the model

Before utilizing the model it can be evaluated by predicting the response of a violin and then by comparing this with experimental data. In this way it is possible to see whether the simplifications which were made in developing the model are valid. However, before this may be done, the parameters which appear in equations (5.17) must be measured on the test violin.

If one were to measure the parameters with the violin fully assembled, the predicted and measured response would have to be similar even if the modelling was not good, for the coupling between the plate and air modes would largely be accounted for. A much more severe test would involve testing the plates separately to obtain the equivalent mass, stiffness, and damping, and then reassembling the violin to measure the frequency response. There are, however, some major problems here: the glue joints may be vastly different on re-assembly, and the plates must be tested on the ribs so that the boundary conditions are similar to those of the assembled instrument. Additionally, the sound-post cannot be positioned between the plates when measuring the parameters in this way, but this should not affect the validity of the comparison.

In order to minimize these problems the plates were tested while mounted one at a time upon the ribs. The glue joint between the

front-plate and the ribs was not broken between measuring the plate parameters and the frequency response of the assembled violin. (The importance of the back plate as a radiator is minimal as discussed in chapter 4 so that altering its glue joint had an unnoticable effect.)

The experiment began by glueing the back plate to the ribs, which were in turn affixed to a rigid wooden frame, open at the center to prevent any cavity modes from affecting the plate. The test facility may be seen in figure 5.4.



Figure 5.4: Setting up a test in the anechoic chamber.

Once the parameters had all been measured the ribs were seperated from the frame and back, and the front plate glued on. After the front plate had been tested, the heavy frame was removed and the back plate glued in its place. The complete violin was then tested as described.

The techniques used to measure the plate parameters were much the same as those described in chapter 4. The equivalent mass for each plate was found by measuring the shift in frequency which occured when a small mass was attached to the antinode. Once the resonant frequency

and equivalent mass were known, and the loss term  $\xi$  had been determined from the resonance peak's 3dB down points, the stiffness was calculated from the expression  $(k_{eq} - \omega^2 m_{eq})^2 + \omega^2 \xi = 0$ . Equivalent areas were found by integrating the product  $\phi_n \psi_m$  over the plate surface, with the normalized pressure distributions  $\phi_0 = 1$  and  $\phi_1 = \cos(\pi x/L)$ , and with the plate displacement  $\psi_m$  determined from

vibration holograms. This tedious

graphical integration was performed by

computer with a great savings in time,

although information from the hologram

still needed to be input manually with a

digitizer by entering the location of each

fringe point by point. A computer plot of

plate displacement is shown in figure 5.5.

The equivalent areas calculated in this

manner are shown in table 5.1 along with

the other parameters.

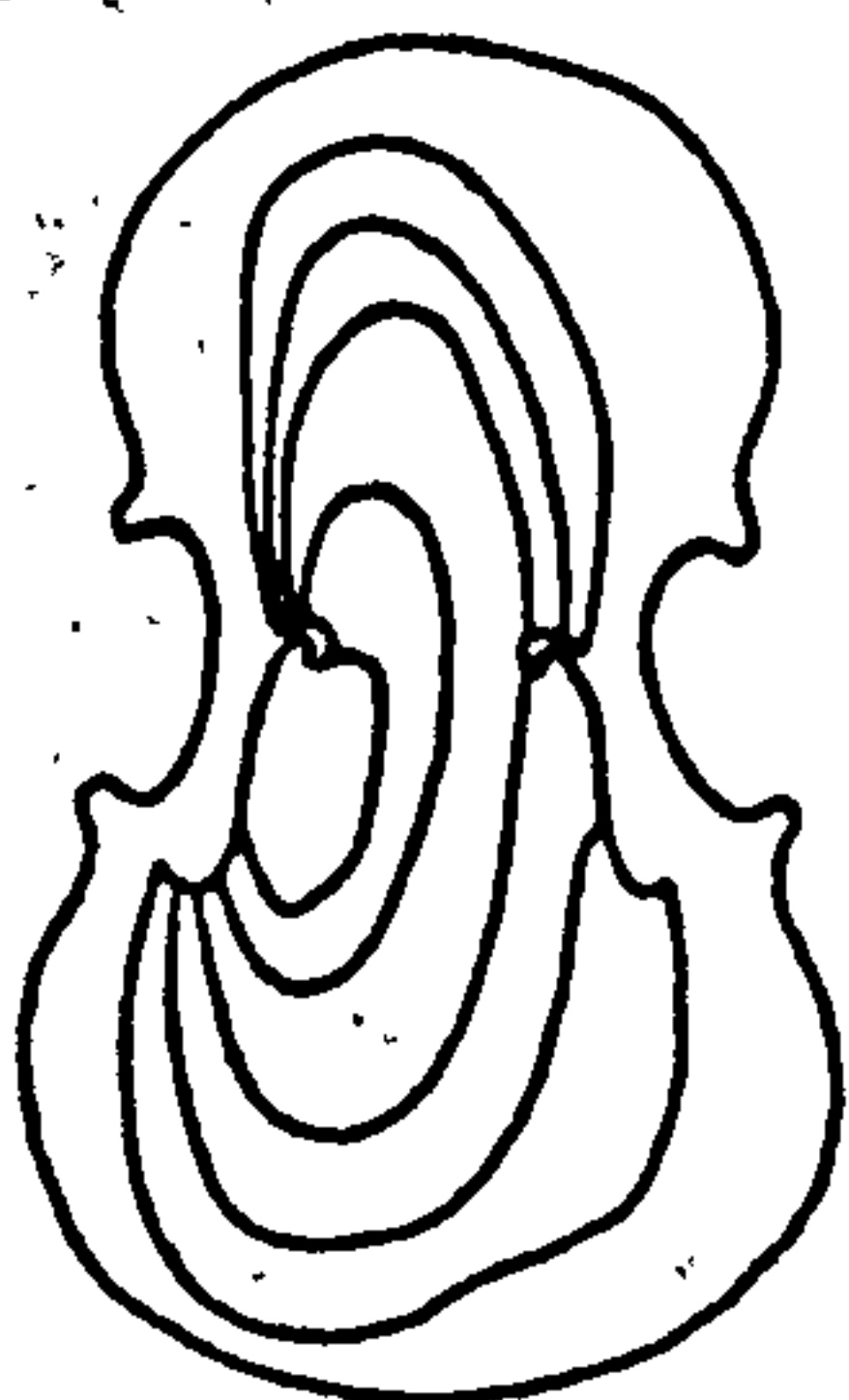


Figure 5.5: Computer version of a vibration hologram used to calculate equivalent areas.

Parameter	Units	front	back	f-holes
$S_{no}$	cm <sup>2</sup>	150*	150*	2x6.3
$S_{nl}$	cm <sup>2</sup>	54*	50*	0
$m$	gm	33	47	.0024*
$k$	gm/s	2.2x10 *	4.5x10 *	-----
$\xi$	gm/s	2130	11700	200*
$f$	Hz	415	515	-----

Table 5.1: The parameters which characterize the violin

at low frequencies, with its sound-post removed. A \*

denotes a calculated value.

The parameters which describe the f-holes were all calculated. Basing them on measurements from an assembled violin gives results which are affected by the plates. Radiation reactance accounted for almost all of the mass loading. This term was 90° out of phase with

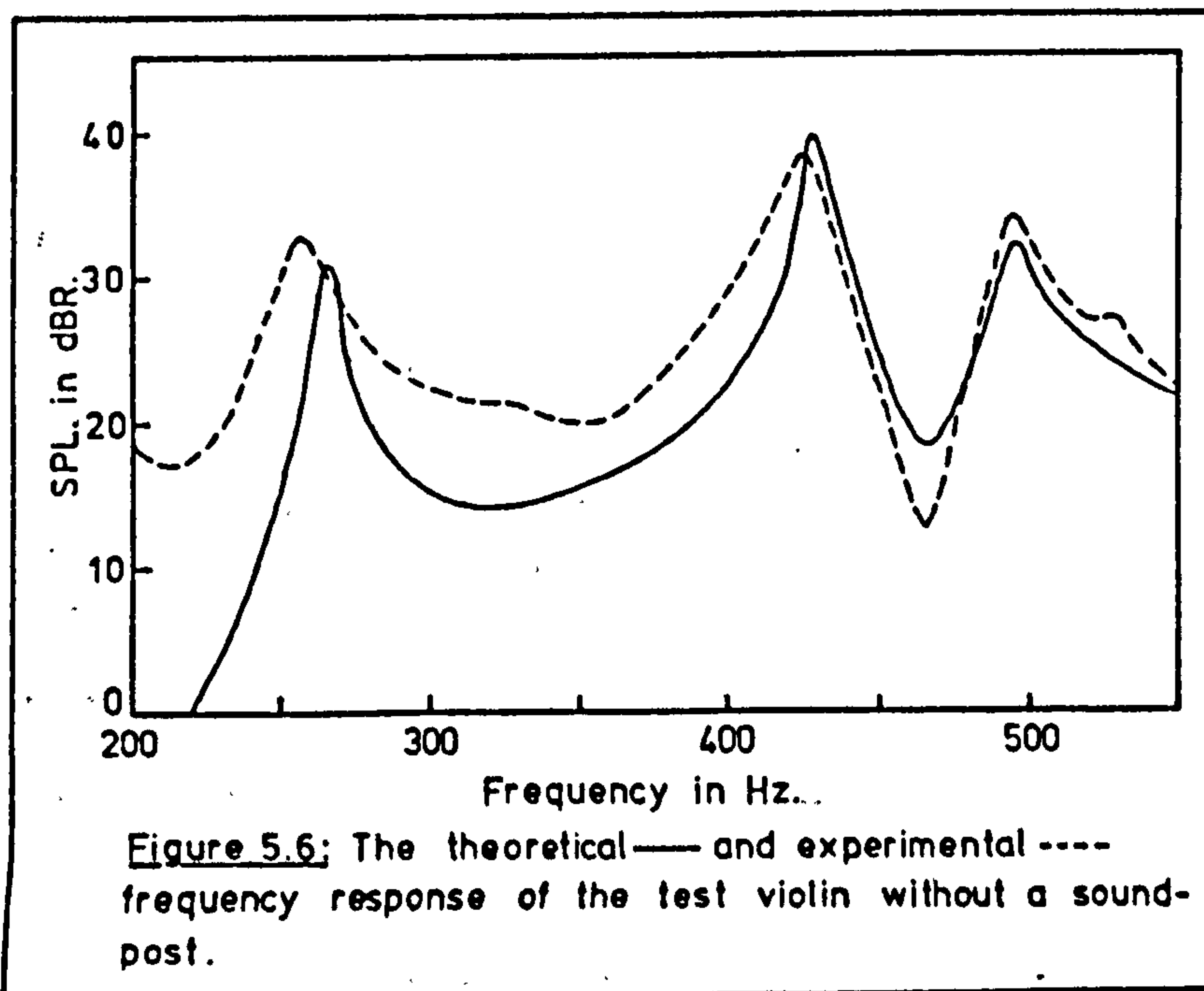
the f-hole velocity so that no energy was radiated, and represented a lossless incompressible flow of air. Both sides of the holes must be considered when calculating the mass-loading due to this near-field effect. The equation which is applied when a surface has dimensions which are  $\ll \lambda$  in air is  $m_{rad} = \rho S [1 + 16\sqrt{S/\pi} / (3\pi)]$  with  $S$  the area of one hole.

The loss term  $\xi$  was calculated in much the same way, however, in this case radiation resistance is in phase with the surface velocity and therefore energy is radiated from the surface. On the inside of the cavity this energy goes to drive the air mode and is already included in the equations of motion. Therefore the radiation losses on only one side of each f-hole need to be considered.

The remaining parameters were measured directly from the test violin: the volume and interior surface areas were 1650 cm<sup>3</sup> and 2000 cm<sup>2</sup>, the length, when modified as described in chapter 4, was 33.2 cm.

A simple computer program used the parameters of table 1 and the equations (5.17) to predict the frequency response at one meter along the normal from the center of the front plate. All of the features which one would expect to find, the single Helmholtz resonance, the doublet of the [1,1] front plate mode, and the anti-resonance due to the energy losses of the [1,0,0] air mode, appear in the calculated frequency response which is plotted in figure 5.6. When the response measured on the assembled violin is plotted so that the two curves have equal areas on the figure, the difference in levels is generally less than three dB and, more importantly, the resonant frequencies are predicted to within a few Hz. Several experiments of this nature produced similar results: the model gives a good description of a real violin.

This is a good point at which to once again consider the effect of

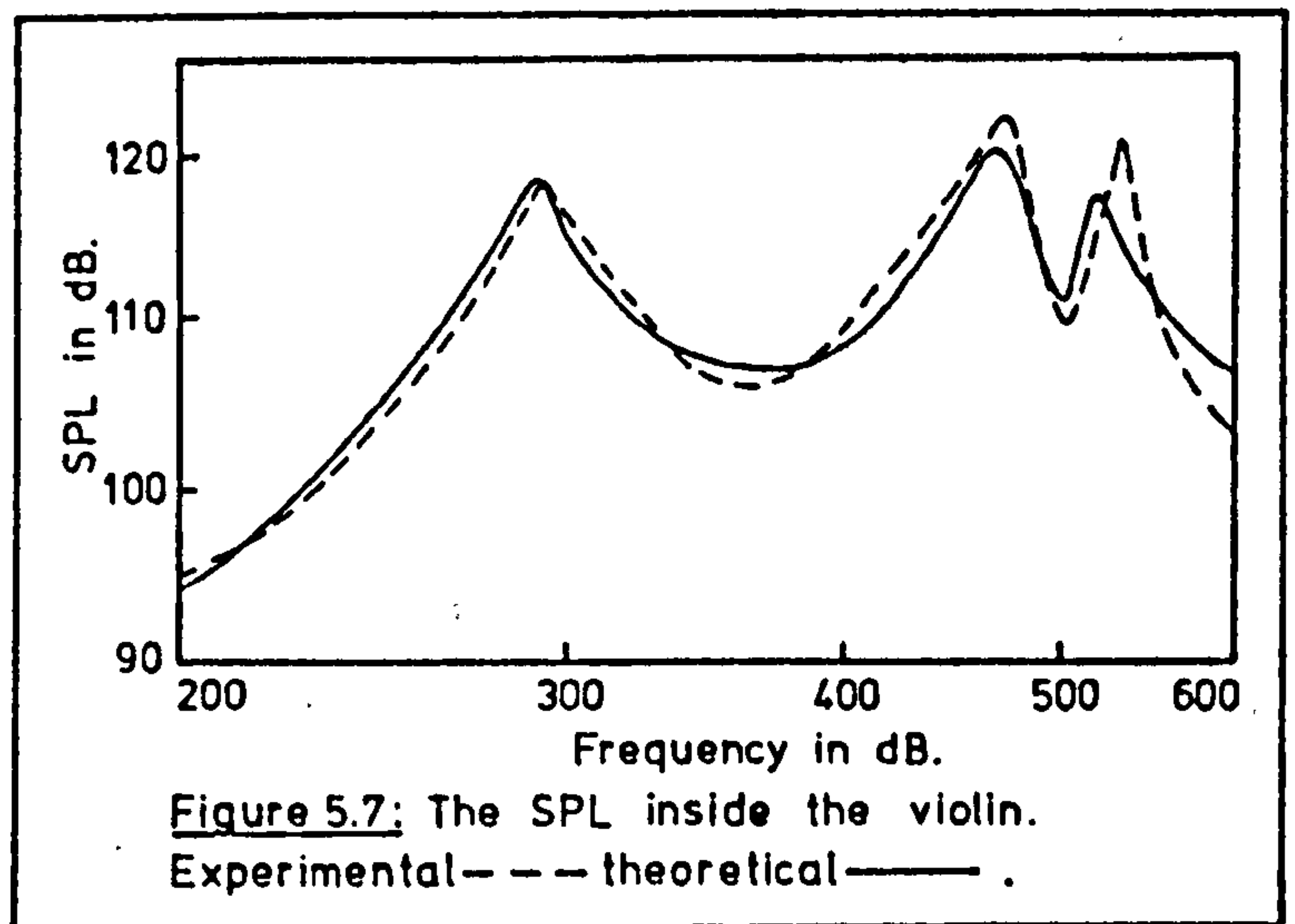


the ribs on the violin's response. It was assumed earlier that they need not enter the model as a separate entity although they would affect the results in various ways. The boundary conditions which they impose on the front plate are implicitly included in the method used to measure its impedance. The surface absorption and compliance as a cavity boundary were included in the impedance terms of equation (5.7). The only other important way in which the walls could affect the violin is as a means of transferring energy between the front and back plates, but as the accuracy of the model is already greater than the changes which can occur in a violin due to humidity, there is nothing to be gained in trying to improve the model by including this effect.

It is interesting to look at the pressure levels which occur inside the violin cavity; for they are remarkably high. A half-inch microphone with a short probe tube was inserted into the air cavity at the center of one f-hole. At this point the  $[1,0,0]$  mode was at a minimum so that the response curve which appears in figure 5.7 is that of the Helmholtz resonance alone. The model predicts sound pressure levels of almost 120 dB., a seemingly impossible figure, and yet the

experimental results confirm this.

These experiments, which were conducted without a soundpost in position, demonstrate that the model is useful for predicting the



frequency response. It is equally valid for use with the soundpost present, although only if no motion occurs where the post contact the plates. Since this is known to be quite often the case, the model can be used to make some interesting observations about the violin, although a new set of parameters must be measured for the complete violin beforehand.

The effective area for each plate may be measured in the same way as before, although their values will be considerably different due to the influence of the sound-post. The coupling of modes prevents one from calculating the stiffness as before, since the resonant frequency of each plate is affected by the air modes when the violin is assembled. By estimating the stiffness and damping, and then using these values in the computer program, it is possible to find the correct values by a process of trial and error.

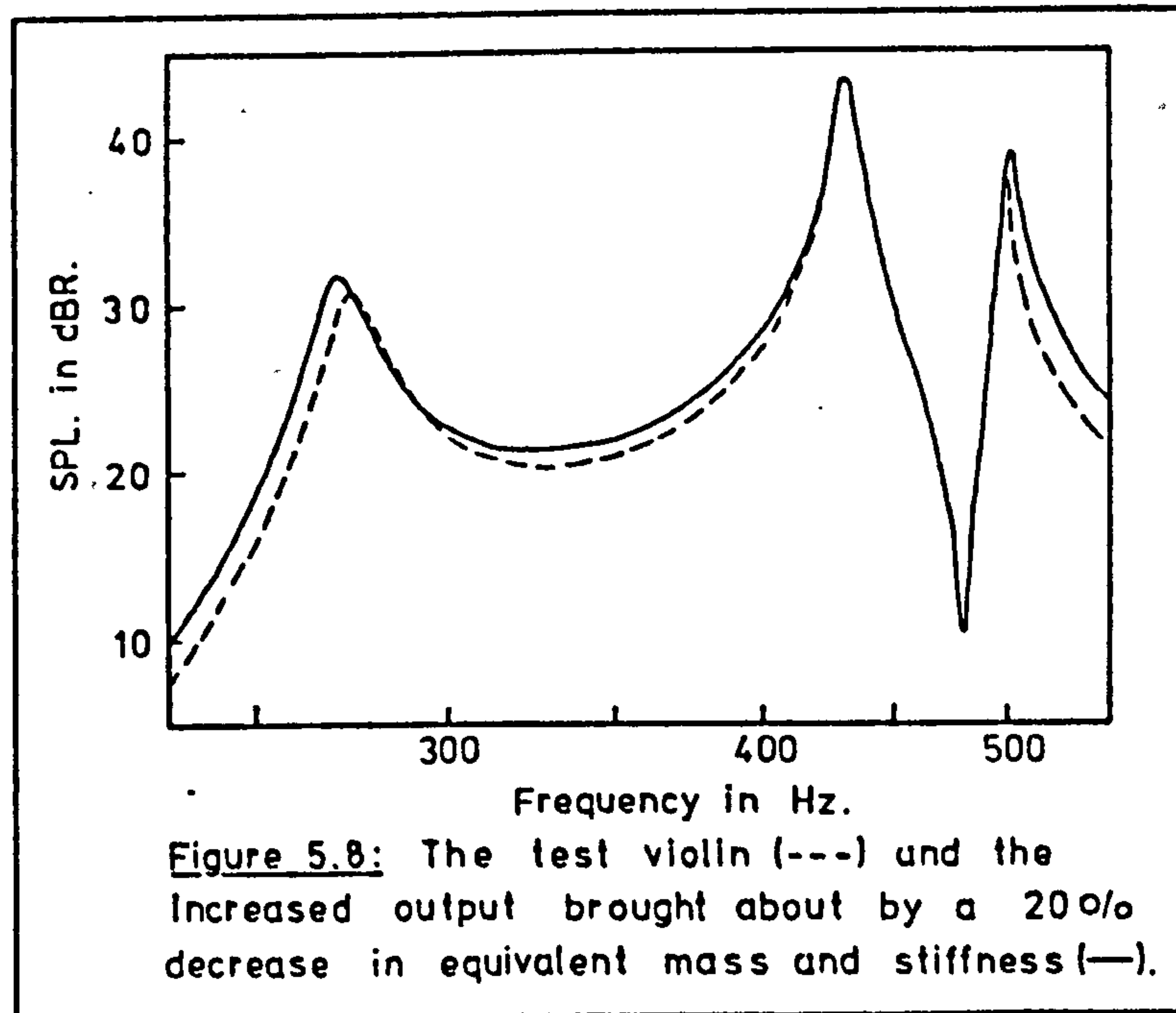
Once these parameters are known it is possible to vary any one of them and then to observe its effect on the whole violin's response in a way which would be impossible by modifying and testing an actual instrument. Of course, this method of predicting the response is of no use to the luthier who wants to know how his individual plates will

behave when he finally glues them together, but this problem will be left for the next chapter.

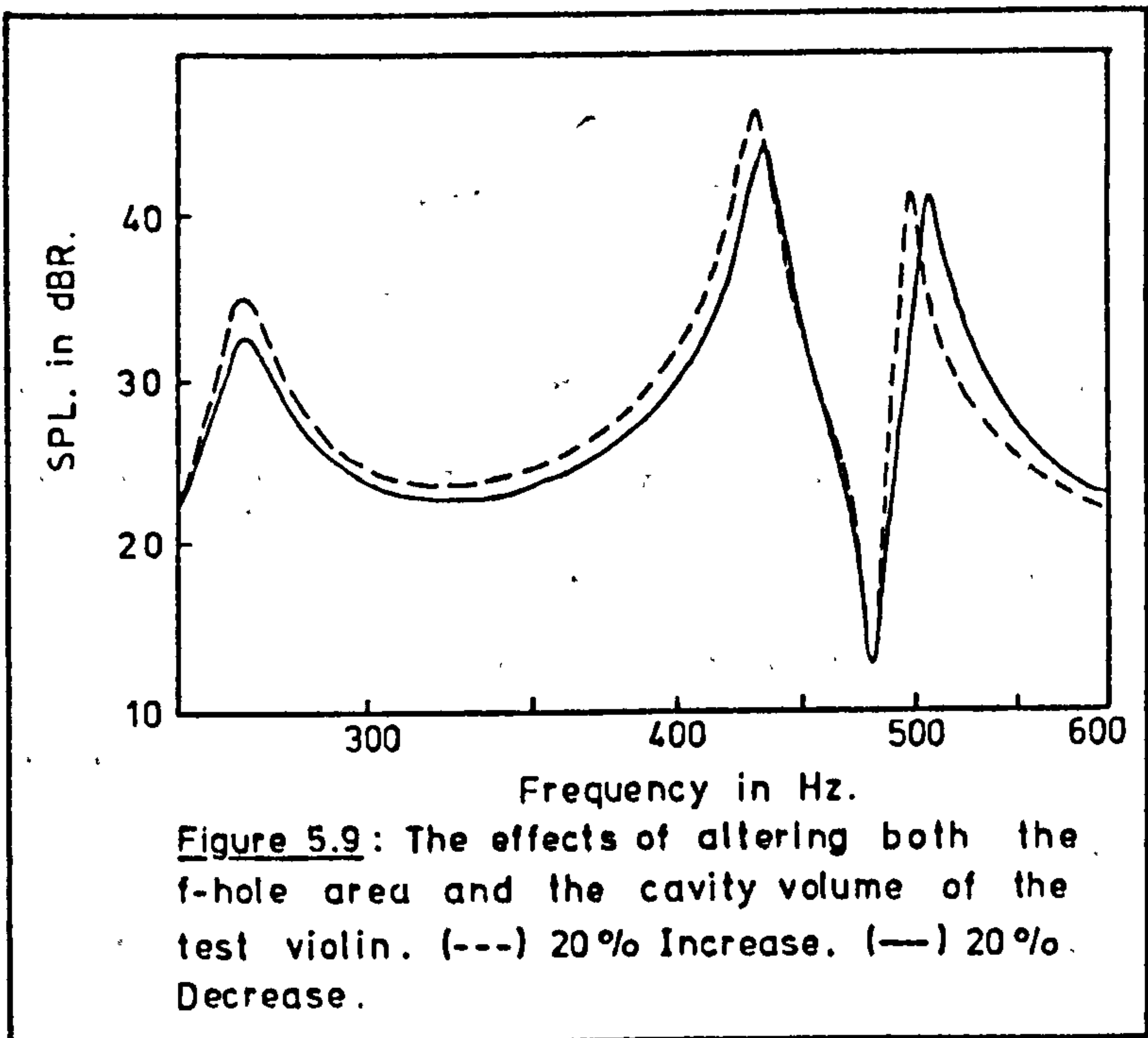
### Investigating Violin Design.

In chapter 4 many aspects of violin design were discussed without the ability to quantify the results from any change. It is now possible to do exactly this, using the equations (5.17).

Perhaps the most obvious requirement is for light, flexible plates rather than massive rigid ones, but the degree to which this is important is rather surprising. In figure (5.8) are shown the response curves of a violin whose [1,1] plate resonance has been held constant



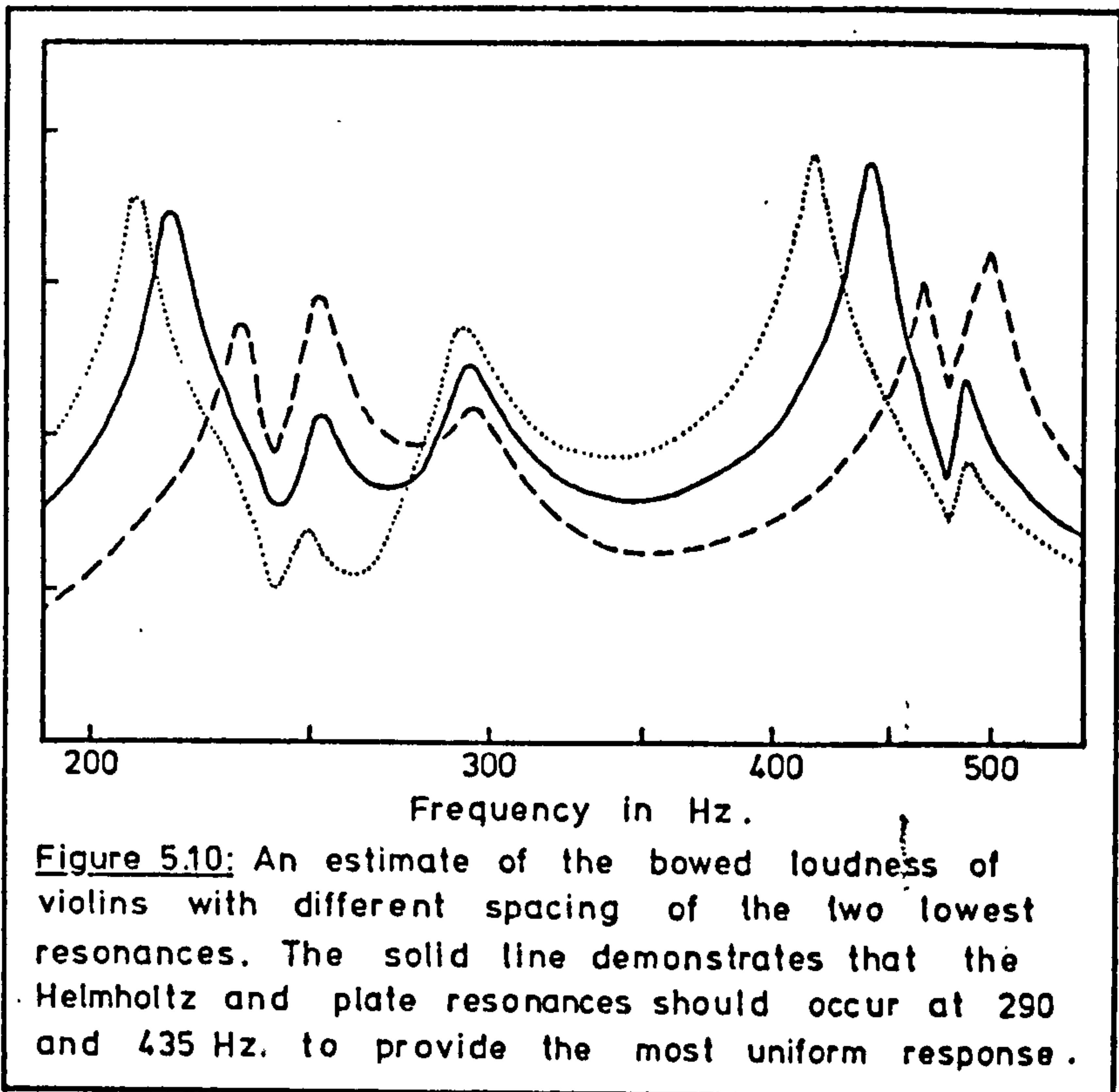
while the effective mass and stiffness have been decreased roughly 20%. An improvement of 2 to 3 dB occurs between the main two resonances and above the doublet. Twenty per cent of the effective mass may seem like a large amount but this is only a small percentage of the total plate mass. The temptation to remove more wood from the plate must be strong, but even a 3 dB increase in output is of little use if the



violin collapses!

Another method for increasing the output involves the Helmholtz mode. Increasing the f-hole area will increase their radiation. It also raises the resonance fre-

quency so that the volume must be increased to counter this. Figure (5.10) shows how a change of roughly 40% produces perhaps a 2 dB difference in the region between the two main resonances, and a 4 dB difference at the Helmholtz peak. Again, this may seem to be an enormous change in the violin design but large differences may be observed between the two violins in figures (1.1) and (1.2), the one a nineteenth century German violin and the

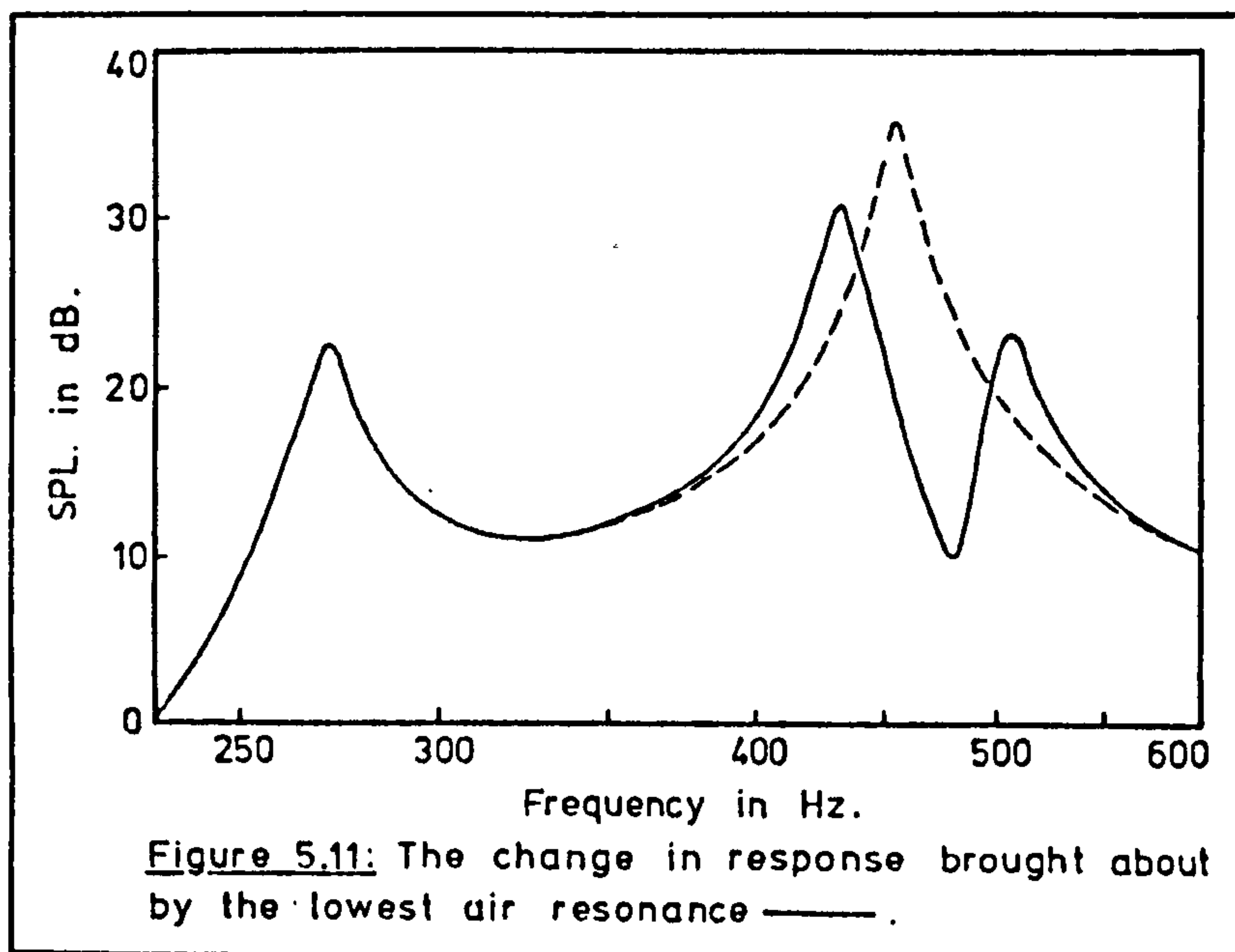


other a copy of a Stradivarius. These large German violins have a reputation for having a powerful G-string, which is not at all surprising considering the differences shown in figure (5.9).

Another basic feature of violin design which should be put to the test is the spacing of the lowest two resonances. It is the loudness curves which are of primary interest in this case and the curves which appear in figure (5.10) were produced by including the second harmonic's contribution to the loudness, calculated for Helmholtz string motion.

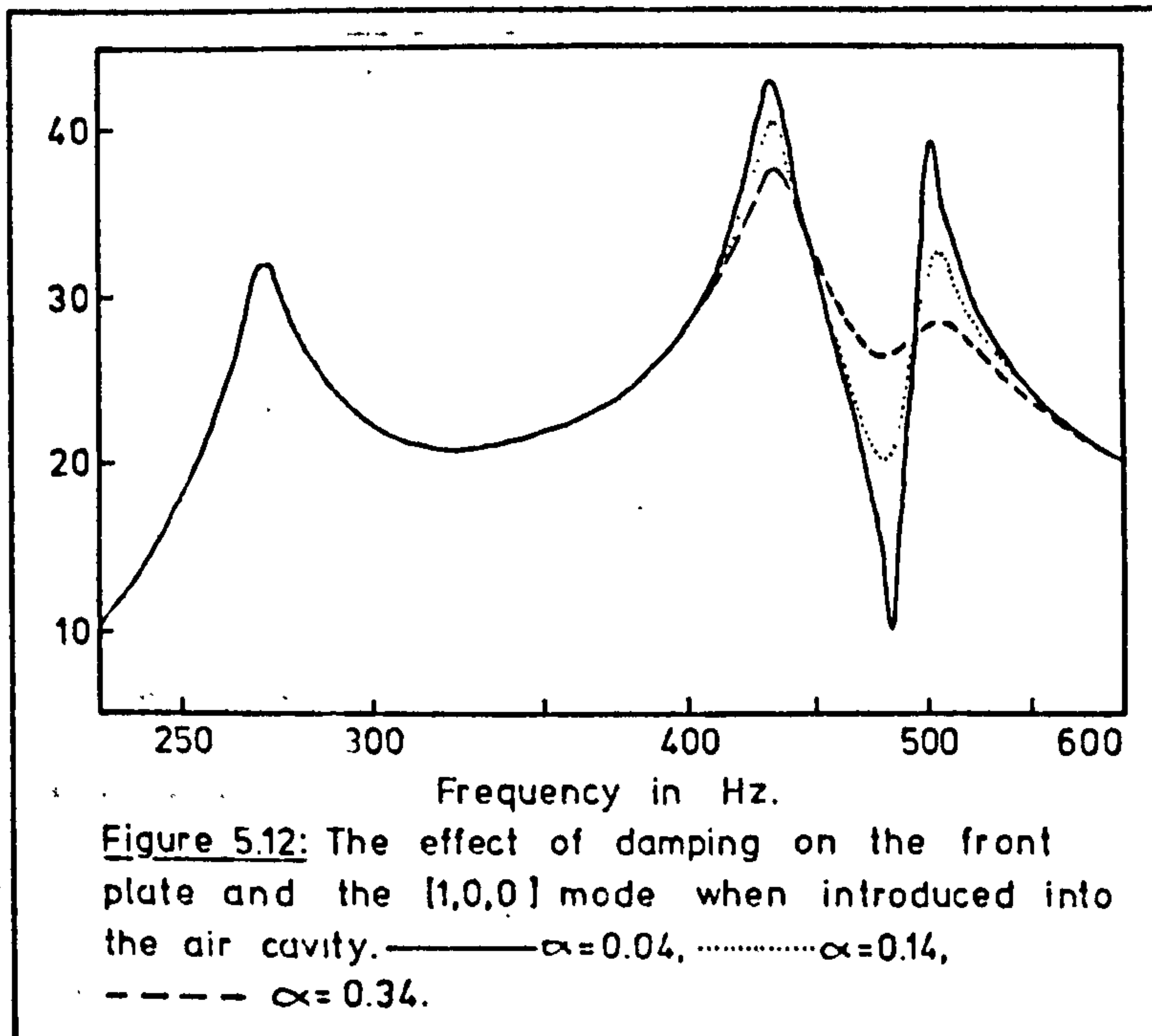
The cavity volume and plate stiffness were altered to change the spacing between the resonances and after trying many combinations the best response was obtained with the peaks at about 290 and 440 Hz. as suggested in the literature [3]. If the other resonance peaks were considered as well as these lowest two the optimum spacing could be slightly different, but the figures suggested should prove to be a good guide.

Including the [1,0,0] mode in the model brings about a remarkable change in the frequency response, as figure (5.11) demonstrates. A



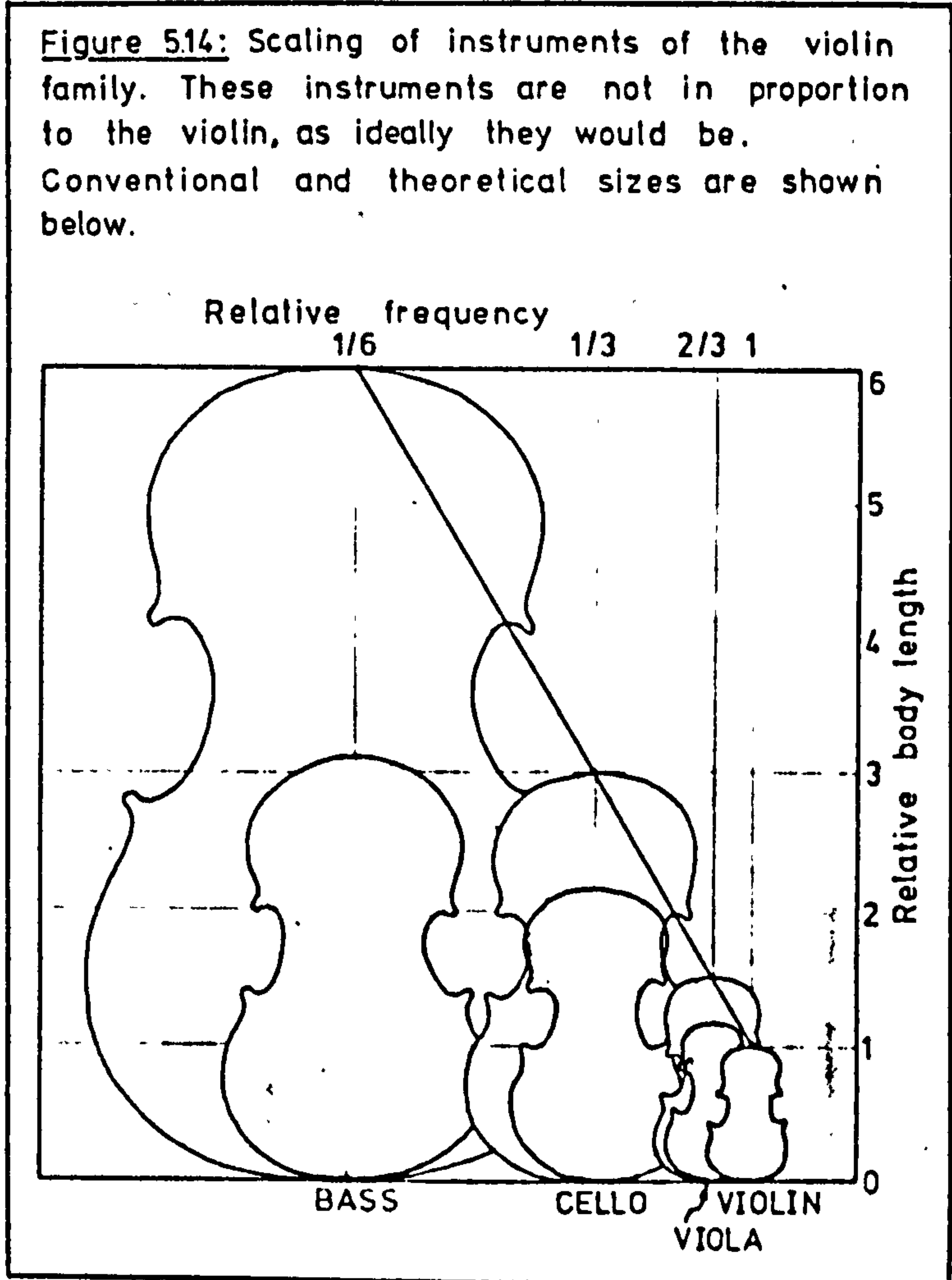
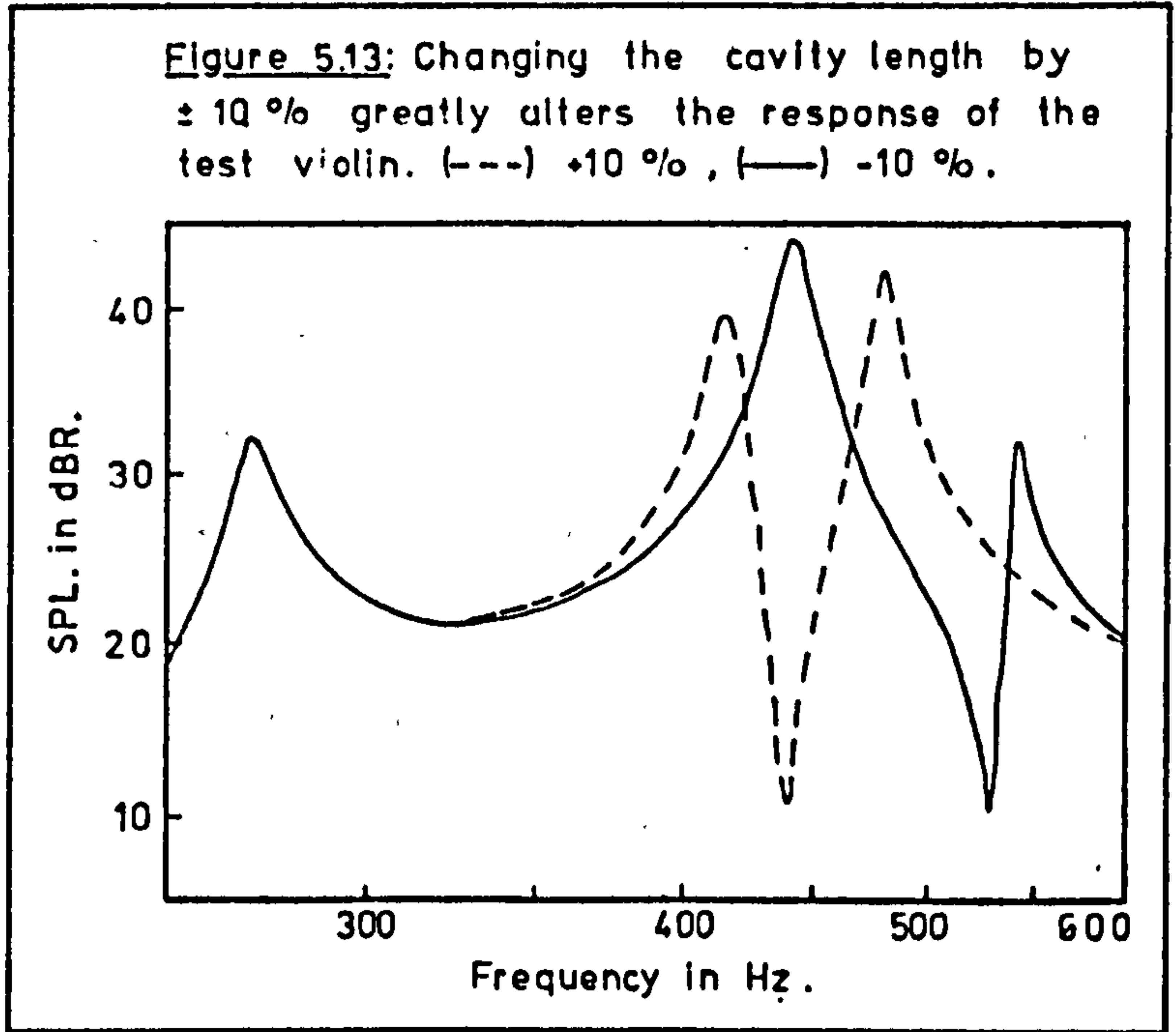
doublet is formed between the air mode and the plate, with a pronounced minimum at the  $[1,0,0]$  resonant frequency. Its function as a vibration absorber can be a great disadvantage if the equivalent area  $S_{f1}$  is too large. The response curve of a violin with  $S_{f1} = 54 \text{ cm}^2$  shows an improvement where the double peaks occur, but the response at both 470 and 235 Hz. would be quite poor. The change in mode shape which the sound-post brings about is responsible for reducing the equivalent area from 54 to 19  $\text{cm}^2$  in the test violin, and this latter curve shows that the response is much more powerful and even with such a value. Ideally the anti-resonance would produce an output level similar to the minimum between the main peaks, with the doublet well spaced and an improvement of a couple of decibels throughout the low frequency range. In frequency response tests of instruments which are held in particular regard this often appears to be the case, although none of the factors which have been discussed are alone enough to produce a good violin [4].

It is not only the area  $S_{f1}$  which affects the doublet, for the cavity length and the damping present in the sound-box are equally im-



portant, as demonstrated in figures (5.12) and (5.13). The lightly damped curve in the first of these figures would be produced by a violin whose interior had been

varnished. Although such a violin would be much less susceptible to the vagaries of the weather, it would certainly have a poor response in the region of the  $[1,0,0]$  resonance. Increasing the damping present reduces the depth of the antiresonance but also reduces the Helmholtz peak. In addition it moves the double peaks of the plate resonance closer together with a reduction in the response between the plate and Helmholtz resonances. Some amount of damping



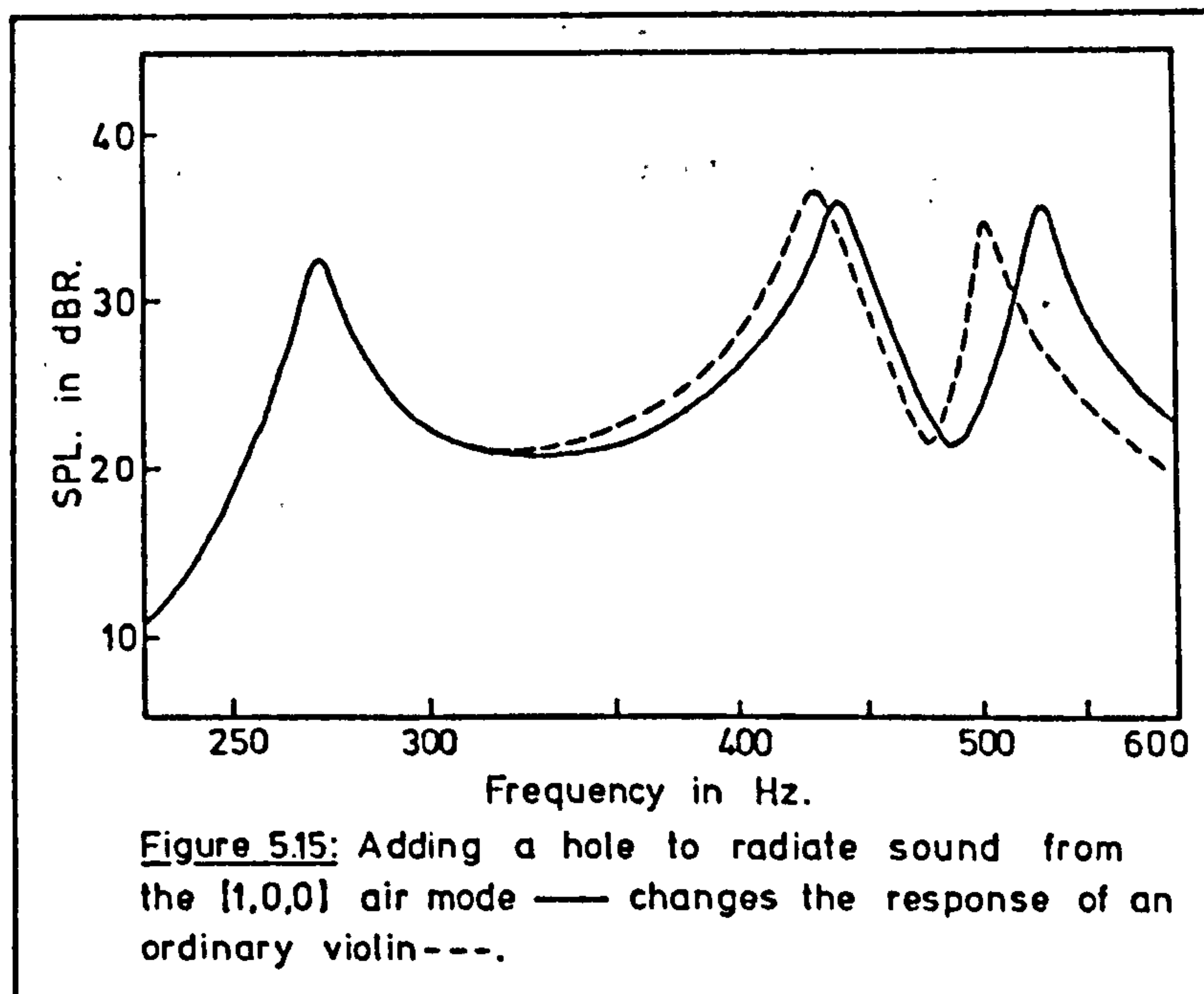
is then necessary but too much, as the figure shows, is counter productive.

The cavity length controls the  $[1,0,0]$  resonant frequency and consequently the relative strengths of the two peaks that form the doublet, although the front plate's impedance is of equal importance in this case. Peaks of almost equal strength were produced in the test violin with a cavity length of 32.5 cm. The differences between the curves in figure (5.13) are small, but perhaps they are enough to explain why the length of a full-size violin seldom varies from one instrument to another.

While the plate sizes of violins are very similar, the same cannot be said about other members of the string family, the viola in particular. Ideally these instruments would be constructed exactly like an enlarged violin, but their size would make them more difficult to play. Figure (5.14) demonstrates how a 'cello would be nearly the size of a typical bass if properly scaled. With these instruments designed so differently than the violin it is not surprising that many sorts of compromises are reached and a standard design does not exist. One modern luthier, Carleen Hutchins, has tried to remedy this situation by producing a new family of stringed instruments which are more accurately scaled [5]. Whether these instruments will gain acceptance is in doubt for most composers have been aware of the weaknesses of violas and 'cellos and exploited their unique tone colors.

It has been suggested that direct radiation of sound from the cavity modes could improve the response of a violin [6]. This possibility is explored at low frequencies in figure (5.15). It would appear that by opening a hole near one end of the violin, (the upper left or lower right corners would be well suited for this) and

increasing the cavity volume to compensate for the shift in the Helmholtz mode that this would produce, the response is not degraded. Experiments with such a construction would be of great interest and could well yield significant improvements at higher frequencies. If, however, this increases the radiation over the important range from 1200 to 2000 Hz., the addition of this extra radiator would not be a welcome one.



In this chapter the violin has been successfully modelled at low frequencies and the ensuing equations used to explore some points about violin design. The function of the sound-post must be included in the model, and although it was accounted for by measuring plate parameters with the sound-post in place, this method cannot be used when predicting the response of a complete violin from its component parts. There are three methods available for doing this. The first of these would be to calculate the effect of the point impedance which the sound-post provides to the front plate, a technique which would be well suited to the green's function approach. A finite element analysis would also be of use, but the computer time necessary for this would be

prohibitive for those who could benefit from such an approach. The third, and most intriguing, possibility is explored in chapter 6.

[1] J. Schelleng, "The violin as a circuit", JASA, vol. 35, pp. 326- 338, (1963).

[2] E. Johnson, "Air coupling between violin plates", Proceedings of the Institute of Acoustics, (1979).

[3] C. Hutchins, "The physics of violins", Scientific American, vol. 138, pp. 73- 86, (1962).

[4] F. Saunders, "The mechanical action of instruments of the violin family", JASA, vol. 17, pp. 169- 186, (1946).

[5] C. Hutchins, "Founding a family of fiddles", Physics Today, vol. 20, pp. 23- (1967).

[6] A. Gabrielsson et. al., "Resonances of a violin body studied by hologram interferometry and acoustical methods", Physica Scripta, vol. 2, pp. 243- 256, (1970).

Manufacturing Techniques.

For the vast majority of violinists, the sound of a Stradivarius is so remotely related to that produced by their own violin that it sounds like an altogether different type of instrument. Many children begin learning to play with an inexpensive, mass-produced violin, which is only to be expected, but these are of discouraging quality. How many give up a lifetime of musical enjoyment simply because their first explorations are unpleasant and physically painful? When viewed this way, the industry has much to answer for.

Most manufacturing processes are similar. It is the individual attention which the luthier pays to his product, as well as his careful selection of wood, which makes these violins so much better than mass produced instruments. These are cut, either by machine or by hand, to specified dimensions so that, while they may appear to be well-made, and may in fact be copies of a fine old violin, perfect in every detail, no attention has been paid to their dynamic characteristics. It would be unreasonable to expect this to be otherwise for a great deal of skill, training, and time are required to employ tap-tones and adjust the plates accordingly.

Of course, some mass-produced violins can be very good- by chance the plates may have the correct spacing of resonances. But, on the whole, factory made instruments are poor as the time and expense of adjusting each one which requires attention makes them uncompetitive in a market where price is usually of primary importance. What is needed is an automated method for predicting the response of an assembled violin before it is put together so that any adjustments may be made quickly and cheaply.

The model which was developed in chapter 5 was meant to meet this

need but a major obstacle remains to be surmounted. In order to include the effects of the direct coupling between back and front plates it is necessary to measure the parameters which describe the plates with the violin assembled and the sound-post in position. This is of no use in production applications. It is possible to predict the new mode shapes and the frequency response of the violin by treating the post as a point impedance and resorting once again to the green's function approach, but a further possibility presents itself which has some additional advantages.

In chapter 4 the back plate was revealed as an impedance device with relatively little radiation when compared to the front. It should then be possible to remove the direct coupling of the sound-post by inserting an internal element to perform the same function, an element which could remain in position while the violin belly is tested and adjusted. A cross-piece, such as illustrated in figure 6.1, serves

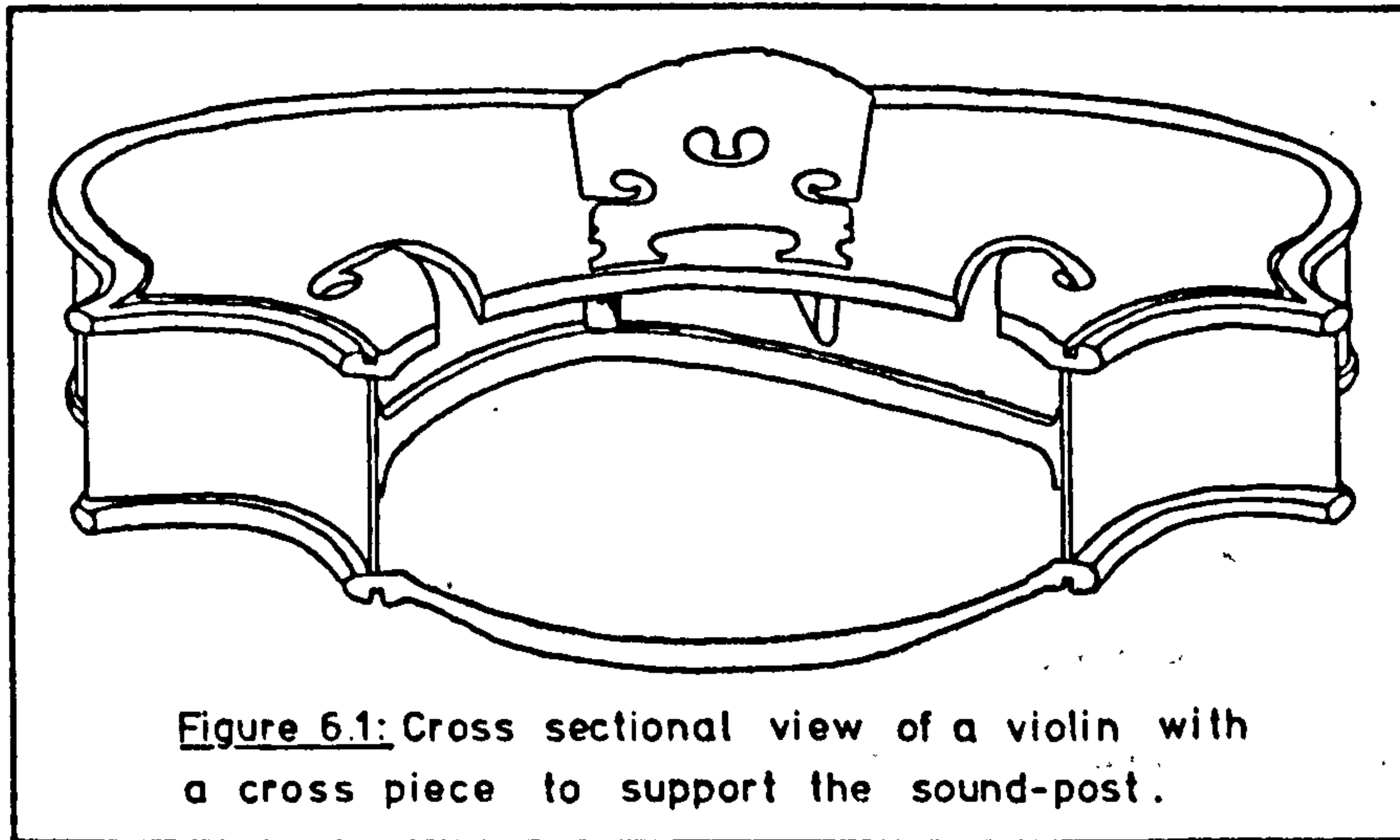


Figure 6.1: Cross sectional view of a violin with a cross piece to support the sound-post.

admirably in this capacity for it is easily made and may itself be easily adjusted to have the best possible impedance characteristics.

Ideally the "cross-bar", as it shall be called, should be made from a material which is both light and has a high modulus of elasticity. only a small section need be used to obtain the dynamic

characteristics which are sought. This is important as reflections from the cross-bar could reduce the effectiveness of the [1,0,0] air cavity mode. Additionally, a material with a coefficient of thermal expansion similar to that of the plates would minimize stresses which could cause cracks under extremes in weather conditions.

If a uniform beam is to be used for this purpose, it is easy to show that spruce is again a good choice of material. The bar must have its lowest resonance at about 700 Hz. where its impedance should match that of the front plate, as was demonstrated in chapter 4. This determines the dimensions of the cross-bar. A match between the resistive part of the front plate and cross-bar impedances may be easily obtained by adding a layer of some lossy material to a surface of the latter.

A beam designed to match the front plate at its second resonance will not of course have an infinite impedance at 440 Hz. as ideally it would. Some compromise must be sought between the two opposing requirements and experimental work with many different cross-bars performed before an optimum is chosen. Such work is beyond the scope of this text, but the feasibility of such a design is demonstrated clearly.

A reasonably good factory made violin was fitted with just such a cross-piece and this prototype is pictured in figure 6.2. A curved spruce beam, with dimensions of 0.3 x 1.0 cm. was attached to the violin ribs, a shortened sound-post wedged between it and the front plate, and the impedance was measured in the usual way. After all of the front plate parameters had been measured the back was glued on and the frequency response, which appears in figure 6.3, was measured.

This frequency response curve is certainly encouraging. Although the spacing of the resonance peaks at low frequencies is not ideal,

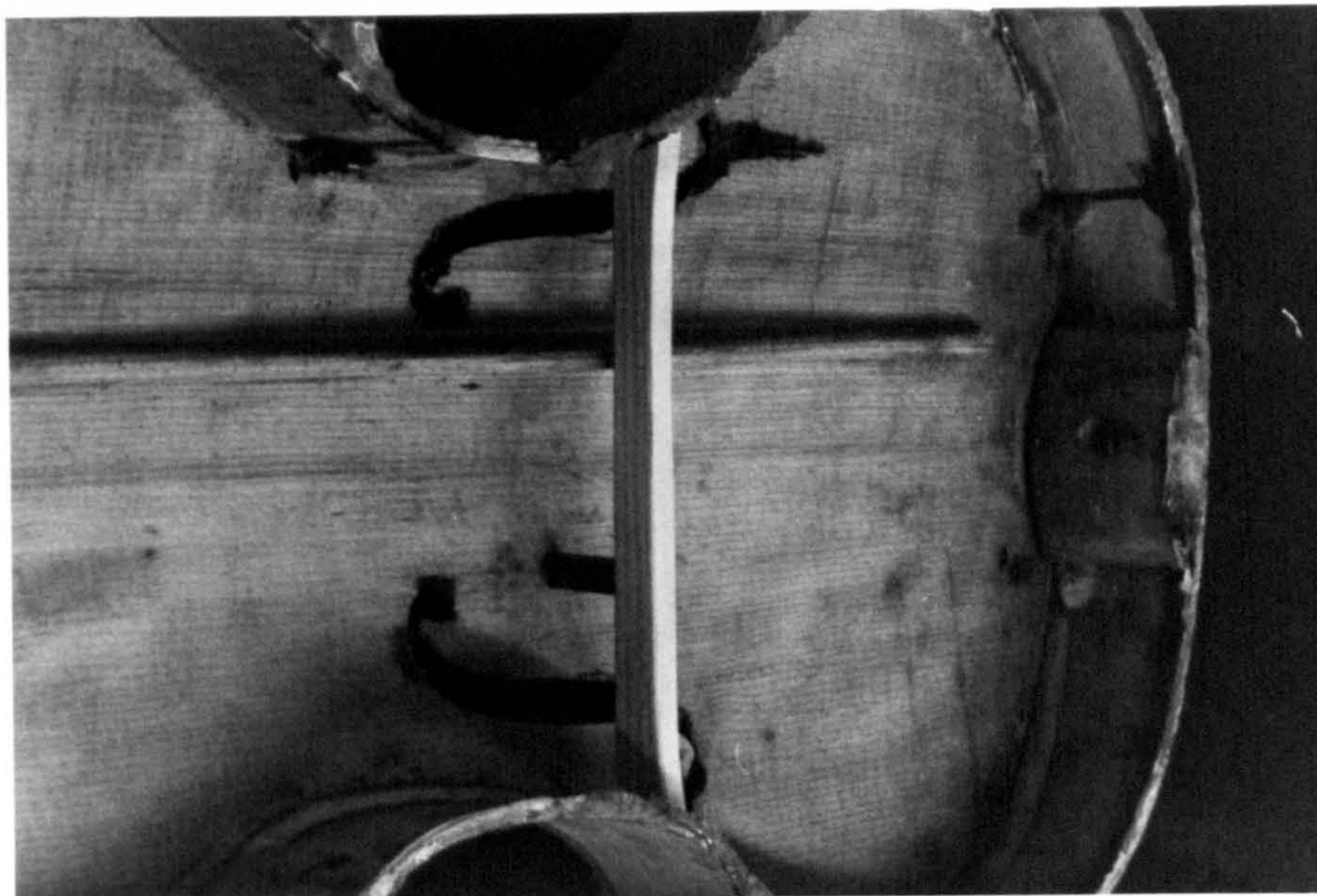


Figure 6.2: The prototype violin with its cross-bar in position.

these could easily be adjusted. The modal density is quite high at frequencies above 1 KHz. so that, with a properly designed bridge, the sort of response curve which was valued so highly in chapter 1 could be obtained.

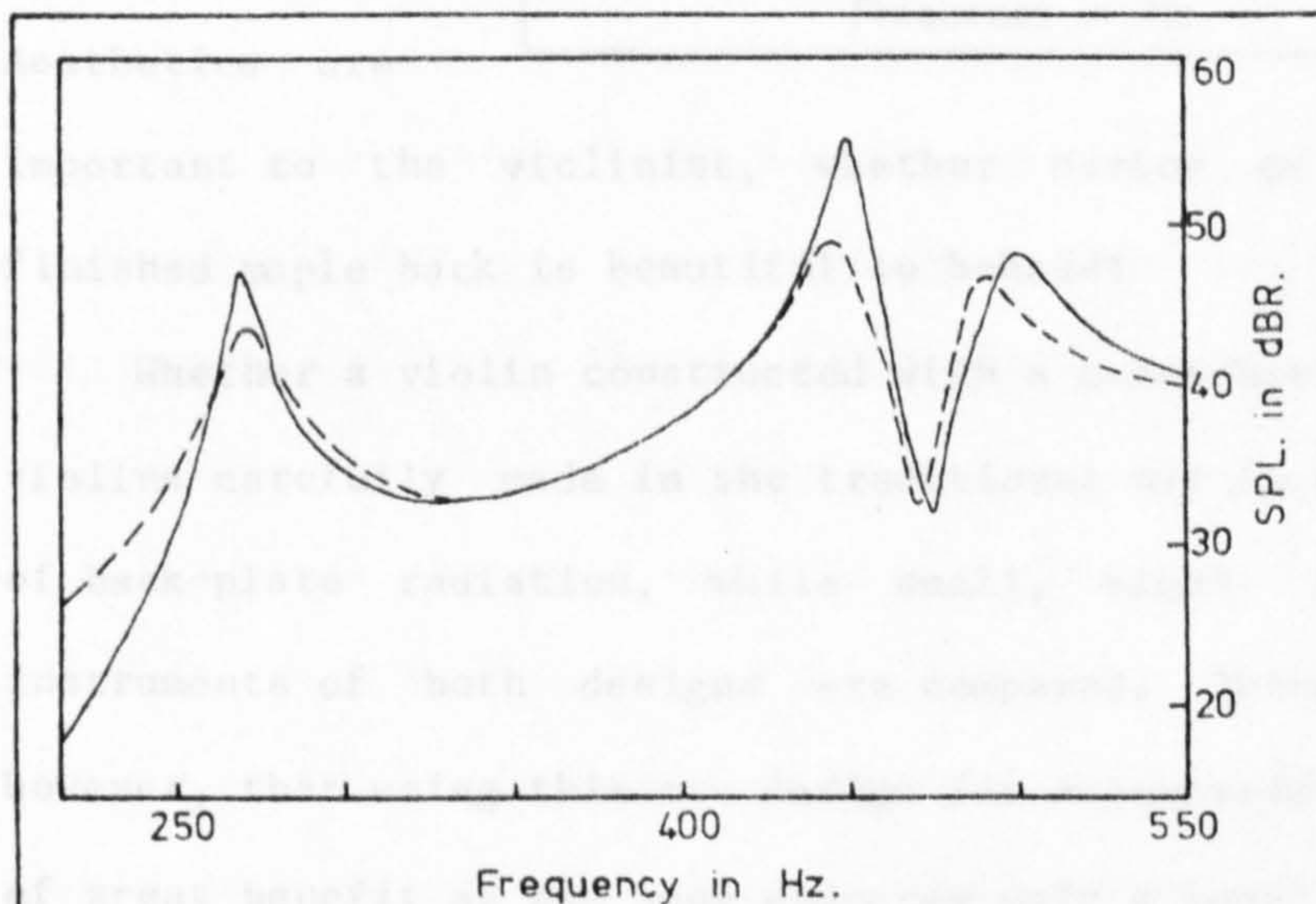


Figure 6.3: The experimental----- and theoretical ——— frequency response of the test violin with a cross-piece to support the sound-post.

Once again the modelling of the violin has made it possible to accurately estimate the frequency response of the instrument itself. This confirms the belief that

by using the crossbar to replace the traditional sound-post it is possible to predict the response of the completed violin from its components.

With the removal of the sound-post an intriguing possibility presents itself. The back plate need no longer be made massive and rigid but could be made of spruce, like the belly. Air coupling between the plates would then drive the back, perhaps to appreciable levels. This possibility was investigated using the model and the frequency responses compared in figure 6.4. Unfortunately only a small difference is noticed between the different curves, and although the

effect may be noticeable, it would probably not be important enough to overcome the resistance to such a change. Aesthetics are

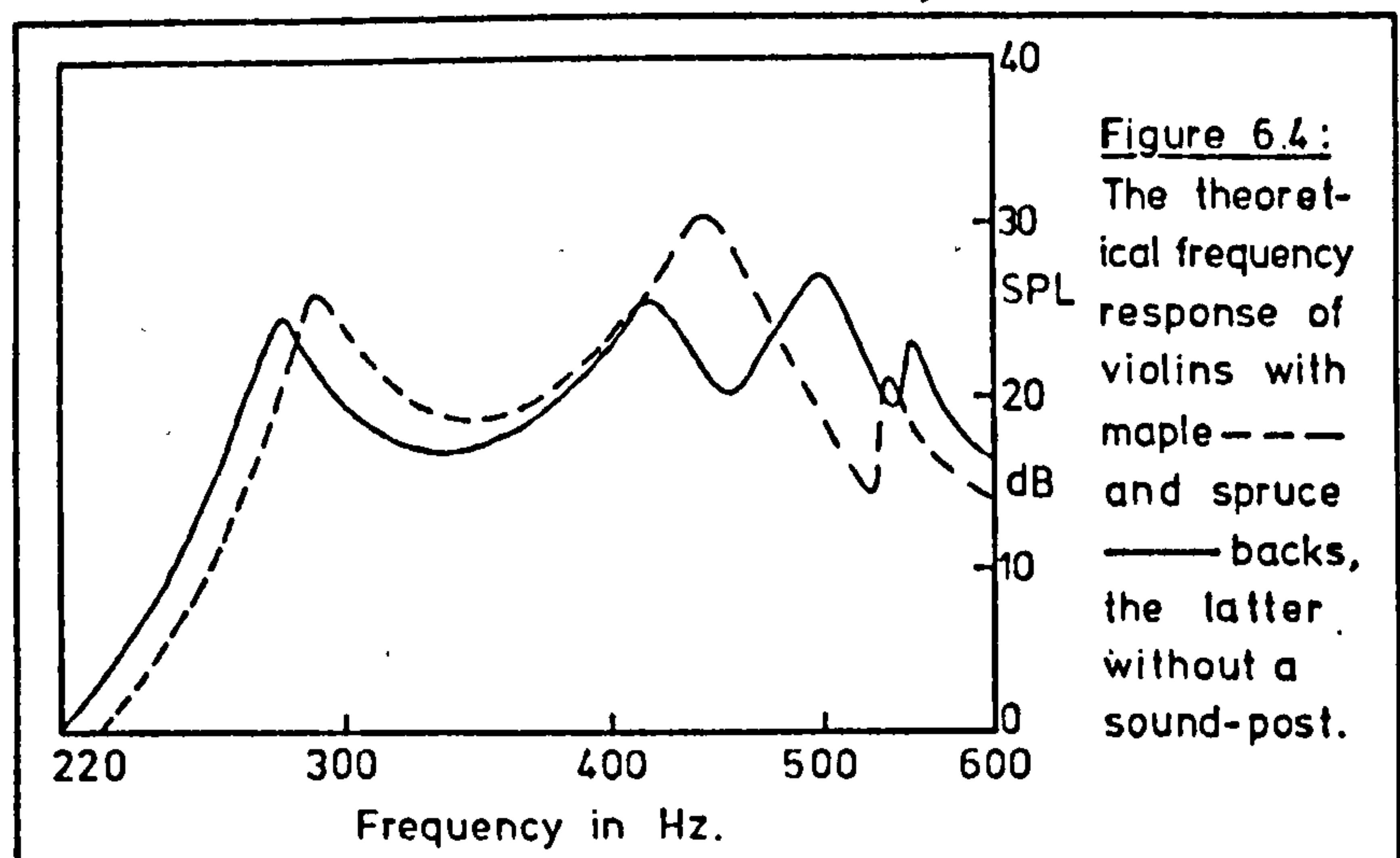
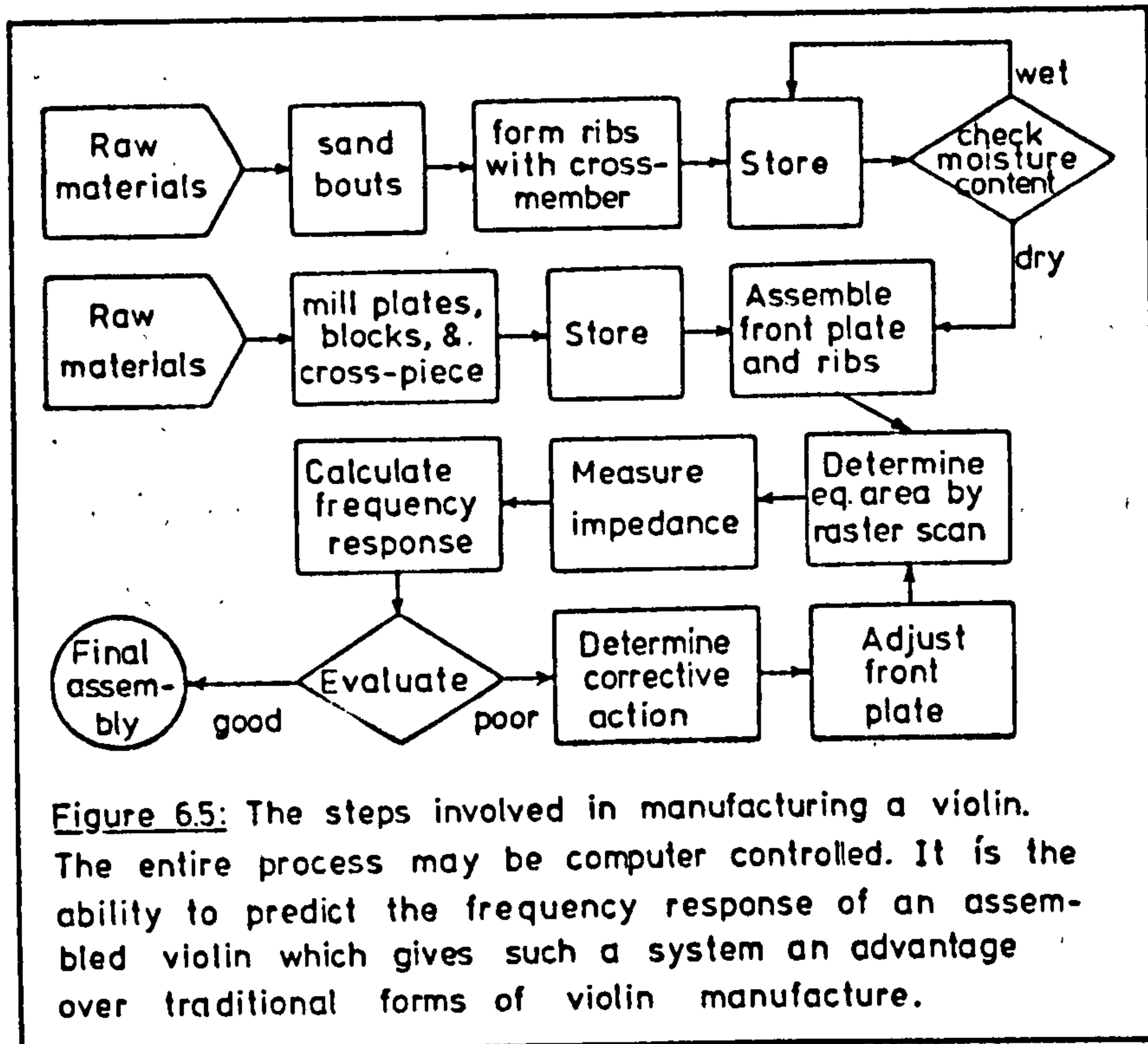


Figure 6.4:  
The theoretical frequency response of violins with maple --- and spruce — backs, the latter without a sound-post.

important to the violinist, whether novice or virtuoso, and a well finished maple back is beautiful to behold!

Whether a violin constructed with a cross-bar could compete with violins carefully made in the traditional way is doubtful. The effect of back-plate radiation, while small, might be noticeable when instruments of both designs are compared. There can be no question, however, that using this new design for mass-produced violins would be of great benefit as the beam obscures only a small portion of the plate when viewed from the back and it is easy to make any necessary adjustments to the frequency response with it still in place. To make



use of this great advantage at a low cost it is necessary to use some advanced production techniques and equipment.

High labour costs and the versatility of micro-processors have combined to make fully automated production centers a reality. Machines need no longer be assigned a single, unchanging function as part of an assembly line; the same milling machine can cut violin plates to size, shape the blocks, make adjustments to the plate thickness, and cut the purfling groove when so directed by a microprocessor. Even the different cutting tools for these operations can be selected automatically.

The steps necessary to build a violin are shown diagrammatically below in figure 6.5, but it should be emphasized that the route which the pieces follow through a production center is not fixed. It depends on the availability of machines when a certain operation is necessary and upon the instructions of the computer. The process is therefore as versatile and efficient as its programmer. The entire production

process is described very briefly below, with the details of all but the last portion, with which this work has been intimately involved, left to the production engineers.

Raw materials, spruce and maple for the plates and for the cross-bar, can all be cut and shaped by a milling machine whose cutter is controlled by computer. Not only violins, but other stringed instruments too, or smaller models such as 3/4 size violins, may have their components cut on the same machine if properly programmed. As components are finished they are sent to storage areas until needed for assembly or for testing.

The bouts must initially be thinned by sanding. When these have reached the required thinness, they are sent to be formed into ribs, along with blocks, corners, and the cross-bar. Vacuum forming processes are frequently used for such applications- heat and moisture are necessary if the wood is to be easily bent, which means that the ribs must be allowed to return to the proper moisture content before being glued to the plates. The micro-processor can select a set of ribs from the holding area with the proper moisture content and join it to a front plate, finally adding the sound-post to complete the first major portion of the assembly process.

In the next portion of the process the modelling is used to calculate the frequency response and then to evaluate the violin. First it is necessary to measure the parameters which characterize the front plate. The impedance may be quite easily measured using a device such as that designed by Ian Firth [1]. Computer control over the positioning, the excitation frequency, and the interpretation of data from the analog "impedance head" makes it possible for this to be done automatically. It is also possible for the computer to measure the equivalent areas  $S_{f_0}$  and  $S_{f_1}$  using a "raster scan" holographic

technique over the plate when it is driven at its resonant frequency.

The most time consuming part of the experimental work required to determine the plate parameters involves measuring the equivalent areas. To do this a vibration hologram must be made, reconstructed, photographed, and the amplitude function integrated either by hand or by a computer, in which case the photograph must somehow be interpreted by it. In a commercial application such a lengthy process would be uneconomical, but once again computer control of the entire operation makes this possible. Rather than recording the intensity produced by the interference of two beams on a photographic emulsion, as is done in conventional holography, a small photocell, which also responds to intensity, can be positioned at programmed points to measure the vibration amplitude. It is possible to use a small, solid-state laser to illuminate a very small area, and the laser and photocell could be combined into a single unit, interfaced to the computer. It would even be possible to use the same machinery to index, or raster-scan, the laser/photocell and to position the impedance head. The computer can then determine the vibration amplitude at any point directly and with no need for sensitive, large lasers.

Once all of this information is available to the computer the frequency response for the complete violin may be predicted, perhaps including many more modes than were used in this research to extend the frequency range, and this response curve evaluated. If changes are necessary the information about the amplitude distribution for each plate mode makes it possible to calculate small changes in the plate thickness which will improve the response. It is of course possible to move the resonant frequencies of any two modes by different amounts, even in opposite directions, providing the alterations are carefully chosen.

Once the predicted response of the violin is acceptable it goes on to its final assembly where the back is glued on, it is varnished, and a bridge, perhaps cut and tested on the same equipment which produced the violin, attached. The automated assembly processes which are only just beginning to be applied in a few leading industries could revolutionize the production of violins.

A violin-maker would no doubt scoff at many of the ideas presented in this work. While he might applaud the intention to raise the quality level of most factory-made instruments, the analysis of the violin's construction, its modelling by computer, testing, and finally the suggestion of a change in design would be dismissed as useless. How can one argue with three-hundred years of experience, the collective genius of Stradivarius, Stainer, the Amatis, Guarneris, and countless others. And yet there is so little of their work in the factory made violin, whose body may be a perfect copy of a master's work but which lacks their spirit, which sought to reconcile the beauties of form and sound. Perhaps through this thesis, or more likely another's work whose object is the same, even the lowly, common mass-produced violin can be made to sing with a richness they lack today.

The violin-maker need not fear for his craft, for although a machine may make a violin with a lovely sound, it is the musician who makes the music, and the luthier, with his individuality, that creates a thing of beauty. But the machine may give us more people to enjoy a lifetime of music, more people to appreciate the genius of man's creativity.

[1] I. Firth, "Small mechanical impedance head for use with musical instruments", *Acustica*, vol. 35, pp. 348- 349, (1976).